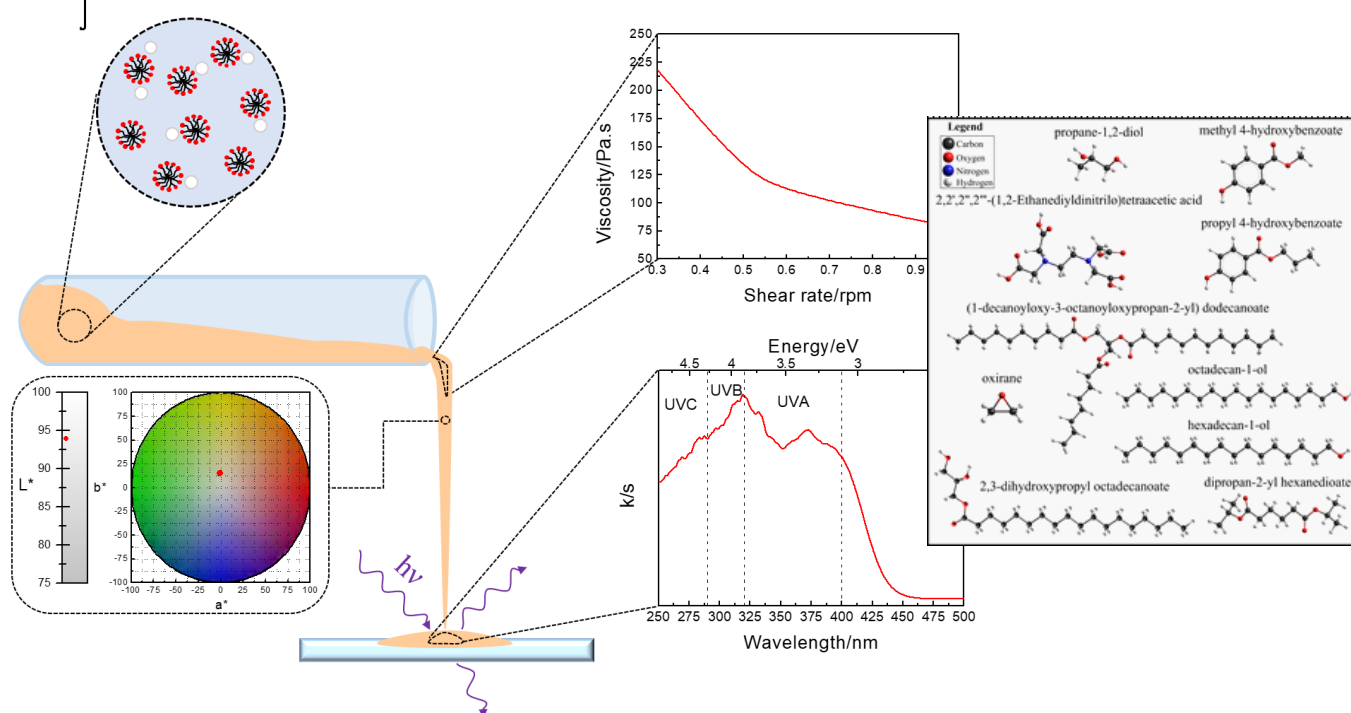


Eclética Química Journal

Volume 44 • number 2 • year 2019



Study of the colloidal stability and optical properties of sunscreen creams

Review

Chemometrics in analytical chemistry – an overview of applications from 2014 to 2018

Arsenic in fish

Direct determination of arsenobetaine and total As in robalo fish liver and tuna fish candidate reference material by slurry sampling graphite furnace atomic absorption spectrometry (SLS-GF AAS)

Aluminum

Effects of garnet particles and chill casting conditions on properties of aluminum matrix hybrid composites

Structural data

Cobalt(II) chloride complexes with some phosphine oxides: compatibility between structural data for the solid complexes and their stability constants in acetone medium



UNIVERSIDADE ESTADUAL PAULISTA

Reitor

Sandro Roberto Valentini

Vice-reitor

Sergio Roberto Nobre

Pró-reitor de Planejamento Estratégico e Gestão

Leonardo Theodoro Büll

Pró-reitora de Graduação

Gladis Massini-Cagliari

Pró-reitora de Pós-Graduação

Telma Teresinha Berchielli

Pró-reitora de Extensão Universitária

Cleopatra da Silva Planeta

Pró-reitor de Pesquisa

Carlos Frederico de Oliveira Graeff



INSTITUTO DE QUÍMICA

Diretor

Eduardo Maffud Cilli

Vice-Diretora

Dulce Helena Siqueira Silva

Editorial Team

Editors

Prof. Assis Vicente Benedetti, Institute of Chemistry Unesp Araraquara, Brazil (Editor-in-Chief)

Prof. Arnaldo Alves Cardoso, Institute of Chemistry Unesp Araraquara, Brazil

Prof. Antonio Eduardo Mauro, Institute of Chemistry Unesp Araraquara, Brazil

Prof. Horacio Heinzen, Faculty of Chemistry UdelaR, Montevideo, Uruguay

Prof. Maysa Furlan, Institute of Chemistry Unesp Araraquara, Brazil

Prof. Maria Célia Bertolini, Institute of Chemistry Unesp Araraquara, Brazil

Prof. Paulo Clairmont Feitosa de Lima Gomes, Institute of Chemistry, Unesp Araraquara, Brazil

Editorial Board

Prof. Jairton Dupont, Instituto de Química, Universidade Federal do Rio Grande do Sul, UFRGS, RS, Brazil

Prof. Enric Brillas, Facultat de Química, Universitat de Barcelona, Spain

Prof. Verónica Cortés de Zea Bermudez, Escola de Ciências da Vida e do Ambiente, Universidade de Trás-os-Montes e Alto Douro, Vila Real, Portugal

Prof. Lauro Kubota, Instituto de Química, Universidade Estadual de Campinas, Unicamp, SP, Brazil

Prof. Ivano Gerardt Rolf Gutz, Instituto de Química, Universidade de São Paulo, USP, SP, Brazil

Prof. Massuo Jorge Kato, Instituto de Química, Universidade de São Paulo, USP, SP, Brazil

Prof. Francisco de Assis Leone, Faculdade de Filosofia, Ciências e Letras, Universidade de São Paulo, Ribeirão Preto, USP-RP, SP, Brazil

Prof. Roberto Santana da Silva, Faculdade de Ciências Farmacêuticas, Universidade de São Paulo, Ribeirão Preto, USP-RP, SP, Brazil

Prof. José Antônio Maia Rodrigues, Faculdade de Ciências, Universidade do Porto, Portugal

Prof. Bayardo Baptista Torres, Instituto de Química, Universidade de São Paulo, USP, SP, Brazil

Technical Staff

Gustavo Marcelino de Souza

Letícia Amanda Miguel

Editorial

It is a pleasure for the Editor to announce the publication of the second issue of this year, containing very interesting subjects for the readers. This issue begins with a review entitled “Chemometrics in analytical chemistry – an overview of applications from 2014 to 2018.” A compilation of recent papers related to multivariate calibration and classification, as well as design of experiments applications and artificial intelligence methods have been reported. Applications of the chemometric techniques in different fields such as medical and pharmaceutical, food analysis, fuels, and biological and forensic were highlighted. The review also presents a promising scenario considering the evolution of the researches in the above-mentioned topics. Sequentially, the synthesis of sunscreen formulations containing inorganic/organic filters, or their mixture is described, and different physicochemical parameters of the colloidal system were determined allowing to evaluate the UV shielding ability. Continuing, a simple and rapid screening method is presented for direct speciation of arsenobetaine in tuna fish tissue and total arsenic in tuna fish tissue and robalo liver; the simplicity of the method enables its use in routine analyses. Following, the microstructural and mechanical properties of an aluminum matrix hybrid reinforced with 6-12 wt. % of garnet are given. For the composite, garnet is the ceramic material and Al-6000 alloys the matrix. This type of composite is of particular interest because of the growing demand for high performance light-weight materials in industrial applications. This issue is closed with the description of a correlation between X-ray structural data of cobalt(II) chloride complexes with some phosphine oxides in the solid state and their stability constants in acetone solution.

The Editor and his team thank all authors for their effective contributions, and reviewers for their outstanding manuscripts evaluation.

Assis Vicente Benedetti
Editor-in-Chief of EQJ

Instructions for Authors

Preparation of manuscripts

- **Only manuscripts in English will be accepted.** British or American usage is acceptable, but they should not be mixed.
- **The corresponding author should submit the manuscript online:** <http://revista.iq.unesp.br/ojs/index.php/eclética/author>
- **Manuscripts must be sent in editable files as *.doc, *.docx or *.odt.** The text must be typed using font style Times New Roman and size 11. Space between lines should be 1.5 mm and paper size A4.
- **The manuscript should be organized in sections as follows:** Introduction, Experimental, Results and Discussion, Conclusions, and References. Sections titles must be written in bold and numbered sequentially; only the first letter should be in uppercase letter. Subsections should be written in normal and italic lowercase letters. For example: **1. Introduction;** *1.1 History;* **2. Experimental;** *2.1 Surface characterization;* *2.1.1 Morphological analysis.*
- **The cover letter should include:** the authors' full names, e-mail addresses, ORCID code and affiliations, and remarks about the novelty and relevance of the work. The cover letter should also contain a declaration of the corresponding author, on behalf of the other authors, that the article being submitted is original and its content has not been published previously and is not under consideration for publication elsewhere, that no conflict of interest exists and if accepted, the article will not be published elsewhere in the same form, in any language, without the written consent of the publisher. Finally, the cover letter should also contain the suggestion of 3 (three) suitable reviewers (please, provide full name, affiliation, and e-mail).
- **The first page of the manuscript** should contain the title, abstract and keywords. *Please, do not give authors names and affiliation, and acknowledgements since a double-blind reviewer system is used. Acknowledgements should be added to the proof only.*
- **All contributions should include** an Abstract (200 words maximum), three to five Keywords and a Graphical Abstract (8 cm wide and 4 cm high) with an explicative text (2 lines maximum).
- **References should be numbered** sequentially in superscript throughout the text and compiled in brackets at the end of the manuscript as follows:

Journal:

[1] Adorno, A. T. V., Benedetti, A. V., Silva, R. A. G. da, Blanco, M., Influence of the Al content on the phase transformations in Cu-Al-Ag Alloys, *Eclét. Quim.* 28 (1) (2003) 33-38. <https://doi.org/10.1590/S0100-46702003000100004>.

Book:

[2] Wendlant, W. W., *Thermal Analysis*, Wiley-Interscience, New York, 3rd ed., 1986, ch1.

Chapter in a book:

[3] Ferreira, A. A. P., Uliana, C. V., Souza Castilho, M. de, Canaverolo Pesquero, N., Foguel, N. V., Pilon dos Santos, G., Fugivara, C. S., Benedetti, A. V., Yamanaka, H., Amperometric Biosensor for Diagnosis of Disease, In: State of the Art in Biosensors - Environmental and Medical Applications, Rincken, T., ed., InTech: Rijeka, Croatia, 2013, Ch. 12.

Material in process of publication:

[4] Valente Jr., M. A. G., Teixeira, D. A., Lima Azevedo, D., Feliciano, G. T., Benedetti, A. V., Fugivara, C. S., Caprylate Salts Based on Amines as Volatile Corrosion Inhibitors for Metallic Zinc: Theoretical and Experimental Studies, *Frontiers in Chemistry*. <https://doi.org/10.3389/fchem.2017.00032>.

- Figures, Schemes, and Tables should be numbered sequentially and presented at the end of the manuscript.
- Nomenclature, abbreviations, and symbols should follow IUPAC recommendations.
- Figures, schemes, and photos already published by the same or different authors in other publications may be reproduced in manuscripts of **Eclet. Quim. J.** only with permission from the editor house that holds the copyright.
- Graphical Abstract (GA) should be a high-resolution figure (900 dpi) summarizing the manuscript in an interesting way to catch the attention of the readers and accompanied by a short explicative text (2 lines maximum). GA must be submitted as *.jpg, *.jpeg or *.tif.
- **Communications** should cover relevant scientific results and are limited to 1,500 words or three pages of the Journal, not including the title, authors' names, figures, tables and references. However, Communications suggesting fragmentation of complete contributions are strongly discouraged by Editors.
- **Review articles** should be original and present state-of-the-art overviews in a coherent and concise form covering the most relevant aspects of the topic that is being revised and indicate the likely future directions of the field. Therefore, before beginning the preparation of a Review manuscript, send a letter (1 page maximum) to the Editor with the subject of interest and the main topics that would be covered in Review manuscript. The Editor will communicate his decision in two weeks. Receiving this type of manuscript does not imply acceptance to be published in **Eclet. Quím. J.** It will be peer-reviewed.
- **Short reviews** should present an overview of the state-of-the-art in a specific topic within the scope of the Journal and limited to 5,000 words. Consider a table or image as corresponding to 100 words. Before beginning the preparation of a Short Review manuscript, send a letter (1 page maximum) to the Editor with the subject of interest and the main topics that would be covered in the Short Review manuscript.
- **Technical Notes:** descriptions of methods, techniques, equipment or accessories developed in the authors' laboratory, as long as they present chemical content of interest. They should follow the usual form of presentation, according to the peculiarities of each work. They should have a maximum of 15 pages, including figures, tables, diagrams, etc.
- **Articles in Education in Chemistry and chemistry-correlated areas:** research manuscript related to undergraduate teaching in Chemistry and innovative experiences in undergraduate and graduate education. They should have a maximum of 15 pages, including figures, tables, diagrams, and other elements.
- **Special issues** with complete articles dedicated to Symposia and Congresses can be published by **Eclet. Quim. J.** under the condition that a previous agreement with Editors is established. All the guides of the journal must be followed by the authors.

• Eclet. Quim. J. Ethical Guides and Publication Copyright:

Before beginning the submission process, please be sure that all ethical aspects mentioned below were followed. Violation of these ethical aspects may prevent authors from submitting and/or publishing articles in **Eclet. Quim. J.**

- The corresponding author is responsible for listing as authors only researchers who have really taken part in the work, and for informing them about the entire manuscript content and for obtaining their permission for submitting and publishing.
- Authors are responsible for carefully searching for all the scientific work relevant to their reasoning irrespective of whether they agree or not with the presented information.
- Authors are responsible for correctly citing and crediting all data used from works of researchers other than the ones who are authors of the manuscript that is being submitted to **Eclet. Quim. J.**
- Citations of Master's Degree Dissertations and PhD Theses are not accepted; instead, the publications resulting from them must be cited.
- Explicit permission of a non-author who has collaborated with personal communication or discussion to the manuscript being submitted to **Eclet. Quim. J.** must be obtained before being cited.
- Simultaneous submission of the same manuscript to more than one journal is considered an ethical deviation and is conflicted to the declaration has been done below by the authors.
- Plagiarism, self-plagiarism, and the suggestion of novelty when the material was already published are unaccepted by **Eclet. Quim. J.**
- The word-for-word reproduction of data or sentences as long as placed between quotation marks and correctly cited is not considered ethical deviation when indispensable for the discussion of a specific set of data or a hypothesis.
- Before reviewing a manuscript, the *turnitin* anti-plagiarism software will be used to detect any ethical deviation.
- The corresponding author transfers the copyright of the submitted manuscript and all its versions to **Eclet. Quim. J.**, after having the consent of all authors, which ceases if the manuscript is rejected or withdrawn during the review process.
- Before submitting manuscripts involving human beings, materials from human or animals, the authors need to confirm that the procedures established, respectively, by the institutional committee on human experimentation and Helsinki's declaration, and the recommendations of the animal care institutional committee were followed. Editors may request complementary information on ethical aspects.
- When a published manuscript in EQJ is also published in other Journal, it will be immediately withdrawn from EQJ and the authors informed of the Editor decision.

• Manuscript Submissions

For the first evaluation: the manuscripts should be submitted in three files: the cover letter as mentioned above, the graphical abstract and the entire manuscript.

The entire manuscript should be submitted as *.doc, *.docx or *.odt files.

The Graphical Abstract (GA) 900 dpi resolution is mandatory for this Journal and should be submitted as *.jpg, *.jpeg or *.tif files as supplementary file.

The cover letter should contain the title of the manuscript, the authors' names and affiliations, and the relevant aspects of the manuscript (no more than 5 lines), and the suggestion of 3 (three) names of experts in the subject: complete name, affiliation, and e-mail).

• Reviewing

The time elapsed between the submission and the first response of the reviewers is around 3 months. The average time elapsed between submission and publication is 7 months.

• **Resubmission** (manuscripts “rejected in the present form” or subjected to “revision”): **A LETTER WITH THE RESPONSES TO THE COMMENTS/CRITICISM AND SUGGESTIONS OF REVIEWERS/EDITORS SHOULD ACCOMPANY THE REVISED MANUSCRIPT. ALL MODIFICATIONS MADE TO THE ORIGINAL MANUSCRIPT MUST BE HIGHLIGHTED.**

• Editor's requirements

Authors who have a manuscript accepted in **Eclética Química Journal** may be invited to act as reviewers.

Only the authors are responsible for the correctness of all information, data and content of the manuscript submitted to **Eclética Química Journal**. Thus, the Editors and the Editorial Board cannot accept responsibility for the correctness of the material published in **Eclética Química Journal**.

• Proofs

After accepting the manuscript, **Eclét. Quim. J.** technical assistants will contact you regarding your manuscript page proofs to correct printing errors only, i.e., other corrections or content improvement are not permitted. The proofs shall be returned in 3 working days (72 h) via e-mail.

• Authors Declaration

The corresponding author declares, on behalf of the other authors, that the article being submitted is original and has been written by the stated authors who are all aware of its content and approve its submission. Declaration should also state that the article has not been published previously and is not under consideration for publication elsewhere, that no conflict of interest exists and if accepted, the article will not be published elsewhere in the same form, in any language, without the written consent of the publisher.

• Appeal

Authors may only appeal once about the decision regarding a manuscript. To appeal against the Editorial decision on your manuscript, the corresponding author can send a rebuttal letter to the editor, including a detailed response to any comments made by the reviewers/editor. The editor will consider the rebuttal letter, and if deemed appropriate, the manuscript will be sent to a new reviewer. The Editor decision is final.

• Contact

Gustavo Marcelino de Souza (ecletica@journal.iq.unesp.br)

Submission Preparation Checklist

As part of the submission process, authors are required to check off their submission's compliance with all of the following items, and submissions may be returned to authors that do not adhere to these guidelines.

In **Step 1**, select the appropriate section for this submission.

Be sure that Authors' names, affiliations and acknowledgements were removed from the manuscript. The manuscript must be in *.doc, *.docx or *.odt format before uploading in **Step 2**.

In **Step 3**, add the full name of each author including the ORCID IDs in its full URL ONLY WITH HTTP, NOT HTTPS (eg. <http://orcid.org/0000-0002-1825-0097>).

Add the authors in the same order as they appear in the manuscript in **step 3**.

Be sure to have the COVER LETTER and GRAPHICAL ABSTRACT (according to the Author Guidelines) to upload them in **Step 4**.

Check if you've followed all the previous steps before continuing the submission of your manuscript.

Copyright Notice

The corresponding author transfers the copyright of the submitted manuscript and all its versions to **Eclét. Quim. J.**, after having the consent of all authors, which ceases if the manuscript is rejected or withdrawn during the review process.

Self-archive to institutional, thematic repositories or personal web page is permitted just after publication.

The articles published by **Eclética Química Journal** are licensed under the Creative Commons Attribution 4.0 International License.

SUMMARY

| | |
|-------------------------------|---|
| EDITORIAL BOARD..... | 3 |
| EDITORIAL..... | 4 |
| INSTRUCTIONS FOR AUTHORS..... | 5 |

ORIGINAL REVIEW

| | |
|--|----|
| Chemometrics in analytical chemistry – an overview of applications from 2014 to 2018..... | 11 |
| <i>Mônica Cardoso Santos, Paloma Andrade Martins Nascimento, Wesley Nascimento Guedes, Edenir Rodrigues Pereira-Filho, Érica Regina Filletti, Fabíola Manhas Verbi Pereira</i> | |

ORIGINAL ARTICLES

| | |
|--|----|
| Study of the colloidal stability and optical properties of sunscreen creams..... | 26 |
| <i>Gustavo Pereira Saito, Mariana Bizari, Marco Aurélio Cebim, Marcos Antonio Correa, Miguel Jafelicci Junior, Marian Rosaly Davolos</i> | |

| | |
|---|----|
| Direct determination of arsenobetaine and total As in robalo fish liver and tuna fish candidate reference material by slurry sampling graphite furnace atomic absorption spectrometry (SLS-GF AAS)..... | 37 |
| <i>Carla Maíra Bossu, Vivian Montes de Oca Carioni, Juliana Naozuka, Pedro Vitoriano de Oliveira, Cassiana Seimi Nomura</i> | |

| | |
|--|----|
| Effects of garnet particles and chill casting conditions on properties of aluminum matrix hybrid composites..... | 45 |
| <i>Haider Tawfiq Naeem, Firas Fouad Abdullah</i> | |

| | |
|--|----|
| Cobalt(II) chloride complexes with some phosphine oxides: compatibility between structural data for the solid complexes and their stability constants in acetone medium..... | 53 |
| <i>Antonio Carlos Massabni, Cristo Bladimiro Melios</i> | |

Chemometrics in analytical chemistry – an overview of applications from 2014 to 2018

Mônica Cardoso Santos¹, Paloma Andrade Martins Nascimento², Wesley Nascimento Guedes¹, Edénir Rodrigues Pereira-Filho³, Érica Regina Filletti¹, Fabíola Manhas Verbi Pereira¹⁺

1 São Paulo State University (UNESP), Institute of Chemistry, 55 Professor Francisco Degni St, Araraquara, São Paulo, Brazil

2 São Paulo State University (UNESP), Faculty of Pharmaceutical Sciences, Km 1 Araraquara-Jaú Hw, Araraquara, São Paulo, Brazil

3 Federal University of São Carlos (UFSCar), Department of Chemistry, Km 235 Washington Luís Hw, São Carlos, São Paulo, Brazil

+Corresponding author: Fabíola Manhas Verbi Pereira, Phone: +55 16 3301 9609, email address: fabiola.verbi@unesp.br

ARTICLE INFO

Article history:

Received: December 2, 2018

Accepted: April 2, 2019

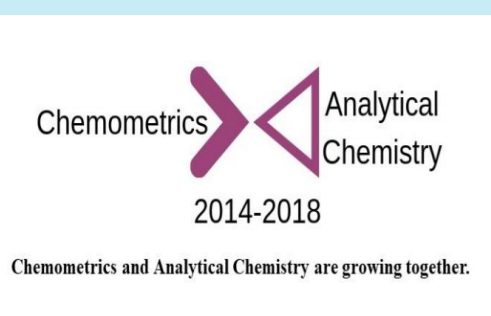
Published: April 25, 2019

Keywords:

1. chemometrics

2. analytical chemistry

ABSTRACT: A compilation of papers published between 2014 and 2018 was evaluated. Many papers related to multivariate calibration and classification have been reported, as well as, design of experiments applications and artificial intelligence methods. Some applications were highlighted, as medical and pharmaceutical, food analysis, fuels, biological and forensic for the chemometric techniques on this review. Most studies are related to developing methods for practical solutions in industry or routine analysis. A promising scenario is shown considering the number of published papers: a total of 832 for this period using the keywords, multivariate classification, multivariate calibration, analysis, chemometrics, prediction, analytical chemistry, artificial neural networks (ANN), design of experiments (DoE) and factorial design. An useful overview for Analytical Chemistry researchers' combined with Chemometrics is presented in this review.



CONTENTS

1. Introduction

2. Materials and methods

2.1. Medical and pharmaceutical applications

2.2 Food analysis

2.3 Fuel

3. Results and discussion

3.1 Biological samples

3.2 Food analysis

3.3 Forensic purposes

3.4 Fuels

4. Artificial intelligence methods for multiple questions

5. Design of Experiments (DoE) and response surface methodology (RSM)

6. Conclusions

7. Acknowledgments

8. References

1. Introduction

With the continuous technological progress of instrumental techniques for analytical purposes, multivariate methods applied to chemical data are mandatory in several applications. Chemometry is a prominent area dedicated to developing multivariate strategies for chemical data evaluation and interpretation^{1,2}. Figure 1 shows the main subjects related to Chemometric techniques according to the most repeated words in a bibliographic searching performed in Science Citation Index Expanded (SCI-E) in Clarivate Analytics' ISI – Web of Science[®], on June 21, 2018.



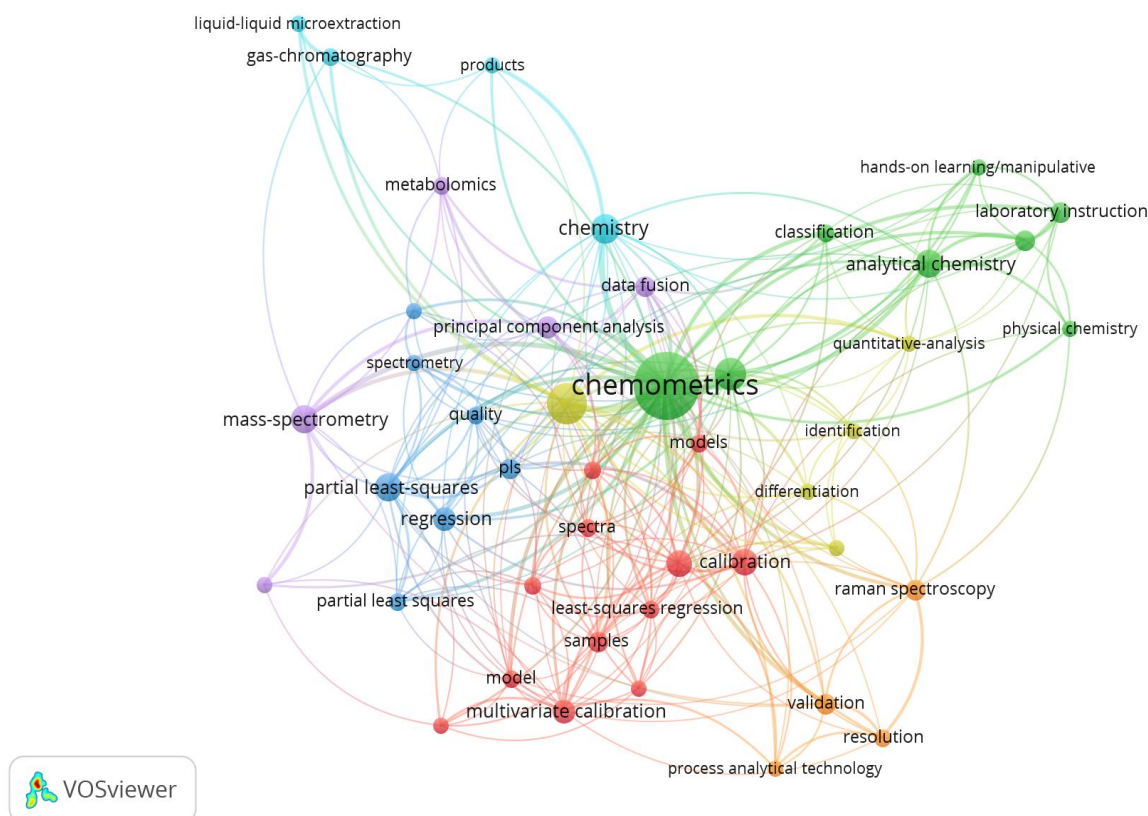


Figure 1. Bibliometric map generated using the more repeated keywords in the authors' search for the period 2014-2018.

The main topics revealed by the search can be verified in the color clusters of Figure 1, as follows: in green symbols classification and educational purposes (“hands-on-learning”, “laboratory instruction” as keywords), light blue circles denote chemistry and separation techniques (chromatography), purple circles represent sophisticated instrumentation as mass-spectrometry, metabolomics, and principal component analysis (PCA), dark blue symbols are related to regression and quality control, as well as the red ones are linked to calibration models and spectral techniques, the process analytical technology (PAT) and identification/differentiation issues appear in the searching as orange and yellow circles, respectively. In the center of the clustering, chemometrics is surrounded by all those words and connected to analytical chemistry.

A total of 832 occurrences were reported by the authors' during the search. Most studies are related to published papers, followed by reviews and proceedings in minor scale. From this amount, studies involving multivariate classification as topic has 390 papers, multivariate calibration 209,

design of experiments (DoE) 136 and artificial neural networks (ANN) 97. It is clear that chemometrics and analytical chemistry are growing together, and the goal of this review was to make a concise compilation of representative studies for the area between 2014 and 2018. Several topics were discussed by using key papers mentioned along the text.

2. Materials and methods

2.1. Medical and pharmaceutical applications

The use of chemometrics to study multifunctional indole alkaloids from *Psychotria nemorosa* (Palicourea comb. nov.) was developed by Júnior *et al.*³. The techniques PCA, partial least squares (PLS) and orthogonal PLS1 (O-PLS1) were helpful for modelling the activities using ultra-high-performance liquid chromatography-diode array detector (UPLC-DAD) data as fingerprint³. Ultraviolet spectral data from monoclonal antibodies compounded into hospital pharmacy were evaluated to build models using PLS-discriminant analysis (PLS-DA). The

challenge was to identify the monoclonal antibodies after compounding and just before administration to the patient for quality control at the hospital⁴. The linear sweep voltammograms generated from integration of three commercial screen-printed electrodes into a voltammetry electronic tongue was combined with PLS to predict concentrations of cysteine, glutathione and homocysteine. The authors applied genetic algorithm and interval PLS (i-PLS) for selection of variables⁵. It was possible to monitor the extraction of indole alkaloids from the toad skin⁶ and the quantification of geniposide in *Gardenia jasminoides* fruit (Chinese medicinal herb)⁷ was performed using near infrared (NIR) spectroscopy and PLS regression (PLSR). The extraction of indole alkaloids from the toad skin showed a coefficient of determination (R^2) value of 0.99 and root mean square error of cross validation (RMSECV) of 8.26 mg mL⁻¹⁶ and the correlation values to quantify the concentration of geniposide in *Gardenia* were between 0.92 – 0.99 and 0.32 - 1.66 mg mL⁻¹ for RMSECV⁷. In order to evaluate the anti-inflammatory properties of extracts from Honeysuckle, Fourier Transform Infrared (FTIR) spectroscopy in combination with PLSR⁸ were used.

Junior *et al.*⁹ used NIR and performed a comparison between two multivariate calibration techniques, PLSR and multiple linear regression (MLR) to monitor the quality control of tablets, and the PLSR model present better results than MLR. Raman spectral imaging technique was also used to predict active ingredient pharmaceutical concentration in microtablets¹⁰, in oral suspensions¹¹, intravaginal rings¹², and in quantitative assessment of pharmaceutical tablets¹³. The PLSR and least squares-support vector machine (LS-SVM) models exhibited excellent prediction abilities for active pharmaceutical ingredient in microtablets with a correlation higher than 0.98 and root mean square error of prediction (RMSEP) of 2.35% (w/w) for PLSR and 2.09% (w/w) for LS-SVM¹⁰. Mazurek and Szostak¹¹, using PLSR model, obtained RMSE of calibration (RMSEC) from 1.59 to 2.92% for oral suspensions¹¹ and Lyndgaard *et al.*¹² achieved RMSECV of 1.82% (w/w) and correlation of 0.99 for intravaginal rings using PLSR model. Then, Sparén *et al.*¹³ in quantitative assessment of tablets obtained RMSE of prediction (RMSEP) from 0.54 to 3.04% (w/w). The ultraviolet visible (UV-Vis) spectroscopy and chemometric models also

allowed determination the presence of impurities in tablets¹⁴. Support vector regression (SVR) model was more accurate when compared to PLSR model with values for RMSEP between 0.18 – 0.27 µg mL⁻¹ while the values for PLSR were RMSEP from 0.27 to 0.30 µg mL⁻¹¹⁴. The synergy PLS (siPLS) model combined with FTIR showed the best results compared to the full spectrum PLS model for the quantification of active ingredient pharmaceutical in tablets which values highlight by authors was RMSECV of 15.28 mg g⁻¹ and R^2 of 0.99 for sulphamethoxazole and RMSECV of 7.52 mg g⁻¹ and correlation of 0.98 for trimethoprim¹⁵. Cantor *et al.*¹⁶ evaluated the ability of different analytical techniques such X ray diffraction, FTIR, Raman and NIR to detect melamine levels in gelatin (pharmaceutical component). The authors highlighted NIR technique and PLSR model that achieved the best results with RMSEP of 2.5% (w/w)¹⁶, besides to quantify the presence of melamine at levels as low as 1.0% (w/w).

The NIR spectroscopy and PLSR were used to determine protein nitrogen in yellow fever vaccine¹⁷. Haghghi, Hemmateenejad and Shamsipur¹⁸ using fluorescence spectroscopy and multivariate curve resolution alternative least square (MCR-ALS) were able to predict enantiomeric excess of some amino acids in frozen plasma which RMSEP values lower than 0.07% and R higher than 0.97. PLS was applied in NIR spectra to analyze the indicator of β -thalassemia in human hemolysate samples¹⁹. FTIR and multivariate calibration method were used to identify three group of clinical bacterial pathogens in human serum²⁰. Both models, PCA and PLS-DA, revealing a feasible tool for discrimination of the samples with percent accuracy of 100%²⁰.

2.2 Food analysis

NIR and PLSR were used to measure both physicochemical²¹ and the antioxidant properties of honey²², as well to detect and to quantify adulterant in honey samples of stingless bees²³. The PLSR model presented a RMSECV between 0.008 – 1.47 and correlation values from 0.90 to 0.98 for physicochemical properties²¹, while the antioxidant properties of honeys from different botanical origin showed high correlation varying from of 0.95-0.96 and RMSECV range from 0.92 to 13.60²². Se *et al.*²³ obtained values for prediction of adulteration in honey samples of stingless bees

with relative errors up 0.58 to 1.49%. The three-dimensional fluorescence spectroscopy technique combined with multivariate calibration was also used for detecting the presence of adulterants in honey²⁴.

A near infrared hyperspectral imaging system was used for predicting viability and vigor in muskmelon seeds using PLS-DA. Variable selection methods, such as variable important projection (VIP), selectivity ratio (SR) and significance multivariate correlation (sMC) were also applied to select the most effective wavelengths²⁵.

In order to determine oxidation parameters in frying canola oil, Talpur *et al.*²⁶ employed FTIR technique and PLSR model, while Uncu and Ozen²⁷ studied various chemical parameters in olive oils and Wu *et al.* evaluated rapeseed oil adulteration²⁸. NIR and PLSR models were also used to study oxidation of edible oils²⁹, to detect adulteration in extra virgin olive oils³⁰, and to monitor vegetable oils quality³¹. The fluorescence spectroscopy and different multivariate calibration methods, PLSR, PCR and MLR were applied for detection of adulteration of sesame oil. The best results highlighted by the authors were using the PLSR model which figures of merit were RMSECV of 0.65 for 80 nm wavelength intervals³².

The applicability of FTIR was used as tool to determine of total sugar content in soy-based drinks³³ and for measuring the concentration of nutrients in grapevine petioles³⁴. For the soy-based drinks, two models were applied for different spectral band: (1) iPLS and (2) siPLS, and both presented high coefficient of correlation (R) (0.98).

Milk samples were evaluated using NIR and PLS-DA to detect contamination by *Salmonella*³⁵. Mid-infrared (MIR) spectroscopy and PLSR were applied for determining the residues of tetracycline in cow's milk³⁶ and for detecting and quantifying the adulteration in milk powder³⁷. Augusto *et al.* used laser-induced breakdown spectroscopy (LIBS) data and PLSR model for the direct determination of mineral elements, such as Ca, K and Mg in powdered milk and dietary supplements³⁸.

2.3 Fuel

Data acquired using C-13 nuclear magnetic resonance (NMR) spectroscopy were evaluated using SVR with variable selection by genetic

algorithm (GA) to determine the contents of saturated, aromatic, and polar compounds in crude oil. The use of small amounts of samples was highlighted by the authors³⁹. Sulfur content in petroleum derivatives was determined using MIR spectroscopy and PLS in association with variable selection methods, among them iPLS, siPLS, uninformative variable elimination (UVE), and GA⁴⁰. The UV spectroscopy integrated different chemometric strategies for quantifying the hydrocarbon contents in fuel oil samples⁴¹.

In order to quantify the presence of adulterants in gasoline, Raman spectroscopy was used, and calibration models were constructed using PLSR, iPLS and PLS-GA which correlations were between 0.80 and 0.99⁴². Gas chromatography data were used to build a PLSR model for quality assessment of gasoline, and low errors from 0.005 to 0.010% were obtained⁴³. Dadson, Pandam and Asiedu evaluated adulterants in gasoline, such as kerosene, diesel, naphta using a multivariate model with FTIR data and PLSR⁴⁴. Mabood *et al.*⁴⁵ also applied PLSR model to detect and estimate gasoline adulteration by NIR spectroscopy.

3. Results and discussion

3.1 Biological samples

Neves *et al.*⁴⁶ used mass spectrometry coupled with PCA, GA with support vector machine (SVM), linear discriminant analysis (LDA) and quadratic discriminant analysis (QDA) as an untargeted lipidomic approach to classify 76 blood plasma samples into negative for intraepithelial lesion or malignancy and squamous intraepithelial lesion. The PCA-SVM models provided the best classification results, achieving values of 80% and 83% for the sensitivity and specificity, respectively. Santos *et al.*⁴⁷ proposed a method to determine 11 polycyclic aromatic hydrocarbons (PAHs) in urine samples based on the coupling of a programmed temperature vaporizer (PTV) with a quadrupole mass spectrometer (qMS) instrument, via a deactivated fused silica tubing. The authors used PLS-DA, LDA, soft independent modeling of class analogy (SIMCA) and SVM to classify the samples according to the presence or absence of the PAHs. Gilany *et al.*⁴⁸ investigated untargeted metabolomic profiling of the seminal plasma in non-obstructive azoospermia men using gas chromatography-mass spectrometry (GC-MS) and QDA chemometric technique to implement on total

ion chromatograms for identification of discriminatory retention times. The receiver operating characteristic (ROC) curves for these classification models presented 88% of accuracy for the discrimination of 36 metabolites that may be considered discriminatory biomarkers for different groups in non-obstructive azoospermia. Boll *et al.*⁴⁹ developed a method using attenuated total reflection (ATR) FTIR spectroscopy combined with PLS-DA model that allowed the discrimination between dyed and non-dyed hair of 380 hair samples. Monakhova, Diehl and Fareed⁵⁰ used PCA, factor discriminant analysis (FDA), PLS-DA and LDA combined with high resolution (600 MHz) NMR spectroscopy data to distinguish 102 authentic samples of heparin and low-molecular weight heparins produced from porcine, bovine and ovine mucosal tissues as well as their blends.

3.2. Food analysis

Chen *et al.*⁵¹ detected 101 volatile compounds in 70 Chinese vinegars through GC-MS and used chemometric techniques such as clusters analysis, LDA, k nearest neighbor (kNN), GA-ANN to classify these compounds. Giannetti *et al.*⁵² evaluated flavor composition of apple cultivars grown in the Northeast Italy through different cultivation forms. The authors used head space-solid phase micro extraction/gas chromatography mass spectrometry (HS-SPME/GC-MS) for the analysis of volatile fraction and PLS-DA model to classify 42 apples varieties. The HS-SPME/GC-MS technique identified 118 volatile compounds and the PLS-DA model classified apples based on their different geographical origin or growing conditions, providing accuracy of 88-100%. Cuevas *et al.*⁵³ applied data fusion (mid-level) using high-performance liquid chromatography high resolution mass spectrometric (HPLC-HR-MS) and HS-SPME/GC-MS to obtain data sets and PLS-DA model for the discrimination between 19 samples of organic and conventional orange juices. The HPLC-HR-MS and HS-SPME/GC-MS techniques identified some flavonoids, fatty acids, aldehydes and esters as potential markers involved in the discrimination of organic juices. Wen *et al.*⁵⁴ characterized the phenolic and proline profiles of four types of unifloral honey collected from beekeepers in China. LDA results showed overall accuracy of 99% and 94% in correct classification of differentiate the floral origin of four Chinese

honeys. Portarena, Baldacchini and Brugnoli⁵⁵ proposed a method to discriminate 38 extra-virgin olive oils from seven regions along the Italian coasts from determination of the isotopic composition and the carotenoid contents. The authors used isotope ratio mass spectrometry (IRMS) and resonant Raman spectroscopy (RRS) to determine isotopic composition and the carotenoid contents, respectively. The LDA model presented 50 – 100% of correct classification for the seven regions, achieving 82% of accuracy for validation set.

Márquez *et al.*⁵⁶ used NIR and FT-Raman data to perform the data fusion in mid and high-level using SIMCA model for classifying the unadulterated and adulterated hazelnut samples. Rodrigues Júnior *et al.*⁵⁷ applied PLS-DA for discrimination of lactose-free samples and classification of adulterated and unadulterated milk powder samples by FT-Raman spectroscopy. Wakholi *et al.*⁵⁸ used short-wave IR (SWIR) hyperspectral imaging coupled with LDA, PLS-DA and SVM models for classification of corn seeds viable (control group) and corn seeds non-viable (microwave treated). The authors used a total of 200 samples of each type of corn: white, yellow and purple. Sandasi *et al.*⁵⁹ applied a fast and non-destructive method for the quality control of herbal tea blends. The authors used hyperspectral images obtained from SWIR combined with PLS-DA to classify herbal tea blends of the species *Sceletium tortuosum* and *Cyclopia genistoides*.

Kimuli *et al.*⁶⁰ also used SWIR hyperspectral imaging system (1000 – 2500 nm) to detect aflatoxin B₁ combined with PCA, PLS-DA and FDA techniques to explore and classify maize kernels of four varieties from different States of the USA. Cortés *et al.*⁶¹ discriminated two nectarine varieties in different spectral ranges of NIR and Vis-NIR using PLS-DA and LDA models. Shrestha *et al.*⁶² used NIR hyperspectral imaging data from 975 to 2500 nm and PLS-DA to investigate seed quality parameters such as year of production and variety in tomato seed lots. Santos, Pereira-Filho and Colnago⁶³ applied ¹H time domain nuclear magnetic resonance (TD-NMR) combined with multivariate analysis for identifying and quantifying the adulteration in 78 samples of milk using whey, urea, hydrogen peroxide and synthetic material (urine or milk).

3.3 Forensic purposes

Chen *et al.*⁶⁴ used NIR combined with hierarchical cluster analysis (HCA), PLS-DA and SVM to authenticate stamps of 12 seals on a Chinese traditional painting. The results obtained were 93% and 100% of accuracy for the PLS-DA and SVM model in validation set, respectively. Oliveira *et al.*⁶⁵ discriminated banknotes authenticity of Brazilian Real (R\$ 20, R\$ 50 and R\$ 100) using a portable NIR spectrometer combined with SIMCA and successive projections algorithm-LDA (SPA-LDA) models. Martins *et al.*⁶⁶ proposed a method for direct analysis of seven whisky brands. The authors used UV-Vis spectroscopy combined with PLS-DA to classify 164 genuine and 73 false samples. The PLS-DA corrected classified 99% and 93% for genuine and false samples, respectively. Costa *et al.*⁶⁷ identified six polymers using different ratios of emission lines and molecular bands (C/H, C/C₂, C/N, C/O, H/C₂, H/N, H/O and O/N) obtained with LIBS. SIMCA and kNN models were computed using 477 samples divided between calibration and validation sets. Both models achieved accuracy of 98% (kNN) and 92% (SIMCA).

3.4 Fuels

Silva *et al.*⁶⁸ developed a method to classify gasoline according to its origin (Brazil, Venezuela and Peru), using IR spectroscopy and multivariate classification. A set of 126 gasoline samples: 56 Brazilian, 66 Venezuelan, and 4 Peruvian, was analyzed. The spectra were standardized using the direct standardization method achieving 100% of correct predictions. In another study, Silva *et al.*⁶⁹ proposed the use of IR spectroscopy and LDA and PLS-DA for classification of gasoline with or without dispersant and detergent additives in 125 samples. The authors selected the variables for the multivariate models using stepwise (SW), successive projections algorithm (SPA) and GA algorithms. Sinkov, Sandercock and Harynuk⁷⁰ developed PLS-DA and SIMCA models for classifying the levels of gasoline in casework arson samples based on GC-MS data.

4. Artificial intelligence methods for multiple questions

An interesting approach for ANN is to handle the samples more efficiently to achieve streamlined processes. Kovalishyn and Poda⁷¹ created a new variable selection method for ANN known as batch pruning algorithm (BPA), being faster and more efficient than traditional methods. ANN was used for Sobol sensitivity estimation⁷² evidencing as advantage, the reduction of computational costs. Still, Bian *et al.*⁷³ allied the advantages of linear and non-linear methods in a novel algorithm called the extreme learning machine (ELM) and compared with PCR, PLS, SVR and back propagation algorithm-ANN (BP-ANN) by three NIR spectral datasets: diesel fuel, ternary mixture and blood, showing that ELM presented the best performance in the spectral quantitative analysis of complex samples.

NIR spectra data acquired for beers from three types of fermentation was used to evaluate foam and color-related parameters⁷⁴, using a robotic pourer and chemical fingerprinting. Results from NIR were used to create PLS and ANN models to predict four parameters such as pH, alcohol, Brix and maximum volume of foam. The ANN was implemented using the Levenberg–Marquardt training algorithm, being able to create more accurate models than PLS⁷⁴. Oliveira *et al.*⁷⁵ determined protein concentration, foam stability, haze, color, total acidity (TA), alcohol content, and bitterness in Ale beers properties using UV-Vis spectra in combination with PCR and also with ANN models.

Many authors also compared ANN and other chemometric methods, such as studies of Das *et al.*⁷⁶ that modeled variations in sucrose, reducing and total sugar content due to water-deficit stress in rice leaves using Vis, NIR and SWIR spectroscopies. They tested the following multivariate techniques, ANN feed-forward model, multivariate adaptive regression splines (MARS), MLR, PLSR, random forest regression and SVM. The variables that affect the performance of ANNs and PLS for spectral interference correction are random noise level, intensity ratio, peak separation and wavelength shift. The results showed that ANNs and PLS are about equally as effective for spectral interference correction^{77,78}. A portable artificial olfaction system for real-time monitoring of black tea fermentation was developed, based on the combination of the kNN and adaptive boosting, namely kNN-AdaBoost with discrimination rate of 100% of correct predictions⁷⁹. The performance of decision tree, kNN, naive bayesian, SVM and ANN

for to classification of orange growing locations based on the NIR using data mining was evaluated⁸⁰. The experimental results showed that the juice NIR spectra is the most suitable dataset for identifying the orange growing locations, and the decision tree is the best and most stable classifier⁸⁰, with the average prediction rate of 97%.

In relation to herbal products, Wang *et al.*⁸¹ used LIBS combined with PCA and BP-ANN to classify Chinese herbal medicine with 99.9% classification accuracy of three types of herbal products, roots of *Angelica pubescens*, *Codonopsis pilosula*, and *Ligusticum wallichii*. The authors established⁸² quality control markers for Chinese herbal medicines using BP-ANN; and the study of Ding *et al.*⁸³ developed a method to improve the markers to Q-markers in Chinese herbal medicines quality management, using PLS-DA for screening analysis of the chemical markers and identification of herbal origin. The BP-ANN algorithm was used to clarify the non-linear relationship between the Q-markers and their integral anti-inflammation effect. Still in relation to herbal medicines, Ito *et al.*⁸⁴ developed a model based on an ANN to quantify proteolytic and amylolytic enzymes using UV-Vis spectra of diluted samples from a particular solid-state fermentation in wheat bran, soybean meal, type II wheat flour and sugarcane bagasse.

Li *et al.*⁸⁵ combined GA with ANN to determine the elements copper and vanadium in steel samples with satisfactory quantitative results. Zhang *et al.*⁸⁶ developed a method combining GA, PCA and ANN to select spectral segments from the original spectra to improve the LIBS performance and proved that use only a fixed-length segment appropriate provides better results than selecting the entire spectral range.

Gurbanov, Bilgin and Severcan⁸⁷ used ANN to evaluate the secondary structural variations in the diabetic kidney cell membrane proteins based in ATR-FTIR spectroscopy analyzing the effects of selenium on diabetes. Hasanjani and Sohrabi⁸⁸ used UV-Vis spectroscopic and back-propagation algorithm ANN to predict fluoxetine and sertraline in tablets. Guo *et al.*⁸⁹ developed a kinetic spectrofluorometric method for the analysis of sibutramine, indapamide, and hydrochlorothiazide, very common in weight-reducing health foods, and the data of the mixtures were processed by parallel factor analysis (PARAFAC), PLS, PCR and radial basis function-artificial neural network (RBF-ANN).

5. Design of Experiments (DoE) and response surface methodology (RSM)

Before the application of any analytical method, it is necessary to optimize some instrumental conditions, named variables. These variables can be related to sample preparation procedure, as volumes of reagents, pressure and temperature or instrumental parameters, as wavelength, power, among others. The goal in several cases is always related to obtain a condition with high analytical signal, signal-to-noise ratio (SNR), and signal-to-background (SBR). In addition, analysts can be also interested in analytical methods with low relative standard deviation, limits of detection, and quantification, and reduced cost per determination. In order to achieve these goals DoE can be applied in almost any type of problem⁹⁰⁻⁹².

DoE can be defined as a group of tools that applies statistical and mathematical knowledge to optimize a system. Several strategies can be used as central composite design (CCD)⁹³, Doehlert (DD)⁹⁴ and, Box-Behnken designs (BBD)⁹⁵. If the goal is only to identify the most important variables, full factorial⁹⁶ or fractional factorial⁹⁷ or Plackett-Burman⁹⁸ designs can be also applied. Figure 2 shows the several possibilities related to the application of DoE in any type of problem.

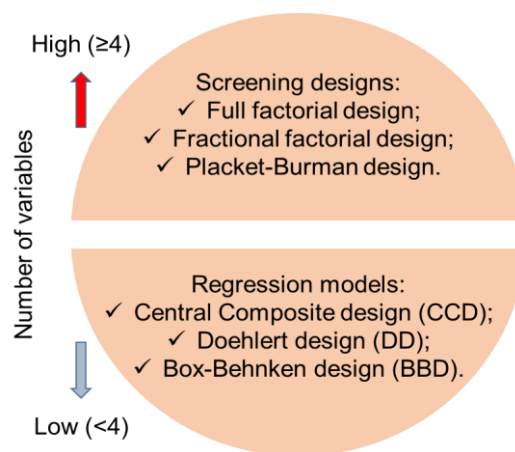


Figure 2. DoE characteristics for optimization.

The applicability and advantages of DoE in analytical chemistry are out of context and hundreds of studies can be easily searched in the scientific literature. In the time span selected for this review we found 125 papers using only the combination of the words “DoE”, “Factorial Design”, “Chemistry” and “Analytical chemistry”.

The scientific literature presents several reviews and tutorial reviews about the use of DoE^{90, 92}. In this case, the fundamentals about the use of DoE will be not discussed in this review, and only

applications will be described and discussed. Table 1 shows the main applications observed and several remarks.

Table 1. Selected analytical problems that applied DoE.

| Analytical chemistry type of application | Problems optimized | References |
|--|--|------------|
| Chromatography | <ul style="list-style-type: none"> - Matrix effects correction in liquid chromatography - Vitamin D3 determination - Synthesis of hydrogel - Single use bioreactors - Supercritical fluid | 99-103 |
| Environmental | <ul style="list-style-type: none"> - Determination of organic pollutants (β-cyclodextrin) - Occupational exposition analysis - NO₂ detection using Raman spectroscopy - N₂O and SF₆ determination - Cloud point extraction - N and S deposition - Cu detection in river water | 104-106 |
| Material | <ul style="list-style-type: none"> - Formation of Ca neptunatos - Signal processing in Raman - Steel production - Environmental aging simulation - Materials proposition for environmental analysis | 107,108 |
| Bioanalytical | <ul style="list-style-type: none"> - Protein translation - Seed growth | 109 |
| Pharmaceutical | <ul style="list-style-type: none"> - Biosensor development - Quantification of cefazolin - Drugs stability - Acetylcholinesterase determination | 110 |
| Electroanalytical | <ul style="list-style-type: none"> - Instrumental conditions of anodic stripping voltammetry for Cu²⁺ determination in water | 111 |
| Food | <ul style="list-style-type: none"> - Ascorbic acid determination - Food safety | 112 |
| NMR | <ul style="list-style-type: none"> - Metabolomics - <i>In vitro</i> mutagenicity | 113,114 |

6. Conclusions

According to authors' search of this review, the most developed methods combined with chemometrics is for food analysis, undoubtedly. In general, the goal of the studies was to improve speediness in the analysis and, to reduce the number of steps in the analytical method. Fuel samples were also a highlighted topic in analytical

chemistry. Sophisticated techniques considering mass spectrometry and chromatography allied to chemometrics have been increasing their applications in the area. Classification techniques have the majority of the papers, following by multivariate calibration, DoE and ANN. Chemometrics and analytical chemistry is a powerful combination to improve robustness, analytical frequency and practicality for methods.

7. Acknowledgements

The authors are grateful to the São Paulo Research Foundation (FAPESP grants number 2018/18212-8 and 2019/01102-8) and the National Council for Scientific and Technological Development (CNPq). This study was financed in part by the Coordination for the Improvement of Higher Education Personnel (CAPES) – Finance Code 001.

8. References

- [1] Olivieri, A. C., Introduction to multivariate calibration: A practical approach, Springer International Publishing, Switzerland, 1st ed., 2018, XVII-243. <https://doi.org/10.1007/978-3-319-97097-4>.
- [2] Lavine, B. K., Rayens, W. S., Classification: basic concepts, in: Brown, S. D., Tauler, R., Walczak, B. (Eds.), Comprehensive Chemometrics: Chemical and Biochemical Data Analysis, 3 Elsevier, Amsterdam, The Netherlands, (2009) 507-515.
- [3] Júnior, L. C. K., Viaene, J., Tuenter, E., Salton, J., Gasper, A. L., Apers, S., Andries, J. P. M., Pieters, L., Henriques, A. T., Heyden, Y. V., The use of chemometrics to study multifunctional indole alkaloids from *Psychotria nemorosa* (*Palicourea comb. nov.*). Part II: Indication of peaks related to the inhibition of butyrylcholinesterase and monoamine oxidase-A, *J. Chromatogr. A* 1463 (2016) 71-80. <https://doi.org/10.1016/j.chroma.2016.08.005>.
- [4] Jaccoulet, E., Boccard, J., Taverna, M., Azevedos, A. S., Rudaz, S., Smadja, C., High-throughput identification of monoclonal antibodies after compounding by UV spectroscopy coupled to chemometrics analysis, *Anal. Bioanal. Chem.* 408 (21) (2016) 5915-5924. <https://doi.org/10.1007/s00216-016-9708-4>.
- [5] Pedroza, R. H. P., Serrano, N., Diaz-Cruz, J. M., Arino, C., Esteban, M., Integration of Commercial screen-printed electrodes into a voltammetric electronic tongue for the analysis of aminothiols, *Electroanalysis* 28 (7) (2016) 1570-1577. <https://doi.org/10.1002/elan.201501112>.
- [6] Tao, L., Liu, B., Jin, Y., Sun, D., Liu, X., Chen, Y., Wu, Y., Characterization of Toad Skin for Traditional Chinese Medicine by Near-Infrared Spectroscopy and Chemometrics, *Anal. Lett.* 50 (8) (2017) 1292-1306. <https://doi.org/10.1080/00032719.2016.1220562>.
- [7] Li, J., Xu, B., Zhang, Y., Dai, S., Sun, F., Shi, X., Qiao, Y., Determination of Geniposide in *Gardenia jasminoides* Ellis fruit by near-infrared spectroscopy and chemometrics, *Anal. Lett.* 49 (13) (2016) 2063-2076. <https://doi.org/10.1080/00032719.2015.1130714>.
- [8] Langerodi, R. N., Ortmann, S., Wenzig, E. M. P., Bochkov, V., Zhao, Y. M., Miao, J. H., Saukel, J., Ladurner, A., Heiss, E. H., Dirsch, V. M., Bauer, R., Atanasov A. G., Assessment of anti-inflammatory properties of extracts from Honeysuckle (*Lonicera* sp. L., *Caprifoliaceae*) by ATR-FTIR spectroscopy, *Talanta* 175 (2017) 264-272. <https://doi.org/10.1016/j.talanta.2017.07.045>.
- [9] Junior, S. G., França, L. M., Pimentel, M. F., Albuquerque, M. M., Santana, D. P., Santana, A. K. M., Souza, J. A. L., Simões, S. S., A process analytical technology approach for the production of fixed-dose combination tablets of zidovudine and lamivudine using near infrared spectroscopy and chemical images, *Microchem. J.* 118 (2015) 252-258. <https://doi.org/10.1016/j.microc.2014.07.009>.
- [10] Kandpal, L. M., Cho, B. K., Tewari, J., Gopinathan, N., Raman spectral imaging technique for API detection in pharmaceutical microtablets, *Sens. Actuators B: Chem.* 260 (2018) 213-222. <https://doi.org/10.1016/j.snb.2017.12.178>.
- [11] Mazurek, S., Szostak, R., Quantification of active ingredients in pharmaceutical suspensions by FT Raman spectroscopy, *Vib. Spectrosc.* 93 (2017) 57-64. <https://doi.org/10.1016/j.vibspec.2017.10.003>.
- [12] Lyndgaard, L. B., Spåberg, R., Gilmour, C., Lyndgaard, C. B., Van Den Berg, F., A process analytical approach for quality control of dapivirine in HIV preventive vaginal rings by Raman spectroscopy, *J. Raman Spectrosc.* 45 (2) (2014) 149-156. <https://doi.org/10.1002/jrs.4433>.
- [13] Sparén, A., Hartman, M., Fransson, M., Johansson, J., Svensson, O., Matrix effects in quantitative assessment of pharmaceutical tablets using transmission Raman and near-infrared (NIR) spectroscopy, *Appl. Spectrosc.* 69 (5) (2015) 580-589. <https://doi.org/10.1366/14-07645>.
- [14] Naguib, I. A., Abdelaleem, E. A., Draz, M. E., Zaazaa, H. E., Linear support vector regression and partial least squares chemometric models for determination of Hydrochlorothiazide and Benazepril hydrochloride in presence of related impurities: A comparative study, *Spectrochim. Acta Part A: Molecular and Biomolecular Spectroscopy* 130 (2014) 350-356. <https://doi.org/10.1016/j.saa.2014.04.024>.

- [15] da Silva, F. E. B., Flores, E. M. M., Parisotto, G., Müller, E. I., Ferrão, M. F., Green method by diffuse reflectance infrared spectroscopy and spectral region selection for the quantification of sulphamethoxazole and trimethoprim in pharmaceutical formulations, *An. Acad. Bras. Ciênc.* 88 (2016) 1-15. <https://doi.org/10.1590/0001-3765201620150057>.
- [16] Cantor, S. L., Gupta, A., Khan, M. A., Analytical methods for the evaluation of melamine contamination, *J. Pharm. Sci.* 103 (2) (2014) 539-544. <https://doi.org/10.1002/jps.23812>.
- [17] Dabkiewicz, V. E., Abrantes, S. M. P., Cassella, R. J., Development of a non-destructive method for determining protein nitrogen in a yellow fever vaccine by near infrared spectroscopy and multivariate calibration, *Spectrochim. Acta Part A: Molecular and Biomolecular Spectroscopy* 201 (2018) 170-177. <https://doi.org/10.1016/j.saa.2018.04.042>.
- [18] Haghighi, A. N., Hemmateenejad, B., Shamsipur, M., Determination of enantiomeric excess of some amino acids by second-order calibration of kinetic-fluorescence data, *Anal. Biochem.* 550 (2018) 15-26. <https://doi.org/10.1016/j.ab.2018.04.004>.
- [19] Chen, J., Peng, L., Han, Y., Yao, L., Zhang, J., Pan, T., A rapid quantification method for the screening indicator for β -thalassemia with near-infrared spectroscopy, *Spectrochim. Acta Part A: Molecular and Biomolecular Spectroscopy* 193 (2018) 499-506. <https://doi.org/10.1016/j.saa.2017.12.068>.
- [20] Lin, W., Chai, Q., Chen, X., Li, Y., Effective identification of clinical bacterial pathogens by Fourier transform near-infrared spectroscopy, In: *Proc - 2017 Chinese Autom. Congr. CAC* (2017) 4587-4592. <https://doi.org/10.1109/CAC.2017.8243589>.
- [21] Anguebes, F., Pat, L., Ali, B., Guerrero, A., Córdova, A. V., Abatal, M., Garduza, J. P., Application of multivariable analysis and FTIR-ATR spectroscopy to the prediction of properties in campeche honey, *J. Anal. Methods Chem.* 2016 (2016) 1-14. <https://doi.org/10.1155/2016/5427526>.
- [22] Tahir, H. E., Xiaobo, Z., Tinting, S., Jiyong, S., Mariod, A. A., Near-Infrared (NIR) spectroscopy for rapid measurement of antioxidant properties and discrimination of sudanese honeys from different botanical origin, *Food Anal. Methods* 9 (9) (2016) 2631-2641. <https://doi.org/10.1007/s12161-016-0453-2>.
- [23] Se, K. W., Ghoshal, S. K., Wahab, R. A., Ibrahim, R. K. R., Lani, M. N., A simple approach for rapid detection and quantification of adulterants in stingless bees (*Heterotrigona itama*) honey, *Food Res. Int.* 105 (2018) 453-460. <https://doi.org/10.1016/j.foodres.2017.11.012>.
- [24] Chen, Q., Qi, S., Li, H., Han, X., Ouyang, Q., Zhao, J., Determination of rice syrup adulterant concentration in honey using three-dimensional fluorescence spectra and multivariate calibrations, *Spectrochim. Acta Part A: Molecular and Biomolecular Spectroscopy* 131 (2014) 177-182. <https://doi.org/10.1016/j.saa.2014.04.071>.
- [25] Kandpal, L. M., Lohumi, S., Kim, M. S., Kang, J. S., Cho, B. K., Near-infrared hyperspectral imaging system coupled with multivariate methods to predict viability and vigor in muskmelon seeds, *Sens. Actuators B: Chem.* 229 (2016) 534-544. <https://doi.org/10.1016/j.snb.2016.02.015>.
- [26] Talpur, M. Y., Hassan, S. S., Sherazi, S. T. H., Mahesar, S. A., Kara, H., Kandhro, A. A., Sirajuddin., A simplified FTIR chemometric method for simultaneous determination of four oxidation parameters of frying canola oil, *Spectrochim. Acta - Part A* 149 (2015) 656-661. <https://doi.org/10.1016/j.saa.2015.04.098>.
- [27] Uncu, O., Ozen, B., Prediction of various chemical parameters of olive oils with Fourier transform infrared spectroscopy, *LWT - Food Sci. Technol.* 63 (2) (2015) 978-984. <https://doi.org/10.1016/j.lwt.2015.05.002>.
- [28] Wu, Z., Li, H., Tu, D., Application of Fourier transform infrared (FT-IR) spectroscopy combined with chemometrics for analysis of rapeseed oil adulterated with refining and purifying waste cooking oil, *Food Anal. Methods* 8 (10) (2015) 2581-2587. <https://doi.org/10.1007/s12161-015-0149-z>.
- [29] Wójcicki, K., Khmelinskii, I., Sikorski, M., Sikorska, E. Near and mid infrared spectroscopy and multivariate data analysis in studies of oxidation of edible oils, *Food Chem.* 187 (2015) 416-423. <https://doi.org/10.1016/j.foodchem.2015.04.046>.
- [30] De Luca, M., Restuccia, D., Lisa, M., Puoci, F., Ragno, G., Chemometric analysis for discrimination of extra virgin olive oils from whole and stoned olive pastes, *Food Chem.* 202 (2016) 432-437. <https://doi.org/10.1016/j.foodchem.2016.02.018>.
- [31] Moreira, S. A., Sarraguça, J., Saraiva, D. F., Carvalho, R., Lopes, J. A., Optimization of NIR spectroscopy based PLSR models for critical properties of vegetable oils used in biodiesel production, *Fuel* 150 (2015) 697-704. <https://doi.org/10.1016/j.fuel.2015.02.082>.
- [32] Temiz, H. T., Tamer, U., Berkkan, A., Boyaci, I. H., Synchronous fluorescence spectroscopy for

- determination of tahini adulteration, *Talanta* 167 (2017) 557-562. <https://doi.org/10.1016/j.talanta.2017.02.044>.
- [33] Rech, A. M., Weiler, F. H., Ferrão, M. F., Determination of total sugar content in soy-based drinks using infrared spectroscopy and chemometrics, *Food Anal. Methods* 11 (7) (2018) 1986-1993. <https://doi.org/10.1007/s12161-018-1170-9>.
- [34] Smith, J. P., Schmidtke, L. M., Müller, M. C., Holzappel, B. P., Measurement of the concentration of nutrients in grapevine petioles by attenuated total reflectance Fourier transform infrared spectroscopy and chemometrics, *Aust. J. Grape Wine Res.* 20 (2) (2014) 299-309. <https://doi.org/10.1111/ajgw.12072>.
- [35] Pereira, J. M., Leme, L. M., Perdoncini, M. R. F. G., Valderrama, P., Março, P. H., Fast Discrimination of milk contaminated with *Salmonella* sp. via near-infrared spectroscopy, *Food Anal. Methods* 11 (7) (2018) 1878-1885. <https://doi.org/10.1007/s12161-017-1090-0>.
- [36] Casarrubias-Torres, L. M., Meza-Márquez, O. G., Osorio-Revilla, G., Gallardo-Velazquez, T., Mid-infrared spectroscopy and multivariate analysis for determination of tetracycline residues in cow's milk, *Acta Vet. Brno.* 87 (2) (2018) 181-188. <https://doi.org/10.2754/avb201887020181>.
- [37] Carvalho, B. M. A., Carvalho, L. M., Coimbra, J. S. R., Minim, L. A., Barcellos, E. S., Júnior, W. F. S., Detmann, E., Carvalho, G. G. P., Rapid detection of whey in milk powder samples by spectrophotometric and multivariate calibration, *Food Chem.* 174 (2015) 1-7. <https://doi.org/10.1016/j.foodchem.2014.11.003>.
- [38] Santos, A. A., Barsanelli, P. L., Pereira, F. M. V., Pereira-Filho, E. R., Calibration strategies for the direct determination of Ca, K, and Mg in commercial samples of powdered milk and solid dietary supplements using laser-induced breakdown spectroscopy (LIBS), *Food Res Int.* 94 (2017) 72-78. <https://doi.org/10.1016/j.foodres.2017.01.027>.
- [39] Filgueiras, P. R., Portela, N. A., Silva, S. R. C., Castro, E. V. R., Oliveira, L. M. S. L., Dias, J. C. M., Neto, A. C., Romão, W., Poppi, R. J., Determination of saturates, aromatics, and polars in crude oil by c -13 nmr and support vector regression with variable selection by genetic algorithm, *Energy and Fuels* 30 (3) (2016) 1972-1978. <https://doi.org/10.1021/acs.energyfuels.5b02377>.
- [40] Rocha, J. T. C., Oliveira, L. M. S. L., Dias, J. C. M., Pinto, U. B., Marques, M. D. S. P., Oliveira, B. P., Filgueiras, P. R., Castro, E. V. R., Oliveira, M. A. L., Sulfur determination in brazilian petroleum fractions by mid-infrared and near-infrared spectroscopy and partial least squares associated with variable selection methods, *Energy and Fuels* 30 (1) (2016) 698-705. <https://doi.org/10.1021/acs.energyfuels.5b02463>.
- [41] Bian, X., Li, S., Lin, L., Tan, X., Fan, Q., Li, M., High and low frequency unfolded partial least squares regression based on empirical mode decomposition for quantitative analysis of fuel oil samples, *Anal. Chim. Acta* 925 (2016) 16-22. <https://doi.org/10.1016/j.aca.2016.04.029>.
- [42] Ardila, J. A., Luis, F., Soares, F., Antônio, M., Farias, S., Carneiro, R. L., Characterization of gasoline by Raman spectroscopy with chemometric analysis, *Anal. Lett.* 50 (7) (2017) 1126-1138. <https://doi.org/10.1080/00032719.2016.1210616>.
- [43] Parastar, H., Mostafapour, S., Azimi, G., Quality assessment of gasoline using comprehensive two-dimensional gas chromatography combined with unfolded partial least squares: A reliable approach for the detection of gasoline adulteration, *J. Sep. Sci.* 39 (2) (2016) 367-374. <https://doi.org/10.1002/jssc.201500720>.
- [44] Dadson, J., Pandam, S., Asiedu, N., Modeling the characteristics and quantification of adulterants in gasoline using FTIR spectroscopy and chemometric calibrations, *Cogent Chem.* 4 (1) (2018) 1-22. <https://doi.org/10.1080/23312009.2018.1482637>.
- [45] Mabood, F., Gilani, S. A., Albroumi, M., Alameru, S., Nabhani, M. M. O. A., Jabeen, F., Hussain, J., Al Harrasi, A., Boqué, R., Farooq, S., Hamaed, A. M., Naureen, Z., Khan, A., Hussain, Z., Detection and estimation of Super premium 95 gasoline adulteration with Premium 91 gasoline using new NIR spectroscopy combined with multivariate methods, *Fuel* 197 (2017) 388-396. <https://doi.org/10.1016/j.fuel.2017.02.041>.
- [46] Neves, A. C. O., Morais, C. L. M., Mendes, T. P. P., Vaz, B. G., Lima, K. M. G., Mass spectrometry and multivariate analysis to classify cervical intraepithelial neoplasia from blood plasma: an untargeted lipidomic study, *Sci. Rep.* 8 (2018) 3954-3963. <https://doi.org/10.1038/s41598-018-22317-6>.
- [47] Santos, P. M., Sánchez, M. N., Pavón, J. L. P., Cordero, B. M., Quantitative and qualitative analysis of polycyclic aromatic hydrocarbons in urine samples using a non-separative method based on mass spectrometry, *Talanta* 181 (2018) 373-379. <https://doi.org/10.1016/j.talanta.2018.01.032>.
- [48] Gilany, K., Mirzajani, F., Rezadoost, H., Sadeghi, M. R., Amini, M., Untargeted metabolomic profiling of seminal plasma in nonobstructive azoospermia men: A noninvasive detection of spermatogenesis, *Biomed.*

Chromatogr. 31 (2017) 1-10.
<https://doi.org/10.1002/bmc.3931>.

[49] Boll, M. S., Doty, K. C., Wickenheiser, R., Lednev, I. K., Differentiation of hair using ATR FT-IR spectroscopy: a statistical classification of dyed and non-dyed hairs, *Forensic Chem.* 6 (2017) 1-9.
<https://doi.org/10.1016/j.forc.2017.08.001>.

[50] Monakhova, Y. B., Diehl, B. W. K., Fareed, J., Authentication of animal origin of heparin and low molecular weight heparin including ovine, porcine and bovine species using 1D NMR spectroscopy and chemometric tools, *J. Pharm. Biomed. Anal.* 149 (2018) 114-119.
<https://doi.org/10.1016/j.jpba.2017.10.020>.

[51] Chen, Y., Bai, Y., Xu, N., Zhou, M., Li, D., Wang, C., Hu, Y., Classification of Chinese vinegars using optimized artificial neural networks by genetic algorithm and other discriminant techniques, *Food Anal. Methods* 10 (2017) 2646-2656.
<https://doi.org/10.1007/s12161-017-0829-y>.

[52] Giannetti, V., Mariani, M. B., M., Mannino, P., Marini, F., Volatile fraction analysis by HS-SPME/GC-MS and chemometric modeling for traceability of apples cultivated in the Northeast Italy, *Food Control* 78 (2017) 215-221.
<https://doi.org/10.1016/j.foodcont.2017.02.036>.

[53] Cuevas, F. J., Pereira-Caro, G., Moreno-Rojas, J. M., Muñoz-Redondo, J. M., Ruiz-Moreno, M. J., Assessment of premium organic orange juices authenticity using HPLC-HR-MS and HS-SPME-GC-MS combining data fusion and chemometrics, *Food Control* 82 (2017) 203-211.
<https://doi.org/10.1016/j.foodcont.2017.06.031>.

[54] Wen, Y.Q., Zhang, J., Li, Y., Chen, L., Zhao, W., Zhou, J., Jin, Y., Characterization of chinese unifloral honeys based on proline and phenolic content as markers of botanical origin, using multivariate analysis, *Molecules* 22 (2017) 735-746.
<https://doi.org/10.3390/molecules22050735>.

[55] Portarena, S., Baldacchini, C., Brugnoli, E., Geographical discrimination of extra-virgin olive oils from the Italian coasts by combining stable isotope data and carotenoid content within a multivariate analysis, *Food Chem.* 215 (2017) 1-6.
<https://doi.org/10.1016/j.foodchem.2016.07.135>.

[56] Márquez, C., López, M. I., Ruisánchez, I., Callao, M. P., FT-Raman and NIR spectroscopy data fusion strategy for multivariate qualitative analysis of food fraud, *Talanta* 161 (2016) 80-86.
<https://doi.org/10.1016/j.talanta.2016.08.003>.

[57] Rodrigues Júnior, P. H., Oliveira, K. S., Almeida, C. E. R., De Oliveira, L. F. C., Stephani, R., Pinto, M. S., Carvalho, A. F., Perrone, Í. T., FT-Raman and chemometric tools for rapid determination of quality parameters in milk powder: Classification of samples for the presence of lactose and fraud detection by addition of maltodextrin, *Food Chem.* 196 (2016) 584-588.
<https://doi.org/10.1016/j.foodchem.2015.09.055>.

[58] Wakholi, C., Kandpal, L. M., Lee, H., Bae, H., Park, E., Kim, M. S., Mo, C., Lee, W.-H., Cho, B.-K., Rapid assessment of corn seed viability using short wave infrared line-scan hyperspectral imaging and chemometrics, *Sens. Actuators B. Chem.* 255 (2018) 498-507.
<https://doi.org/10.1016/j.snb.2017.08.036>.

[59] Sandasi, M., Chen, W., Vermaak, I., Viljoen, A., Non-destructive quality assessment of herbal tea blends using hyperspectral imaging, *Phytochem. Lett.* 24 (2018) 94-101.
<https://doi.org/10.1016/j.phytol.2018.01.016>.

[60] Kimuli, D., Wang, W., Wang, W., Jiang, H., Zhao, X., Chu, X., Application of SWIR hyperspectral imaging and chemometrics for identification of aflatoxin B1 contaminated maize kernels, *Infrared Phys. Technol.* 89 (2018) 351-362.
<https://doi.org/10.1016/j.infrared.2018.01.026>.

[61] Cortés, V., Cubero, S., Aleixos, N., Blasco, J., Talens, P., Sweet and nonsweet taste discrimination of nectarines using visible and near-infrared spectroscopy, *Postharvest Biol. Technol.* 133 (2017) 113-120.
<https://doi.org/10.1016/j.postharvbio.2017.07.015>.

[62] Shrestha, S., Knapic, M., Zibrat, U., Deleuran, L. C., Gislum, R., Single seed near-infrared hyperspectral imaging in determining tomato (*Solanum lycopersicum* L.) seed quality in association with multivariate data analysis, *Sens. Actuators B Chem.* 237 (2016) 1027-1034.
<https://doi.org/10.1016/j.snb.2016.08.170>.

[63] Santos, P. M., Pereira-Filho, E. R., Colnago, L. A. Detection and quantification of milk adulteration using time domain nuclear magnetic resonance (TD-NMR), *Microchem. J.* 124 (2016) 15-19.
<https://doi.org/10.1016/j.microc.2015.07.013>.

[64] Chen, Z., Gu, A., Zhang, X., Zhang, Z., Authentication and inference of seal stamps on Chinese traditional painting by using multivariate classification and near-infrared spectroscopy, *Chemom. Intell. Lab. Syst.* 171 (2017) 226-233.
<https://doi.org/10.1016/j.chemolab.2017.10.017>.

[65] Oliveira, V. S., Honorato, R. S., Honorato, F. A., Pereira, C. F., Authenticity assessment of banknotes using portable near infrared spectrometer and

- chemometrics, *Forensic Sci. Int.* 286 (2018) 121-127. <https://doi.org/10.1016/j.forsciint.2018.03.001>.
- [66] Martins, A. R., Talhavini, M., Vieira, M. L., Zacca, J. J., Braga, J. W. B., Discrimination of whisky brands and counterfeit identification by UV-Vis spectroscopy and multivariate data analysis, *Food Chem.* 229 (2017) 142-151. <https://doi.org/10.1016/j.foodchem.2017.02.024>.
- [67] Costa, V. C., Aquino, F. W. B., Paranhos, C. M., Pereira-Filho, E. R., Identification and classification of polymer e-waste using laser-induced breakdown spectroscopy (LIBS) and chemometric tools, *Polym. Test.* 59 (2017) 390-395. <https://doi.org/10.1016/j.polymertesting.2017.02.017>.
- [68] Silva, N. C., Pimentel, M. F., Honorato, R. S., Talhavini, M., Maldaner, A. O., Honorato, F. A., Classification of Brazilian and foreign gasolines adulterated with alcohol using infrared spectroscopy, *Forensic Sci. Int.* 253 (2015) 33-42. <https://doi.org/10.1016/j.forsciint.2015.05.011>.
- [69] Silva, M. P. F., Rodrigues e Brito, L., Honorato, F. A., Paim, A. P. S., Pasquini, C., Pimentel, M. F., Classification of gasoline as with or without dispersant and detergent additives using infrared spectroscopy and multivariate classification, *Fuel* 116 (2014) 151-157. <https://doi.org/10.1016/j.fuel.2013.07.110>.
- [70] Sinkov, N. A., Sandercock, P. M. L., Harynyuk, J. J., Chemometric classification of casework arson samples based on gasoline content, *Forensic Sci. Int.* 235 (2014) 24-31. <https://doi.org/10.1016/j.forsciint.2013.11.014>.
- [71] Kovalishyn, V., Poda, G., Efficient variable selection batch pruning algorithm for artificial neural networks, *Chem. Intell. Lab. Syst.* 149 (2015) 10-16. <https://doi.org/10.1016/j.chemolab.2015.10.005>.
- [72] Li, S., Yang, B., Qi, F., Accelerate global sensitivity analysis using artificial neural network algorithm: Case studies for combustion kinetic model, *Combust. Flame* 168 (2016) 53-64. <https://doi.org/10.1016/j.combustflame.2016.03.028>.
- [73] Bian, X. H., Li, S. J., Fan, M. R., Guo, Y. G., Chang, N., Wang, J. J., Spectral quantitative analysis of complex samples based on the extreme learning machine, *Anal. Methods* 8 (23) (2016) 4674-4679. <https://doi.org/10.1039/C6AY00731G>.
- [74] Viejo, C. G., Fuentes, S., Torrico, D., Howell, K., Dunshea, F. R., Assessment of beer quality based on foamability and chemical composition using computer vision algorithms, near infrared spectroscopy and machine learning algorithms, *J. Sci. Food Agr.* 9 8 (2) (2018) 618-627. <https://doi.org/10.1002/jsfa.8506>.
- [75] Oliveira, H. C., Cunha, J. C. E., Rocha, J. C., Nunez, E. G. F., Rapid monitoring of beer-quality attributes based on UV-Vis spectral data, *Int. J. Food Prop.* 20 (2017) 1686-1699. <https://doi.org/10.1080/10942912.2017.1352602>.
- [76] Das, B., Sahoo, R. N., Pargal, S., Krishna, G., Verma, R., Chinnusamy, V., Sehgal, V. K., Gupta, V. K., Dash, S. K., Swain, P., Quantitative monitoring of sucrose, reducing sugar and total sugar dynamics for phenotyping of water-deficit stress tolerance in rice through spectroscopy and chemometrics, *Spectrochim. Acta Part A* 192 (2018) 41-51. <https://doi.org/10.1016/j.saa.2017.10.076>.
- [77] Li, Z., Zhang, X., Karanassios, V., Verification of the performance of artificial neural networks (ANNs) versus partial least squares (PLS) for spectral interference correction in optical emission spectrometry, *Proceedings of SPIE 9118, Independent Component Analyses, Compressive Sampling, Wavelets, Neural Net, Biosystems, and Nanoengineering XII*, 911812 (2014). <https://doi.org/10.1117/12.2050326>.
- [78] Li, Z., Zhang, X., Karanassios, V., How do artificial neural networks (ANNs) compare to partial least squares (PLS) for spectral interference correction in optical emission spectrometry? *Proc. SPIE 9496, Independent Component Analyses, Compressive Sampling, Large Data Analyses (LDA), Neural Networks, Biosystems, and Nanoengineering XIII*, 94960M (2015). <https://doi.org/10.1117/12.2177516>.
- [79] Li, H. H., Zhang, B., Hu, W. W., Liu, Y., Dong, C. W., Chen, Q. S., Monitoring black tea fermentation using a colorimetric sensor array-based artificial olfaction system, *J. Food Process. Pres.* 42 (1) (2018). <https://doi.org/10.1111/jfpp.13348>.
- [80] Dan, S. J., Yang, S. X., Tian, F. C., Den, L., Classification of orange growing locations based on the near-infrared spectroscopy using data mining, *Intell. Autom. Soft Co.* 22 (2) (2016) 229-236. <https://doi.org/10.1080/10798587.2015.1095474>.
- [81] Wang, J. M., Liao, X. Y., Zheng, P. C., Xue, S. W., Peng, R., Classification of Chinese herbal medicine by laser-induced breakdown spectroscopy with principal component analysis and artificial neural network, *Anal. Lett.* 51(4) (2018) 575-586. <https://doi.org/10.1080/00032719.2017.1340949>.
- [82] Wang, F., Wang, B., Wang, L., Xiong, Z. Y., Gao, W., Li, P., Li, H. J., Discovery of discriminatory quality control markers for Chinese herbal medicines and

related processed products by combination of chromatographic analysis and chemometrics methods: *Radix Scutellariae* as a case study, *J. Pharmaceut. Biomed.* 138 (2017) 70-79. <https://doi.org/10.1016/j.jpba.2017.02.004>.

[83] Ding, G. Y., Wang, Y. S., Liu, A. N., Hou, Y. Y., Zhang, T. J., Bai, G., Liu, C. X., From chemical markers to quality markers: an integrated approach of UPLC/Q-TOF, NIRS, and chemometrics for the quality assessment of honeysuckle buds, *RSC Adv.* 7 (36) (2017) 22034-22044. <https://doi.org/10.1039/C6RA28152D>.

[84] Ito, S., Barchi, A. C., Escaramboni, B., Neto, P. D., Herculano, R. D., Borges, F. A., Miranda, M. C. R., Nunez, E. G. F., UV/Vis spectroscopy combined with chemometrics for monitoring solid-state fermentation with *Rhizopus microsporus* var. *oligosporus*, *J. Chem. Technol. Biot.* 92 (10) (2017) 2563-2572. <https://doi.org/10.1002/jctb.5271>.

[85] Li, K. H., Guo, L. B., Li, J. M., Yang, X. Y., Yi, R. X., Li, X. Y., Lu, Y. F., Zeng, X. Y., Quantitative analysis of steel samples using laser-induced breakdown spectroscopy with an artificial neural network incorporating a genetic algorithm, *Appl. Optics* 56 (4) (2017) 935-941. <https://doi.org/10.1364/AO.56.000935>.

[86] Zhang, P., Sun, L. X., Kong, H. Y., Yu, H. B., Guo, M. T., Zeng, P., A method derived from genetic algorithm, principal component analysis and artificial neural networks to enhance classification capability of laser-induced breakdown spectroscopy, *Proc. SPIE* 10461, AOPC 2017: Optical Spectroscopy and Imaging, 1046107 (24 October 2017). <https://doi.org/10.1117/12.2281493>.

[87] Gurbanov, R., Bilgin, M., Severcan, F., Restoring effect of selenium on the molecular content, structure and fluidity of diabetic rat kidney brush border cell membrane, *Biochim. Biophys. Acta – Biomembr.* 1858 (4) (2016) 845-854. <https://doi.org/10.1016/j.bbmem.2016.02.001>.

[88] Akbari Hasanjani, H. R., Sohrabi, M. R., Artificial neural networks (ANN) for the simultaneous spectrophotometric determination of fluoxetine and sertraline in pharmaceutical formulations and biological fluid, *Iran J. Pharm. Res.* 16 (2) (2017) 478-489.

[89] Guo, Y., Ni, Y. N., Chen, J. F., Kokot, S., A kinetic spectrofluorometric method, aided by chemometrics, for the analysis of sibutramine, indapamide and hydrochlorothiazide compounds found in weight-reducing tonic samples, *Anal. Methods* 8 (1) (2016) 197-204. <https://doi.org/10.1039/C5AY02191J>.

[90] Leardi, R., Experimental design in chemistry: A tutorial, *Anal. Chim. Acta* 652 (2009) 161-172. <https://doi.org/10.1016/j.aca.2009.06.015>.

[91] Barros Neto, B., Scarminio, I. S., Bruns, R. E. Como fazer experimentos, Bookman: Porto Alegre, 2010.

[92] Pereira, F. M. V., Pereira-Filho, E. R., Aplicação de programa computacional livre em planejamento de experimentos: um tutorial, *Quim. Nova* 41 (2018) 1061-1071. <https://doi.org/10.21577/0100-4042.20170254>.

[93] Pereira Filho, E. R., Planejamento fatorial em química: maximizando a obtenção de resultados. Edufscar: São Carlos, 2015.

[94] Ferreira, S. L. C., Santos, W. N. L., Quintella, C. M., Barros Neto, B., Bosque-Sendra, J. M., Doehlert matrix: a chemometric tool for analytical chemistry – review, *Talanta* 63 (2004) 1061-1067. <https://doi.org/10.1016/j.talanta.2004.01.015>.

[95] Ferreira, S. L. C., Bruns, R. E., Ferreira, H. S., Matos, G. D., David, J. M., Brandão, G. C., da Silva, E. G. P., Portugal, L. A., dos Reis, P. S., Souza, A. S., dos Santos, W. N. L., Box-Behnken desing: an alternative for the optimization of analytical methods, *Anal. Chim. Acta* 597 (2007) 179-186. <https://doi.org/10.1016/j.aca.2007.07.011>.

[96] Ferreira, S. L. C., Introdução às técnicas de planejamento de experimentos. Vento Leste: Salvador, 2015.





[97] Teófilo, R. F., Ferreira, M. M. C., Quimiometria II: planilhas eletrônicas para cálculos de planejamentos experimentais, um tutorial, *Quim. Nova.* 29 (2006) 338-350. http://quimicanova.sbq.org.br/imagebank/pdf/Vol29No2_338_25-DV04378.pdf.

[98] Myers, R. H., Montgomery, D. C., Anderson-Cook, C. M., Response surface methodology: process and product optimization using designed experiments, Wiley: Hoboken, 2009.

[99] Hewavitharana, A. K., Abu Kassim, N. S., Shaw, P. N., Standard addition with internal standardization as an alternative to using stable isotope labelled internal standard to correct for matrix effects-comparison and validation using liquid chromatography – tandem mass spectrometric assay of vitamin D, *J. Chromatogr. A* 1553 (2018) 101-107. <https://doi.org/10.1016/j.chroma.2018.04.026>.

- [100] Andri, B., Dispas, A., Klinkenberg, R., Streeb, B., Marini, R. D., Ziemons, E., Hubert, P., Is supercritical fluid chromatography hyphenated to mass spectrometry suitable for the quality control of vitamin D3 oily formulations? *J. Chromatogr. A* 1515 (2017) 209-217. <https://doi.org/10.1016/j.chroma.2017.07.057>.
- [101] Finetti, C., Sola, L., Elliott, J., Chiari, M., Synthesis of hydrogel via click chemistry for DNA electrophoresis, *J. Chromatogr. A* 1513 (2017) 226-234. <https://doi.org/10.1016/j.chroma.2017.07.042>.
- [102] Doriva-Garcia, N., Bones, J., Monitoring leachables from single-use bioreactor bags for mammalian cell culture by dispersive liquid-liquid microextraction followed by ultra high performance liquid chromatography quadrupole time of flight mass spectrometry. *J. Chromatogr. A* 1512 (2017) 51-60. <https://doi.org/10.1016/j.chroma.2017.06.077>.
- [103] Zimmermann, A., Totoli, E. G., Fernandes, F. H. A., Salgado, H. R. N., An eco-friendly and low-cost method for the quantification of cefazolin sodium in powder for injectable solution using thin-layer chromatography assisted by digital images, *JPC-J. Planar Chromat.* 30 (2017) 285-290. <https://doi.org/10.1556/1006.2017.30.4.8>.
- [104] Risoluti, R., Materazzi, S., MicroNIR/Chemometrics assesment of occupational exposure to hydroxyurea, *Front. Chem.* 6 (2018) 1-9. <https://doi.org/10.3389/fchem.2018.00228>.
- [105] Dunst, K. J., Trzcinski, K., Scheibe, B., Study of the NO₂ sensing mechanism of PEDOT-RGO film using *in situ* Raman spectroscopy, *Sens. Actuator B-Chem.* 260 (2018) 1025-1033. <https://doi.org/10.1016/j.snb.2018.01.089>.
- [106] Hogmalm, K. J., Zack, T., Karlsson, A. K. O., Sjoqvist, A. S. L., Garbe-Schonberg, D., *In situ* Rb-Sr and K-Ca dating by LA-ICP-MS/MS: an evaluation of N₂O and SF₆ as reaction gases, *J. Anal. At. Spectrom.* 32 (2017) 305-313. <https://doi.org/10.1039/C6JA00362A>.
- [107] Fellhauer, D., Gaona, X., Rothe, J., Altmaier, M., Fanghanel, T., Neptunium(VI) solubility in alkaline CaCl₂ solutions: evidence for the formation of calcium neptunates Ca_x NpO_{3+x} (s,hyd), *Monatsh. Chem.* 149 (2018) 237-252. <https://doi.org/10.1007/s00706-017-2116-4>.
- [108] Wang, X., He, H., Fan, X. G., Tang, M., Signal processing method for Raman spectra based on matching pursuit, *Spectrosc. Spect. Anal.* 38 (2018) 93-98. [https://doi.org/10.3964/j.issn.1000-0593\(2018\)01-0093-06](https://doi.org/10.3964/j.issn.1000-0593(2018)01-0093-06).
- [109] Liu, T., Zhang, W. J., Zhang, Z., Chen, M. L., Wang, J. H., Qian, X. H., Qin, W. J., Sensitive western-blot analysis of azide-tagged protein post translation modifications using thermoresponsive polymer self-assembly, *Anal. Chem.* 90 (2018) 2186-2192. <https://doi.org/10.1021/acs.analchem.7b04531>.
- [110] Orihara, K., Hikichi, A., Arita, T., Muguruma, H., Yoshimi, Y., Heparin molecularly imprinted Polymer thin film on gold electrode by plasma-induced graft polymerization for label-free biosensor, *J. Pharmaceut. Biomed.* 151 (2018) 324-330. <https://doi.org/10.1016/j.jpba.2018.01.012>.
- [111] Cinti, S., Mazzaracchio, V., Orturk, G., Moscone, D., Arduini, F., A lab-on-a-tip approach to make electroanalysis user-friendly and decentralized: detection of copper ions in river water, *Anal. Chim. Acta* 1029 (2018) 1-7. <https://doi.org/10.1016/j.aca.2018.04.065>.
- [112] Coutinho, M. S., Morais, C. L. M., Neves, A. C. O., Menezes, F. G., Lima, K. M. G., J., Colorimetric determination of ascorbic acid based on its interfering effect in the enzymatic analysis of glucose: an approach using smartphone image analysis, *J. Braz. Chem. Soc.* 28 (2017) 2500-2505. <https://doi.org/10.21577/0103-5053.20170086>.
- [113] Sandusky, P. O., Introducing undergraduate students to metabolomics using a NMR-based analysis of coffee beans, *J. Chem. Educ.* 94 (2017) 1324-1328. <https://doi.org/10.1021/acs.jchemed.6b00559>.
- [114] Ayed, L., Bakir, K., Ben Mansour, H., Hammami, S., Cheref, A., Bakhrouf, A., *In vitro* mutagenicity, NMR metabolite characterization of azo and triphenylmethanes dyes by adherents bacteria and the role of the “can” adhesion gene in activated sludge, *Microb Pathog* 103 (2017) 29-39. <https://doi.org/10.1016/j.micpath.2016.12.016>.

Study of the colloidal stability and optical properties of sunscreen creams

Gustavo Pereira Saito¹, Mariana Bizari¹, Marco Aurélio Cebim¹, Marcos Antonio Correa², Miguel Jafelicci Junior¹, Marian Rosaly Davolos¹⁺

1 São Paulo State University (Unesp), Institute of Chemistry, 55 Prof. Francisco Degni St, Araraquara, São Paulo, Brazil

2 São Paulo State University (Unesp), Faculty of Pharmaceutical Sciences, Km 1 Araraquara-Jaú Hw, Araraquara, São Paulo, Brazil

+ Corresponding author: Marian Rosaly Davolos, phone: +55 16 3301-9634, email address: marian.davolos@unesp.br

ARTICLE INFO

Article history:

Received: September 06, 2018

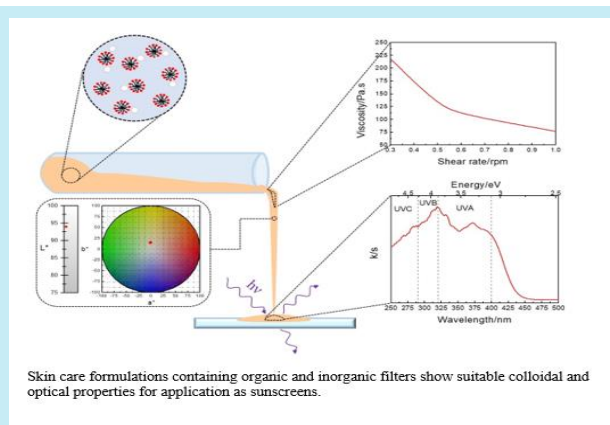
Accepted: January 29, 2019

Published: April 25, 2019

Keywords:

1. viscosity
2. colloidal stability
3. thixotropic fluid
4. optical absorption
5. UV protection

ABSTRACT: Sunscreen formulations containing inorganic/organic filters or mixture of them were synthesized by oil/water dispersion. The viscosity measurements show that sunscreen formulations are time-dependent non-newtonian fluids. In the CIELab color diagram, the white and/or beige colors presented by formulations do not compromise the aesthetics of the cosmetic product. UV-VIS absorption spectra show that sunscreen creams have high UV shielding ability, mainly the formulations containing inorganic and organic filters mixtures, which provide *in vitro* SPF and critical wavelength values recommended for UV protection.



1. Introduction

The excessive sun exposure causes cellular damage and immune system function modifications^{1,2}. These damaging biological effects are caused by ultraviolet radiation (UV), which is responsible for the photochemical reactions in the human organism. UV radiation may be subdivided into following regions: UVC (100-290 nm), UVB (290-320 nm) and UVA (320-400 nm)³. However, the solar UV radiation which reaches the earth's surface is commonly composed by a combination of UVB and UVA radiation⁴. UVB radiation, although restricted to penetration of the upper layers of the skin, causes sunburns and direct DNA damage via pyrimidine dimer formation⁵. While

the UVA radiation penetrates deeper into the skin causing photoaging, irregular pigmentation, immune system depression and gene modifications due mainly to the generation of reactive oxygen species by photosensitized oxidation⁶. Therefore, the sunscreen use to minimize the human health risks induced by UVB and UVA radiation exposure is very relevant⁷.

Sunscreens are skin care products whose main function is to protect the human skin from solar UV radiation⁸. Analyzing from physical-chemical point of view, sunscreens are colloidal systems containing emulsions and/or particle dispersions. Generally, these colloidal systems are constituted by hydrophilic (e.g. water), hydrophobic (e.g. emollients) and amphiphilic (e.g. surfactants)

compounds; therefore, sunscreens have suitable water-soluble and liposoluble properties to form films over the skin surface. Moreover, these properties provide sensory characteristics to sunscreens, which stimulate their use as skin cosmetics due to the facility of the cream removal with water and the skin hydration⁹.

Sunscreen application over human skin and the formation of the sunscreen film depend on their rheological properties, especially the colloidal stability. In this perspective, viscosity is an important property to evaluate the colloidal stability of sunscreens¹⁰, since it is directly associated to the surface interactions between sunscreen ingredients.

Inorganic and organic filters are sunscreen active ingredients¹¹, i.e., the compounds responsible to the UV photoprotection of the human skin. Among inorganic and organic commercial filters, zinc oxide, 1-(4-methoxyphenyl)-3-(4-tertbutylphenyl)propane-1,3-dione and hexyl 2-(4-diethylamino-2-hydroxybenzoyl)-benzoate have been widely used as broad spectrum filters in sunscreens due to their high UV shielding ability⁶.

Therefore, sunscreens must exhibit optical and rheological properties that allow photo-protective film formation on the human skin. In this perspective, the understanding of the intermolecular interactions between sunscreen ingredients, especially organic and inorganic filters, is very important for the development of stable and broad-spectrum sunscreens. In addition, the nature, amount and mixture of the filters directly influence optical and rheological properties of sunscreens due to the modification and/or formation of the new intermolecular interactions between their ingredients.

In the literature, several scientific publications show rheological and optical properties of sunscreen creams containing different and/or mixtures of sunscreen active ingredients^{10,12-18}. However, the understanding of possible surface interactions between sunscreen constituents that influence the colloidal stability, mechanical and optical properties of sunscreen creams require more detailed studies. Thus, this work aims to investigate the colloidal stability and mechanical properties of sunscreen formulations containing different and/or mixture of organic and inorganic filters using the viscosity measurements as parameter to evaluate the surface interactions between sunscreen ingredients. Moreover, the

optical properties of the sunscreen formulations were analyzed by UV-VIS spectrophotometric measurements to investigate sunscreen active ingredients interactions and potential UV shielding capacity of the sunscreen creams.

2. Materials and methods

2.1 Sunscreen formulations

Dipropan-2-yl hexanedioate (Dhymers), 2,3-dihydroxypropyl octadecanoate (Via Farma), mixture of hexadecan-1-ol and octadecan-1-ol (Cetostearyl alcohol, Via Farma), mixture of hexadecan-1-ol, octadecan-1-ol and oxirane (Cosmowax[®] J, Croda), (1-decanoyloxy-3-octanoyloxypropan-2-yl) dodecanoate (Via Farma), propane-1,2-diol (Qhemis), methyl 4-hydroxybenzoate (Synth), propyl 4-hydroxybenzoate (Synth), 2,2',2'',2'''-(1,2-Ethanediyldinitrilo)tetraacetic acid (Qhemis), 1-(4-methoxyphenyl)-3-(4-tertbutylphenyl)propane-1,3-dione (Eusolex[®] 9020, Merck) and hexyl 2-(4-diethylamino-2-hydroxybenzoyl)-benzoate (Uvinul[®] A Plus, BASF) and zinc oxide (ZnO, Sigma-Aldrich) were used without further purification. The quantities of sunscreen active ingredients used meet the standards established by the Brazilian Health Surveillance Agency¹⁹. The molecular structures of sunscreen ingredients are shown in the Fig. 1 and Fig. 2.

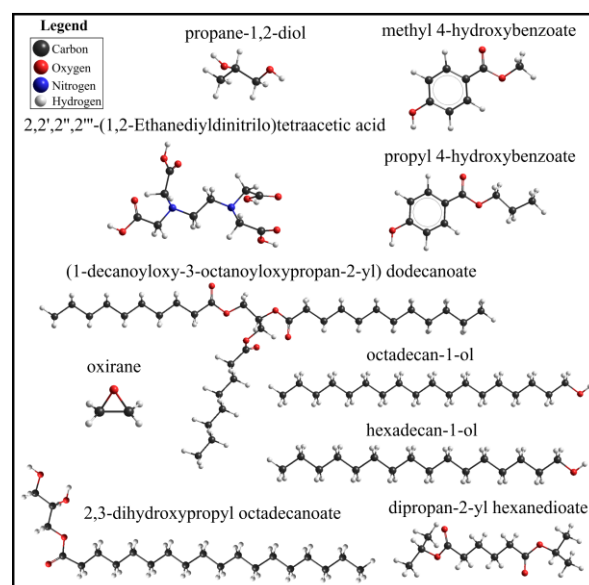


Figure 1. Molecular structures of sunscreen ingredients described in the Table 1.

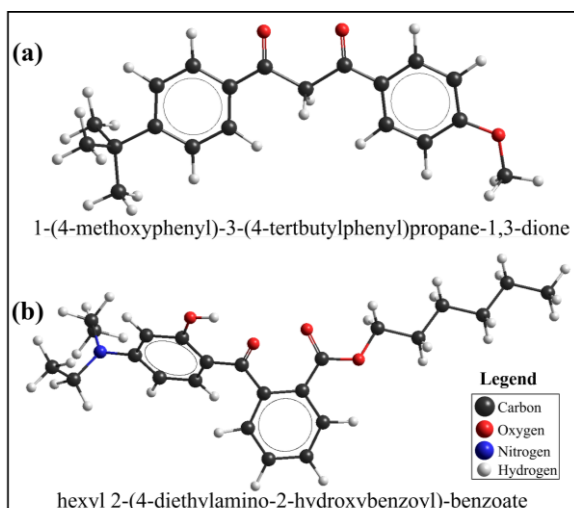


Figure 2. (a) Eusolex[®] 9020 and (b) Uvinul[®] A Plus molecular structures.

Table 1. Mass percentage of the ingredients of the sunscreen formulations containing different UV filters.

| Ingredients | Phase | Sunscreen formulations/% | | | |
|---|---------|--------------------------|-------|-------|-------|
| | | B | E | U | Z |
| Cetostearyl alcohol | Oil | 2.00 | 2.00 | 2.00 | 2.00 |
| 2,3-dihydroxypropyl octadecanoate | Oil | 2.00 | 2.00 | 2.00 | 2.00 |
| Cosmowax [®] J. | Oil | 8.00 | 8.00 | 8.00 | 8.00 |
| Dipropan-2-yl hexanedioate | Oil | 1.50 | 1.50 | 1.50 | 1.50 |
| (1-decanoyloxy-3-octanoyloxypropan-2-yl)dodecanoate | Oil | 1.50 | 1.50 | 1.50 | 1.50 |
| Uvinul [®] A Plus | Oil | - | - | 10.00 | - |
| Eusolex [®] 9020 | Oil | - | 5.00 | - | - |
| ZnO | Oil | - | - | - | 25.00 |
| Propane-1,2-diol | Aqueous | 4.00 | 4.00 | 4.00 | 4.00 |
| Methyl 4-hydroxybenzoate | Aqueous | 0.18 | 0.18 | 0.18 | 0.18 |
| Propyl 4-hydroxybenzoate | Aqueous | 0.02 | 0.02 | 0.02 | 0.02 |
| 2,2',2'',2'''-(1,2-Ethanediyldinitrilo)tetraacetic acid | Aqueous | 0.05 | 0.05 | 0.05 | 0.05 |
| Water | Aqueous | 80.75 | 75.75 | 70.75 | 55.75 |

Table 2. Mass percentage of the ingredients of the sunscreen formulations containing Uvinul[®] A Plus, ZnO or mixtures of them.

| Ingredients | Sunscreen formulations/% | | | | | | | | |
|----------------------------|--------------------------|-------|-------|-------|-------|-------|-------|-------|-------|
| | U1 | U2 | U3 | Z1 | Z2 | Z3 | UZ | UZ1 | UZ2 |
| Oil phase ingredients | 15.00 | 15.00 | 15.00 | 15.00 | 15.00 | 15.00 | 15.00 | 15.00 | 15.00 |
| Uvinul [®] A Plus | 5.00 | 2.50 | 1.00 | - | - | - | 10.00 | 5.00 | 1.00 |
| ZnO | - | - | - | 10.00 | 5.00 | 1.00 | 1.00 | 1.00 | 1.00 |
| Aqueous phase ingredients | 4.25 | 4.25 | 4.25 | 4.25 | 4.25 | 4.25 | 4.25 | 4.25 | 4.25 |
| Water | 75.75 | 78.25 | 79.75 | 70.75 | 75.75 | 79.75 | 69.75 | 74.75 | 78.75 |

2.2 Characterization techniques

The viscosity curves of sunscreen formulations were collected on a Brookfield rotational viscometer, model LVDV-E, equipped with a temperature control system (28-60 °C temperature range) using a cylindrical sample holder and No. 63

The sunscreen formulations were obtained by dispersion of the oil phase constituents (Table 1) under aqueous phase constituents (Table 1). The oil phase and aqueous phase ingredients were weighed and subjected to heating at 75 °C for 5 minutes.

Then, the oil phase was poured under the aqueous phase and the sunscreen cream obtained was kept under stirring for 1h. The mass percentage of the sunscreen ingredients and the respective sunscreen formulations are shown in Tables 1 and 2.

spindle (11 mm spindle diameter). Diffuse reflectance spectra of sunscreen formulations were recorded on a Cary spectrophotometer, model 500 UV-VIS-NIR, equipped with diffuse reflectance accessory. Color index was obtained in a Konica Minolta spectrophotometer, model CM-2500d, equipped with d/8° integrating sphere (CIELab

color space). The sun protection factor (SPF) of sunscreen formulations was obtained from diffuse reflectance relative measurements using the *in vitro* SPF assessment²⁰, which is defined by

$$\text{SPF} = \frac{\int_{290}^{400} E(\lambda)S(\lambda)d\lambda}{\int_{290}^{400} E(\lambda)S(\lambda)T(\lambda)d\lambda} \quad (1)$$

In the Eq. 1, the $T(\lambda)$ corresponds to the optical diffuse transmittance of sunscreen creams as a function of wavelength (λ) and the wavelength integration limits refers to the combined UVB and UVA wavelength range. $E(\lambda)$ is the erythema action spectrum and $S(\lambda)$ is the spectral irradiance of terrestrial sunlight under defined conditions by International Organization for Standardization²¹. The UVA protection of sunscreen creams was analyzed using the critical wavelength (λ_c), i.e., the wavelength value where the area under UV spectrum from 290 nm to a specific wavelength correspond to 90% of the integral of the absorption spectrum in the 290-400 nm region²².

3. Results and discussion

3.1 Colloidal stability

Viscosity is a physical property that provides important information about colloidal structure of various chemical systems, mainly emulsions and particle dispersions²³. Thus, viscosity can be used to evaluate colloidal stability of sunscreens. The viscosity-shear rate curves (Fig. 3) show that viscosity of the sunscreen formulations decreases as the shear rate increases. This viscoelastic behavior indicates that the viscosity decrease is a consequence of the changes in the relaxation properties of these colloidal systems due to the deformation of dispersed molecules and/or particles in determined shear flows²⁴. Therefore, the sunscreen formulations obtained are non-newtonian fluids.

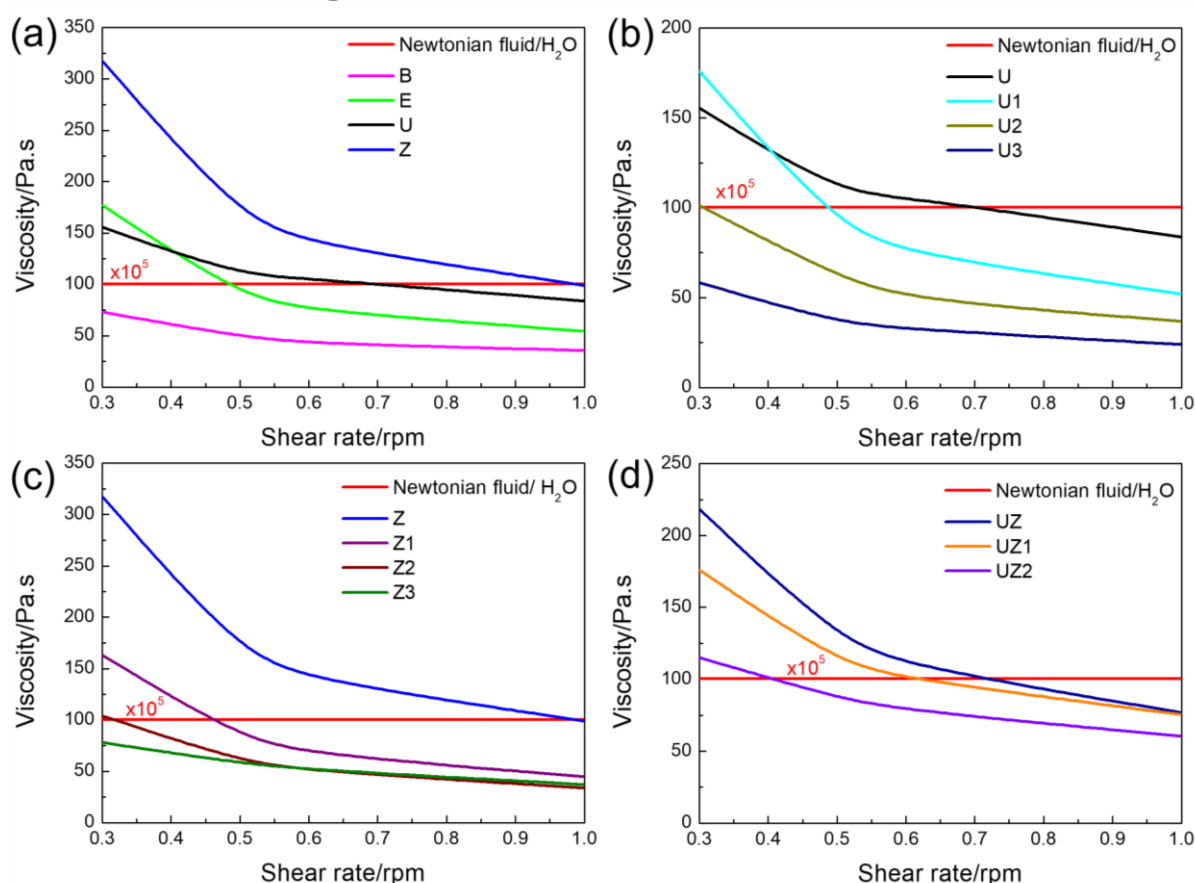


Figure 3. Viscosity-shear rate curves of sunscreen formulations containing different mass percentages of (a) sunscreen active ingredients, (b) Uvinul® A Plus, (c) ZnO and (d) mixture of Uvinul® A Plus and ZnO, as shown in Tables 1 and 2.

The inorganic or organic filter presence and/or their increase in the cosmetic formulations cause the viscosity increase; it is associated with interfacial structuring in sunscreen formulations that contributes significantly to the colloidal stability. Thus, the sunscreen active ingredients used and their amount present in formulations provide modifications in the colloidal stability due to the conformation, rearrangement and degree of interaction of these chemical compounds with the ingredients of the colloidal systems, especially with the surfactants^{25,26}. In sunscreen formulations, Cetostearyl alcohol, Cosmowax[®] J and 2,3-dihydroxypropyl octadecenoate compounds (Fig. 1) are the emulsifying agents or surfactants of these colloidal systems.

The sunscreen formulations containing ZnO have higher viscosity values when compared to the others. This fact indicates possible surface interactions of the zinc oxide with sunscreen ingredients and/or the formation of zinc oxide agglomerates. According to the literature, surface interactions between zinc oxide particles and ions or molecules depend on the surface charge of these particles, which is correlated with the pH of the particle dispersion²⁷. Moreover, particle

agglomeration in colloidal systems is associated to the ionic strength, the nature of the chemical environment and the morphological properties of the ZnO particles²⁸.

The viscosity-time curves under constant shear rate (Fig. 4) show that the viscosity of sunscreen formulations decreases as the measurement time increases. This rheological behavior exhibited indicates the formulations are thixotropic fluids, i.e., time-dependent non-newtonian fluids²⁹. Therefore, the creams have essential rheological characteristics for application as sunscreens because thixotropic fluids when subjected to an external force present viscosity decrease providing their application in the human skin. Moreover, the viscosity returns the initial state after the force removal allowing the formation of a photo-protective film on the skin surface.

Comparing the viscosity-time curves of B and E formulations to others, it is observed an initially viscosity increase in the 0-60 s time interval. This viscosity increase is associated to the interfacial region changes due to the deformation and reorganization of dispersed molecules in the interface^{24,29}, which provide specific viscoelastic properties for these colloidal systems.

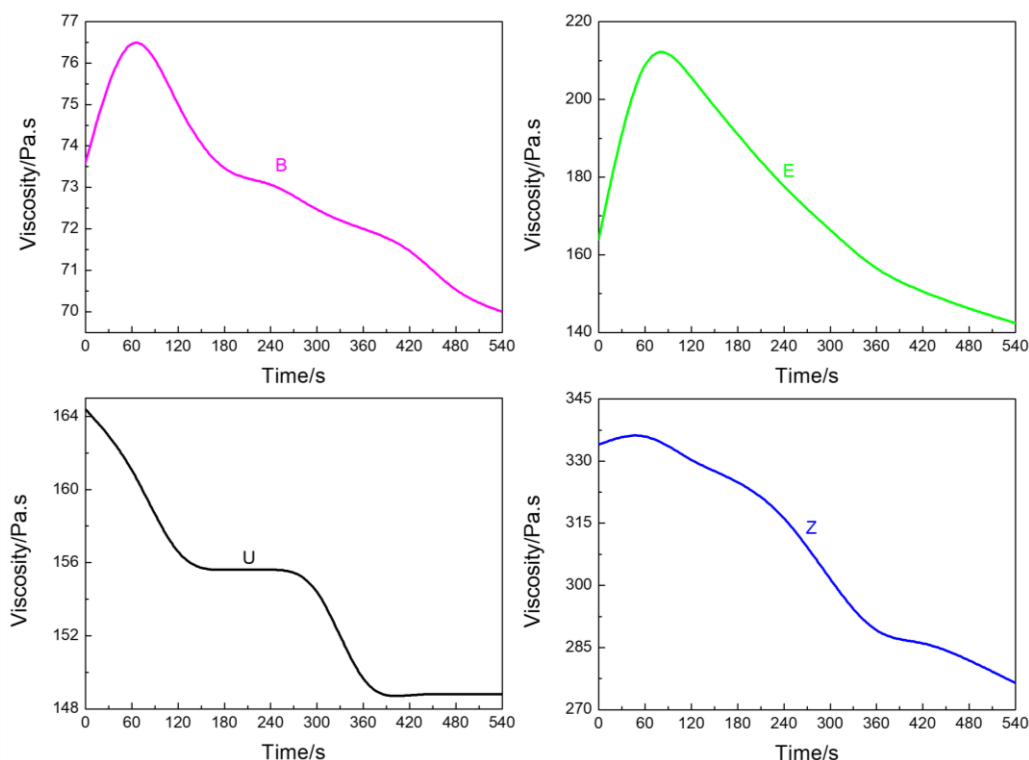


Figure 4. Viscosity-times curves of B, E, U and Z sunscreen formulations indicated in Tables 1 and 2.

The colloidal stability of sunscreen formulations depends on the interfacial structuring, which is maintained by surface interactions between sunscreen ingredients. Thus, the temperature variation changes the interfacial region promoting loss and/or gain of the colloidal stability; consequently, the sunscreen viscosities are modified. The Fig. 5 shows the temperature effect on the viscosity of the sunscreen creams.

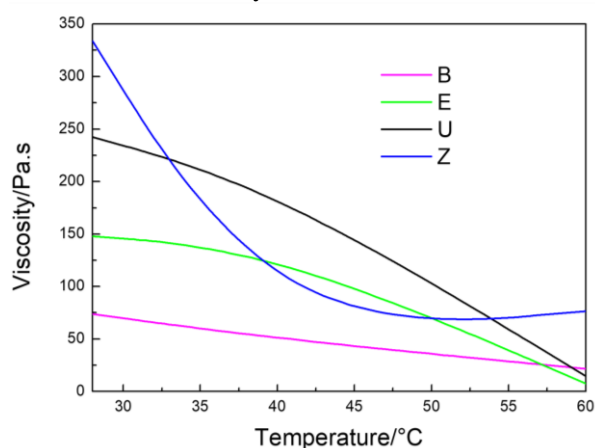


Figure 5. Viscosity-temperature curves of B, E, U and Z sunscreen formulations indicated in Tables 1 and 2.

In the temperature-viscosity curves, it is observed the viscosity decrease of the sunscreen formulations with the temperature increase. This viscosity decrease is attributed to the break of intermolecular interactions in the interfacial region, which provides the loss of the colloidal stability. In addition, the sunscreen formulation containing ZnO exhibits different rheological behavior compared to the other formulations in the 40-60 °C temperature range. This rheological behavior can be associated to the agglomeration and/or dispersion of the ZnO particles in the formulation.

The temperature-dependence of sunscreen viscosity can be correlated with the Arrhenius equation³⁰ according to Eq. 2:

$$\eta = \eta_0 e^{\left(\frac{E_a}{RT}\right)} \quad (2)$$

where η is the viscosity of formulations, η_0 is the empirical constant and E_a is the flow activation energy. The flow activation energy (E_a) is the potential energy barrier that interfacial molecules need to overcome in order to the fluid flow to occur; consequently, the E_a values show the degree

of the temperature-dependence of viscosity³¹. Thus, temperature-dependence of viscosity is small for viscous fluids that have low E_a values.

In this perspective, flow activation energy can be a parameter used to evaluate the temperature influence on the colloidal stability of sunscreen creams containing different UV filters. The flow activation energy values of the sunscreen formulations are shown in Table 3. Independent of sunscreen active ingredient used in the colloidal system, the experimental E_a values show that sunscreen creams have high temperature-dependence of their viscosity; therefore, the colloidal stability of them is directly affected by the temperature restricting their application as stable cosmetic cream in a temperature range. In addition, the flow active energy values presented by the sunscreen formulation containing ZnO show a non-newtonian rheological behavior in the investigated temperature range. Consequently, the difference of E_a values indicates that surface relaxations between zinc oxide and sunscreen ingredients medium depend on the temperature, giving rise to different interfacial structuring of the colloidal dispersion³².

Table 3. Flow activation energy (E_a) values of B, E, U and Z formulations.

| Sunscreen formulation | E_a / kJ mol ⁻¹ |
|-----------------------|---|
| B | 32.15 |
| E | 81.09 |
| U | 76.42 |
| Z | 121.19 ^a /17.00 ^b |

^a E_a value obtained in 28-40 °C temperature range.

^b E_a value obtained in 40-60 °C temperature range.

3.2 Optical properties

The diffuse reflectance spectra (Fig. 6) show that each sunscreen formulation has a specific visible light scattering (400-800 nm), which is associated to micellar structures formed and their size in the cosmetic cream; therefore, organic or inorganic filter used have significant contribution to the formation of the micellar structures. Moreover, the visible light scattering in the sunscreen formulations containing inorganic filter is also related to the ZnO particles depending on their size⁸.

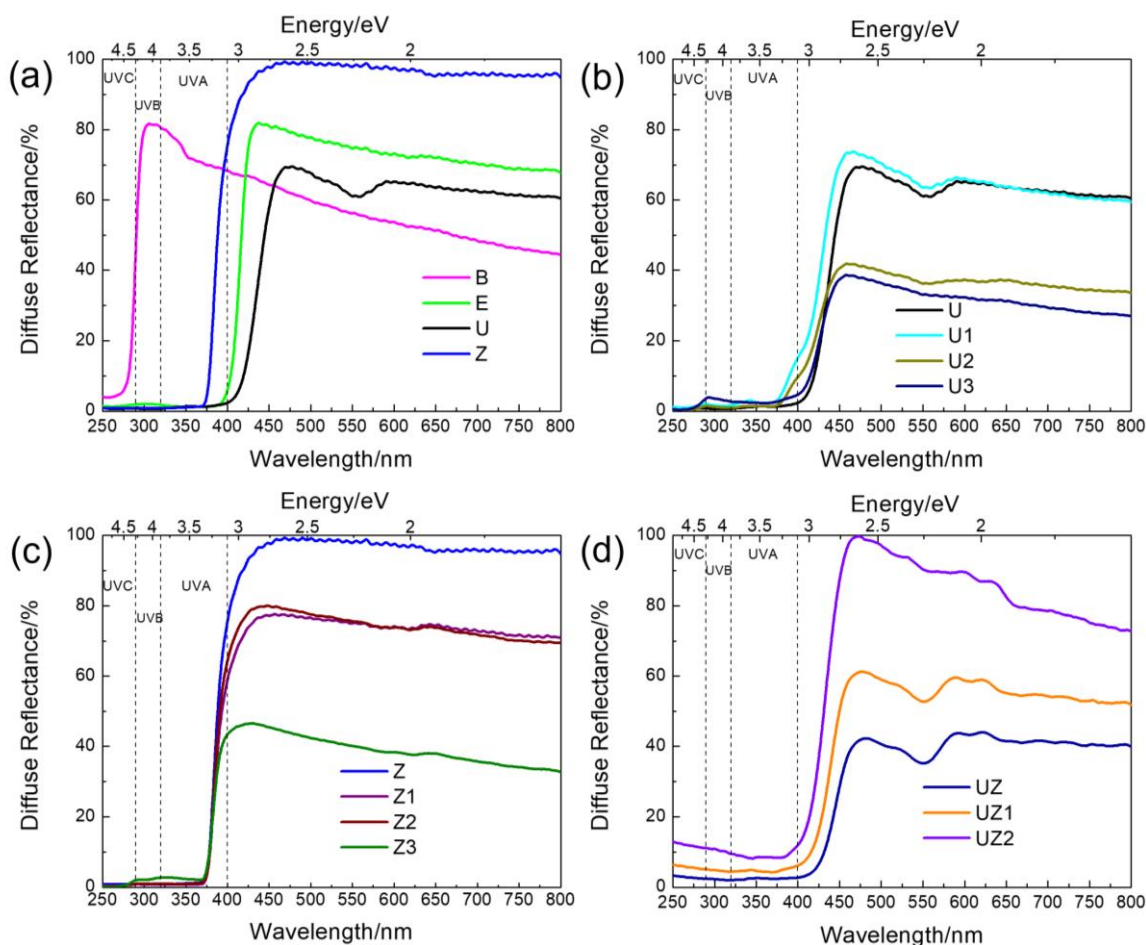


Figure 6. Diffuse reflectance spectra of the sunscreen formulations containing several mass percentages of (a) different UV filters, (b) Uvinul® A Plus, (c) ZnO and (d) mixture of Uvinul® A Plus and ZnO, as shown in Tables 1 and 2.

The UV-VIS absorption spectra of sunscreen formulations obtained by Kubelka-Munk equation³³ are shown in Fig. 7. In the absorption spectrum of the B cream (Fig. 7a), it is observed a broad and low intensity absorption band in the 250-290 nm region attributed to the $\pi \rightarrow \pi^*$ and/or $\eta \rightarrow \pi^*$ transitions³⁴ due to aromatic rings and/or carbonyl groups present in the molecular structures of sunscreen ingredients (Fig. 1). The absorption spectra of sunscreen formulations containing organic and inorganic filters or mixture of them (Fig. 7) show a typical band of sunscreen ingredients and characteristic absorption bands of the UV filters.

In the sunscreen creams containing organic filters (Fig. 7a and Fig. 7b), the broad absorption bands with maximum values at 312 and 370 nm are attributed to $\pi \rightarrow \pi^*$ and/or $\eta \rightarrow \pi^*$ transitions. These electronic transitions assigned are characteristics of the beta-diketones³⁵ and benzophenone-derived compounds³⁶, such as the Eusolex® and Uvinul® A Plus filters used in the sunscreen formulations. In

addition, the mass percentages variation of the Uvinul® A Plus causes absorption edge shifts and intensity modifications of these absorption bands probably due to the different micellar structures obtained, which provide energy changes in the frontier molecular orbitals of the organic filter.

The sunscreen creams containing inorganic filter (Fig. 7c) present a broad and high intensity absorption band in the 290-380 nm region attributed to VB \rightarrow CB transitions from the ZnO semiconductor⁸. In the sunscreen formulations containing mixtures of Uvinul® A Plus and ZnO (Fig. 7d), it is observed the enlargement, overlapping and displacement of the specific absorption bands of these UV filters when compared to the other formulations. Probably, this optical behavior is correlated to the interactions between Uvinul® A Plus and ZnO surface, which cause modifications in the energy levels of the organic filter and/or the formation of new molecular orbitals that give rise to different electronic transitions.

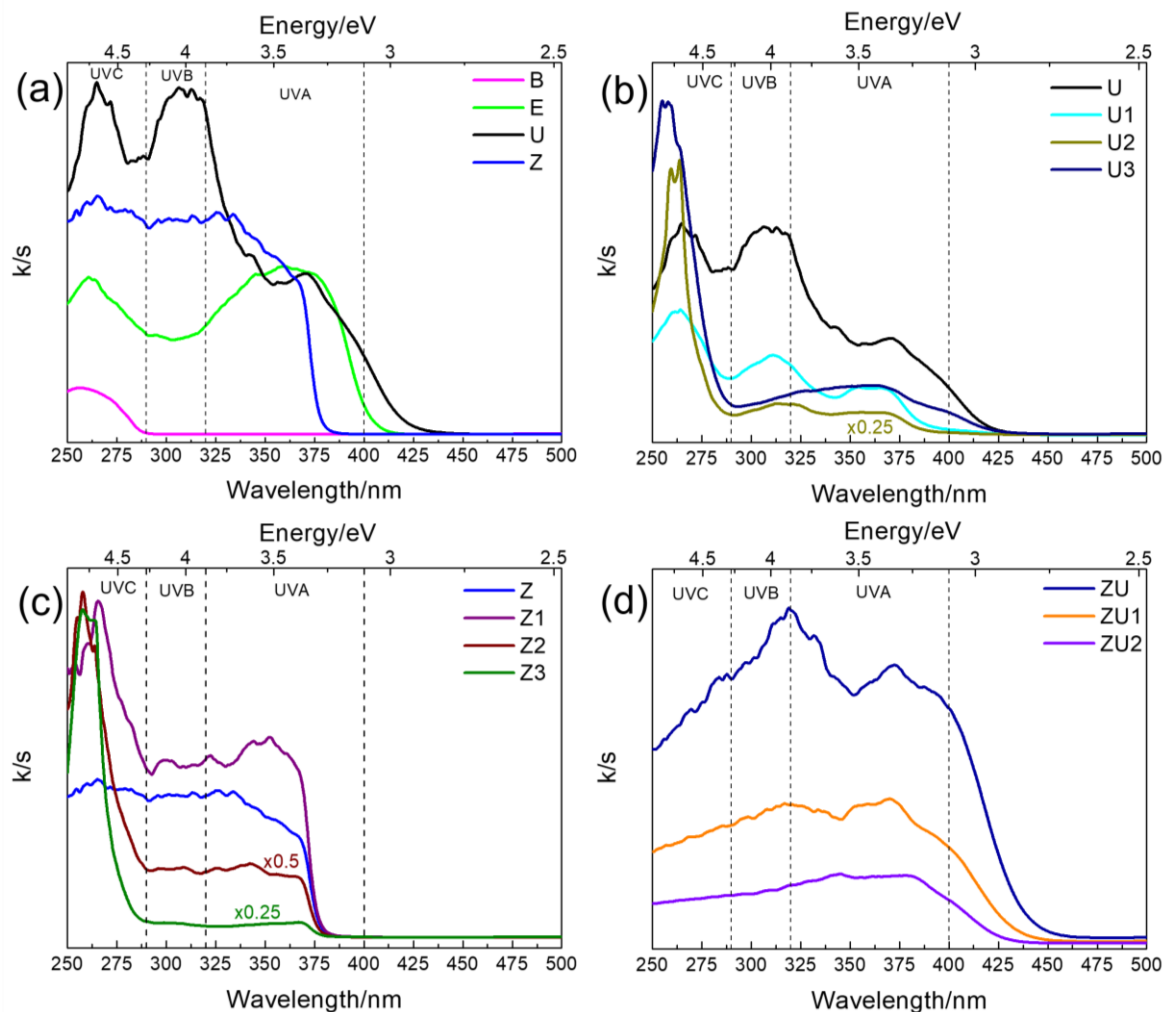


Figure 7. Absorption spectra of the sunscreen formulations containing several mass percentages of (a) different UV filters, (b) Uvinul® A Plus, (c) ZnO and (d) mixture of Uvinul® A Plus and ZnO, as shown in Tables 1 and 2.

The CIELab color diagram (Fig. 8) shows that sunscreen formulations are white or beige depending on the UV filter present in their composition; consequently, their colors do not compromise the desired aesthetics appearance for the cosmetic products.

The UV shielding performance of the skin care products was analyzed by *in vitro* sunscreen measurement methods³⁷, which are based on UV-VIS spectrophotometric measurements. Comparing the sun protection factor (SPF) and critical wavelength values (Fig. 9) of sunscreen creams with a commercial sunscreen product (SPF labelled equal to 10) and also comparing them to sunscreens described in the BASF sunscreen simulator³⁸, it is verified the *in vitro* method used shows coherent and satisfactory results allowing the evaluation of UV shielding capacity of sunscreen creams.

According to the literature³⁹, sunscreens that have SPF values ≤ 15 prevent skin damages caused by UVB radiation, moreover, critical wavelength values greater than 370 nm show that sunscreens have potential for UVA protection. Therefore, all sunscreen formulations obtained present UVB protection (Fig. 9), however, only formulations containing organic filter have potential UVA shielding capacity. In addition, UZ and UZ1 creams present better UV shielding ability when compared to the others due to synergistic effect from the mixture of ZnO and Uvinul® A Plus filters in specific mass percentages. This synergistic effect is probably associated to surface interactions between inorganic and organic filters, which are observed in the absorption spectra of these sunscreen creams (Fig. 7d).

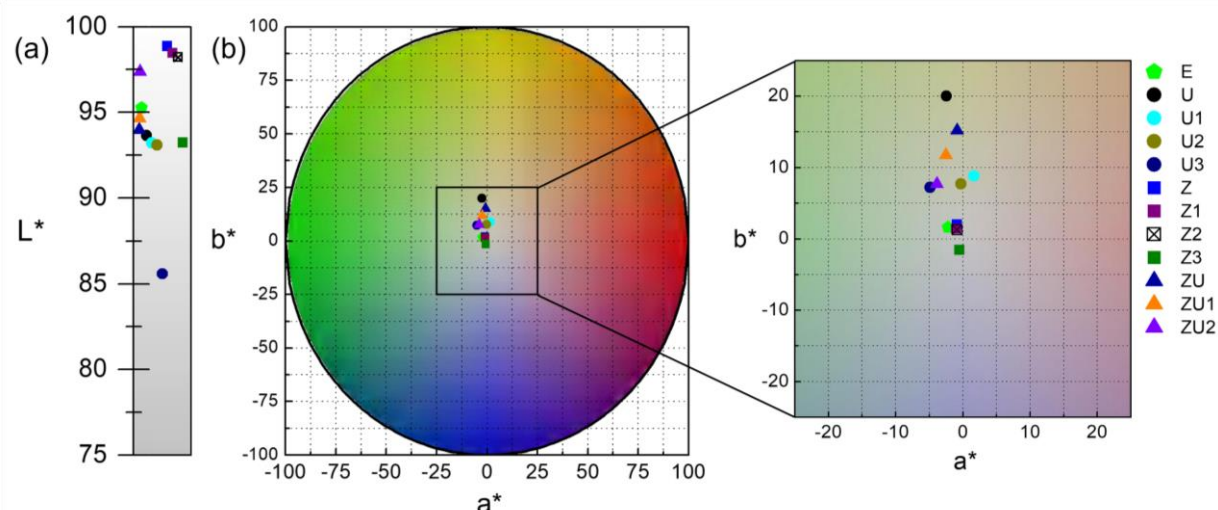


Figure 8. (a) Brightness scale and (b) color scale corresponding to the CIELab color diagram of sunscreen formulations described in Tables 1 and 2.

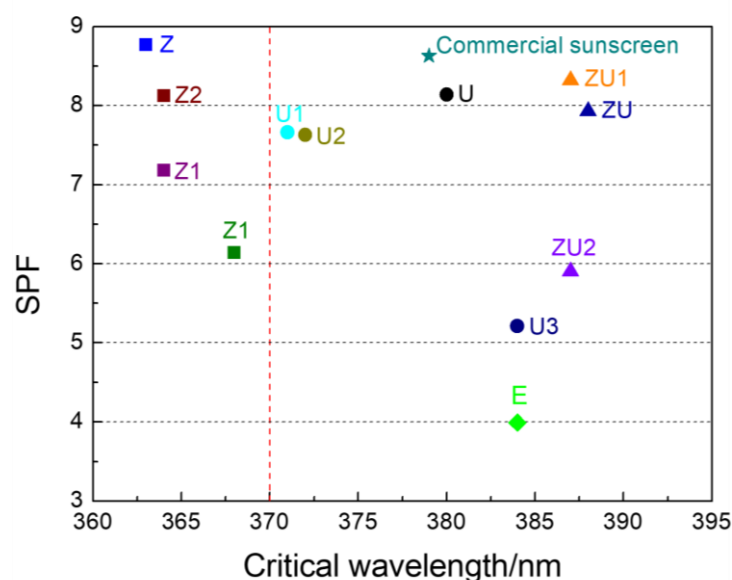


Figure 9. SPF and critical wavelengths of sunscreen formulations described in the Tables 1 and 2.

4. Conclusions

The sunscreen formulations obtained are time-dependent non-newtonian colloidal systems classified as thixotropic fluids. The colloidal stability of these thixotropic fluids depends on both the temperature and the sunscreen active ingredients presence in their composition. It can be remarked that the flow activation energy (E_a) obtained by the viscosity measurements is an essential parameter to evaluate the temperature influence on the colloidal stability of sunscreen formulations. The UV-VIS absorption/scattering properties of the sunscreen creams are also

correlated to the inorganic/organic filters or mixture of them, which provide SPF and critical wavelength values recommended for UV protection. It is important to emphasize that the synergistic effects from the inorganic and organic filters mixtures result in a better UV shielding performance of the sunscreen formulations as observed for UZ and UZ1 samples containing 10.00 or 5.00 wt% Uvinul® A Plus, respectively, and 1.00 wt% zinc oxide. Furthermore, white and beige colors presented by creams do not compromise the desired aesthetics appearance for the skin care products. Therefore, sunscreen formulations investigated in this work have

colloidal stability and suitable optical properties for application as sunscreens.

5. Acknowledgments

This work was developed with institutional infrastructure financed by FAPESP, CNPq and CAPES (Brazilian Agencies). G.P.S thanks CNPq for the granted scholarship.

6. References

- [1] Baker, L. A., Marchetti, B., Karsili, T. N. V., Stavros, V. G., Ashfold, M. N. R., Photoprotection: extending lessons learned from studying natural sunscreens to the design of artificial sunscreen constituents, *Chem. Soc. Rev.* 46 (2017) 3770-3791. <https://doi.org/10.1039/C7CS00102A>.
- [2] Cole, C., Appa Y., Ou-Yang, H., A broad spectrum high-SPF photostable sunscreen with a high UVA-PF can protect against cellular damage at high UV exposure doses, *Photodermatol. Photoimmunol. Photomed.* 30 (2014) 212-219. <https://doi.org/10.1111/phpp.12124>.
- [3] Velasco, M. V. R., Sarruf, F. D., Salgado-Santos, I. M. N., Haroutiounian-Filho, C. A., Kaneki, T. M., Baby, A. R., Broad spectrum bioactive sunscreens, *Int. J. Pharm.* 363 (2008) 50-57. <https://doi.org/10.1016/j.ijpharm.2008.06.031>.
- [4] Fourtanier, A., Moyal, D., Seite, S., UVA filters in sun-protection products: regulatory and biological aspects, *Photochem. Photobiol. Sci.* 11 (2012) 81-89. <https://doi.org/10.1039/C1PP05152K>.
- [5] Sambandan, D. R., Ratner, D., Sunscreens: An overview and update, *J. Am. Acad. Dermatol.* 64 (2011) 748-758. <https://doi.org/10.1016/j.jaad.2010.01.005>.
- [6] Kockler, J., Oelgemöller, M., Robertson, S., Glass, B. D., Photostability of sunscreens, *J. Photochem. Photobiol., C.* 13 (2012) 91-110. <https://doi.org/10.1016/j.jphotochemrev.2011.12.001>.
- [7] Sohn, M., Herzog, B., Osterwalder, U., Imanidis, G., Calculation of the sun protection factor of sunscreens with different vehicles using measured film thickness distribution-Comparison with the SPF *in vitro*, *J. Photochem. Photobiol., B.* 159 (2016) 74-81. <https://doi.org/10.1016/j.jphotobiol.2016.02.038>.
- [8] Flor, J., Davolos, M. R., Correa, M. A., Sunscreens, *Quim. Nova.* 30 (2007) 153-158. <https://doi.org/10.1590/S0100-40422007000100027>.
- [9] Cross, S. E., Jiang, R., Benson, H. A. E., Roberts, M. S., Can Increasing the Viscosity of Formulations be used to Reduce the Human Skin Penetration of the Sunscreen Oxybenzone?, *J. Invest. Dermatol.* 117 (2001) 147-150. <https://doi.org/10.1046/j.1523-1747.2001.01398.x>.
- [10] Calixto, L. S., Maia Campos, P. M. B. G., Physical-Mechanical characterization of cosmetic formulations and correlation between instrumental measurements and sensorial properties, *Int. J. Cosmet. Sci.* 39 (2017) 527-534. <https://doi.org/10.1111/ics.12406>.
- [11] Hernández, J. M. G., Escalante, A., Vázquez, R. N. M., Delgado, E., González, F. J., Toríz, G., Use of Agave tequilana-lignin and zinc oxide nanoparticles for skin photoprotection, *J. Photochem. Photobiol. B.* 163 (2016) 156-161. <https://doi.org/10.1016/j.jphotobiol.2016.08.027>.
- [12] Gaspar, L. R., Maia Campos, P. M. B. G., Rheological behavior and the SPF of sunscreens, *Int. J. Pharm.* 250 (2003) 35-44. [https://doi.org/10.1016/S0378-5173\(02\)00462-3](https://doi.org/10.1016/S0378-5173(02)00462-3).
- [13] Santoro, M. I. R. M., Oliveira, D. A. G. C. E., Kedor-Hackmann, E. R. M., Singh, A. K., The effect of packaging materials on the stability of sunscreen emulsions, *Int. J. Pharm.* 297 (2005) 197-203. <https://doi.org/10.1016/j.ijpharm.2005.03.021>.
- [14] Nasu, A., Otsubo, Y., Rheology and UV protection properties of suspensions of fine titanium dioxides in a silicone oil, *J. Colloid Interface Sci.* 296 (2006) 558-564. <https://doi.org/10.1016/j.jcis.2005.09.036>.
- [15] Rigo, L. A., Rascovetzki, R. H., Beck, R. C. R., Sunscreen formulations containing rice bran or soybean oil: rheological properties, spreadability and *in vitro* sun protection factor, *Lat. Am. J. Pharm.* 30 (2) (2011) 246-52. <http://hdl.handle.net/10915/8130>.
- [16] Sierra, A. F., Ramírez, M. L. G., Campmany, A. C. C., Martínez, A. R., Naveros, B. C., *In vivo* and *in vitro* evaluation of the use of a newly developed melatonin loaded emulsion combined with UV filters as a protective agent against skin irradiation, *J. Dermatol. Sci.* 69 (2013) 202-214. <https://doi.org/10.1016/j.jdermsci.2012.10.013>.
- [17] Amnuait, T., Boonme, P., Formulation and characterization of sunscreen creams with synergistic efficacy on SPF by combination of UV filters, *J. Appl. Pharm. Sci.* 3 (2013) 1-5. <https://doi.org/10.7324/JAPS.2013.3801>.
- [18] Seixas, V. C., Serra, O. A., Stability of Sunscreens Containing CePO₄: Proposal for a New Inorganic UV

Filter, *Molecules* 19 (2014) 9907-9925. <https://doi.org/10.3390/molecules19079907>.

[19] Technical Regulation MERCOSUR on ultraviolet filter list permitted for toiletries, cosmetics and perfumes. Brazilian Health Surveillance Agency. Resolution RDC No. 69. Ministry of Health (Brazil): National Press; 2016.

[20] Binks, B. P., Fletcher, P. D. I., Johnson, A. J., Marinopoulos, I., Crowther, J., Thompson, M. A., How the sun protection factor (SPF) of sunscreen films change during solar irradiation, *J. Photochem. Photobiol. A* 333 (2017) 186-199. <https://doi.org/10.1016/j.jphotochem.2016.10.027>.

[21] ISO 24443:2012, Determination of sunscreen UVA photoprotection *in vitro*, International Organization for Standardization, 2012.

[22] Diffey, B. L., A method for broad spectrum classification of sunscreens, *Int. J. Cosmet. Sci.* 16 (1994) 47-52. <https://doi.org/10.1111/j.1467-2494.1994.tb00082.x>.

[23] Vand, V., Viscosity of solutions and suspensions. I. Theory, *J. Phys. Colloid. Chem.* 52 (1948) 277-299. <https://pubs.acs.org/doi/pdf/10.1021/j150458a001>.

[24] Malkin, A.Y., Non-Newtonian viscosity in steady-state shear flows, *J. Nonnewton. Fluid. Mech.* 192 (2013) 48-65. <https://doi.org/10.1016/j.jnnfm.2012.09.015>.

[25] Tambe, D. E., Sharma, M. M., The effect of colloidal particles on fluid-fluid interfacial properties and emulsion stability, *Adv. Colloid Interface Sci.* 52 (1994) 1-63. [https://doi.org/10.1016/0001-8686\(94\)80039-1](https://doi.org/10.1016/0001-8686(94)80039-1).

[26] Tambe, D., Paulis, J., Sharma, M. M., Factors Controlling the Stability of Colloid-Stabilized Emulsions: IV. Evaluating the Effectiveness of Demulsifiers, *J. Colloid Interface Sci.* 171 (1995) 463-469. <https://doi.org/10.1006/jcis.1995.1203>.

[27] Degen, A., Kosec, M., Effect of pH and impurities on the surface charge of zinc oxide in aqueous solution, *J. Eur. Ceram. Soc.* 20 (2000) 667-673. [https://doi.org/10.1016/S0955-2219\(99\)00203-4](https://doi.org/10.1016/S0955-2219(99)00203-4).

[28] Bian, S. W., Mudunkotuwa, I. A., Rupasinghe, T., Grassian, V. H., Aggregation and Dissolution of 4 nm ZnO Nanoparticles in Aqueous Environments: Influence of pH, Ionic Strength, Size, and Adsorption of Humic Acid, *Lagmuir* 27 (2011) 6059-6068. <https://doi.org/10.1021/la200570n>.

[29] Lee, C. H., Moturi, V., Lee, Y., Thixotropic property in pharmaceutical formulations, *J. Control. Release* 136 (2009) 88-98. <https://doi.org/10.1016/j.jconrel.2009.02.013>.

[30] Juszczak, L., Fortuna, T., Rheology of selected Polish honeys, *J. Food. Eng.* 75 (2006) 43-49. <https://doi.org/10.1016/j.jfoodeng.2005.03.049>.

[31] Huang, B., Liang, S., Qu, X., The rheology of metal injection molding, *J. Mater. Process. Technol.* 137 (2003) 132-137. [https://doi.org/10.1016/S0924-0136\(02\)01100-7](https://doi.org/10.1016/S0924-0136(02)01100-7).

[32] Morrison, F. A., Experimental Data, In: Understanding rheology, first ed., Oxford University Press, New York, 2001, Ch. 6.

[33] Loyalka, S. K., Riggs, C. A., Inverse problem in diffuse reflectance spectroscopy: Accuracy of the Kubelka-Munk equations, *Appl. Spectrosc.* 49 (1995) 1107-1110.

[34] Pavia, D. L., Lampman, G. M., Kriz, G. S., Vyvyan, J. A., Ultraviolet spectroscopy, In: Introduction to spectroscopy, fourth ed., Cengage Learning, Belmont, 2009, Ch. 7.

[35] Wetz, F., Routaboul, C., Lavabre, D., Garrigues, J. C., Lattes, I. R., Pernep, I., Denis, A., Photochemical Behavior of a New Long-chain UV Absorber Derived from 4-tert-Butyl-4'-Methoxydibenzoylmethane, *J. Photochem. Photobiol.* 80 (2004) 316-321. <https://doi.org/10.1111/j.1751-1097.2004.tb00089.x>.

[36] Porter, G., Suppan, P., Primary photochemical processes in aromatic molecules. Part 12.-Excited states of benzophenone derivatives, *Trans. Faraday Soc.* 61 (1965) 1664-1673. <https://doi.org/10.1039/TF9656101664>.

[37] Stanfield, J., Osterwalder, U., Herzog, B., *In vitro* measurements of sunscreen protection, *Photochem. Photobiol. Sci.* 9 (2010) 489-494. <https://doi.org/10.1039/B9PP00181F>.

[38] BASF Sunscreen Simulator, Prediction of SPF and UVA-Metrics. https://www.sunscreensimulator.basf.com/Sunscreen_Simulator/Input_show.action, 2018.

[39] Wang, S. Q., Lim, H. W., Current status of the sunscreen regulation in the United States: 2011 Food and Drug Administration's final rule on labeling and effectiveness testing, *J. Am. Acad. Dermatol.* 65 (2011) 863-869. <https://doi.org/10.1016/j.jaad.2011.07.025>.

Direct determination of arsenobetaine and total As in robalo fish liver and tuna fish candidate reference material by slurry sampling graphite furnace atomic absorption spectrometry (SLS-GF AAS)

Carla Maíra Bossu¹⁺, Vivian Montes de Oca Carioni², Juliana Naozuka³, Pedro Vitoriano de Oliveira⁴, Cassiana Seimi Nomura⁴

1 São Paulo State University (Unesp), Institute of Chemistry, 55 Prof. Francisco Degni St, Araraquara, São Paulo, Brazil

2 University of Missouri (MU), Research Reactor Center, 1513 Research Park Dr, Columbia, Missouri, United States of America

3 Federal University of São Paulo (Unifesp), 275 Prof. Artur Riedel St, Diadema, São Paulo, Brazil

4 University of São Paulo (USP), Institute of Chemistry, 748 Prof. Lineu Prestes Hw, São Paulo, São Paulo, Brazil

+Corresponding author: Carla Maíra Bossu, email address: carla.bossu@gmail.com

ARTICLE INFO

Article history:

Received: October 21, 2018

Accepted: January 9, 2019

Published: April 25, 2019

Keywords:

1. arsenic
2. direct chemical speciation
3. tuna fish
4. robalo liver
5. reference material

ABSTRACT: This work describes a simple and rapid screening method for direct speciation of arsenobetaine (AsB) in tuna fish tissue and total As in tuna fish tissue and robalo liver using SLS-GF AAS. All procedures were proposed after careful optimization of pyrolysis and evaluation of chemical modifiers. Best results for total As were acquired using 25 μg Pd + 15 μg Mg + 0.1% w/v Triton X-100 in tuna fish ($4.4 \pm 0.3 \text{ mg kg}^{-1}$) and 100 μg Pd + 0.1 % w/v Triton X-100 solution in robalo liver ($10.3 \pm 0.6 \text{ mg kg}^{-1}$) as chemical modifiers. The direct speciation of AsB ($3.6 \pm 0.4 \text{ mg kg}^{-1}$) in tuna fish was achieved when 5 μg Pd + 3 μg Mg + 0.1% w/v Triton X-100 was used as a chemical modifier. Accuracy was verified using a tuna fish certified reference material (CRM BCR 627), with statistically equivalent concentrations (Student's *t*-test) for both total As and AsB.



1. Introduction

Marine organisms have been intensively used as bioindicators for ecological risk assessment, enabling the monitoring of potentially toxic elements, such as arsenic (As), which provides information about the risk of human contamination¹. Consequences of exposure to As in humans include progressive deterioration in motor and sensory responses, problematic pregnancy outcomes, cardiovascular disease and skin hyperpigmentation, as well as lung, skin and bladder cancer, and even death^{2,3}. However, the toxicity of As depends on its chemical species. The most toxic As species present in marine organisms are the arsenite (As(III)) and arsenate (As(V)),

followed by the methylated (MMA) and dimethylated (DMA) forms¹. Although fishes can contribute with up to 90% of all arsenic exposure originated from food, only a low portion of this element is present in its inorganic form. This is related to the presence of large amount of arsenobetaine (AsB), which is a relatively non-toxic form of arsenic. In general, AsB correspond to 80-90% of As in fish^{1,4,5}.

Taking into consideration that different As species induce different toxicity levels, some countries have established regulations for inorganic As content in food. China, for example, set maximum inorganic As levels for inspection of aquatic products (fish and products from fish, with the exception of live fishes). In this case, inorganic

arsenic (iAs) was regulated to a maximum of 0.01 mg kg⁻¹ and 0.5 mg kg⁻¹ for finfish and other fishes, respectively⁶. The maximum level of iAs in marine organisms was also regulated by Australia and was set as 2.0, 2.0, 1.0 and 1.0 mg kg⁻¹ for crustaceans, fish, shellfish, and algae, respectively⁷. The European Union has not established legislation to limit of the arsenic species in marine organisms but recommends the monitoring of iAs levels in fish feed, algae and animal feed. In this case, the maximum iAs content recommended is 2 mg kg⁻¹^{8,9}.

The determination of total arsenic concentration can be performed using many analytical techniques. Although As speciation has been frequently reported in the literature, incorrect results are not uncommon. The errors are generally related to the matrix complexity and the wide variety of materials that are routinely analyzed. This problem becomes even more evident when analyses of samples with low analyte content are required. One way to ensure the quality of analytical results in this case is the use of reference materials (RMs), which allow the assessment of the method accuracy and ensure the quality of the analytical results. Additionally, RMs are also used for instrument calibration, especially when direct solid sampling techniques are required^{10,11}.

According to the COMAR database (International database of certified reference materials)¹², the development of new RMs has been continually growing, because of the market development and the production of new industrial materials. The demand of RMs for speciation analyses has been also increasing, especially the ones dedicated to do the screening and identification of toxic and non-toxic species^{13,14}. Generally, speciation analyses are based on chromatographic methods with, including liquid chromatography coupled to inductively coupled plasma mass spectrometry (LC-ICP-MS), which remains the main choice for arsenic species determination^{15,16,17}.

The use of instrumental neutron activation analysis (INAA) to As detecting has been used to validate As species mass fractions combined with LC-ICP-MS¹⁴. It was demonstrated by the results that INAA can account for 100% of arsenic species distribution in analytical processes, complementing LC-ICP-MS technique in validation of the As species characterization in the development of RMs to such chemicals species.

The sample preparation for speciation analysis is generally a crucial and laborious step, as interconversion, losses or degradation of species must be avoided. The use of direct solid sampling in graphite furnace atomic absorption spectrometry (GF AAS) can be a good alternative to avoid or minimize the sample treatment step^{18,19}. In this case, the use of different chemical modifiers and/or different heating program conditions may result in the measurement of different species²⁰.

Recently, some studies have used electrothermal atomic absorption spectrometry (ET AAS) for As(III), As(V), MMA, DMA and AsB speciation in fish-based foods²⁰⁻²⁵. Significant differences were reported for the atomization of iAs and AsB or arsenocholine (AC) when using different chemical modifiers. These studies have shown evidence that the behavior of these species in the atomizer is different and depends on the chemical modifier used for the measurements²⁰.

López-García and co-workers have developed a method to measure iAs (As(III) and As(V)), MA, DMA and AsB in fish-based baby foods by ET AAS, using slurries prepared in tetramethylammonium hydroxide (TMAH) solution and a chemical modifier based on palladium salt, which was used for total As determination, whereas a chemical modifier based on Ce(IV) was used for determination of inorganic arsenic (As(III) and As(V)) + MA. The authors also used a zirconium coated atomizer for determination of DMA and AsB²⁵.

In this context, the present work aimed to develop a simple procedure for direct measurement of total As and some As species by SLS-GF AAS. Direct chemical speciation of As in tuna fish (RM) and robalo liver prepared in our laboratory was evaluated using different masses of Pd and Mg as chemical modifier solutions. The results found in this work were compared to those obtained for the same samples by INAA and LC-ICP-MS in a previous work¹⁴. The accuracy of the proposed method was also verified using tuna fish certified reference material (CRM) BCR 627 from the Institute for Reference Materials and Measurements (IRMM, Belgium).

2. Materials and methods

2.1 Instrumentation

The measurement of arsenic species was carried out using a Model ZEE nit 60 atomic absorption spectrometer (Analytik Jena AG, Jena, Germany), equipped with a hollow arsenic cathode lamp, a transverse heated graphite tube atomizer, and a Zeeman background corrector. Pyrolytically coated transverse heated graphite tubes and

pyrolytically coated boat-type solid sampling platforms (Analytik Jena) were used throughout. A manual solid sampling accessory (SSA-6 Z, Analytik Jena AG, Germany) with pre-adjusted micro-tweezers was used to transfer the boat-type platform to the graphite tube. For purging and protection gas, argon (99.998%, v/v; Air Liquide Brazil, São Paulo, Brazil) was used. Table 1 presents the instrumental parameters used after optimizing the pyrolysis temperature.

Table 1. Instrumental parameters, experimental conditions, and heating program used in the total and direct chemical speciation of arsenic by SLS-GF AAS.

| Instrumental parameters | | | | |
|--|----------------|-------------------------|-------------|-----------------------------|
| Wavelength | 193.7 nm | | | |
| Slit | 0.8 nm | | | |
| Lamp current | 6 mA | | | |
| Heating program for total As determination by SLS-GF AAS | | | | |
| Step | Temperature/°C | Ramp/°C s ⁻¹ | Hold time/s | Ar Flow/L min ⁻¹ |
| Drying | 130 | 10 | 20 | 1.0 |
| Pyrolysis | 1200 | 100 | 40 | 1.0 |
| Atomization | 2500 | 2600 | 6 | 0 |
| Cleaning | 2600 | 1200 | 3 | 1.0 |

A freeze-dryer (Thermo Electron Corporation), a food cutting mill (GM 200 model, Retsch, Germany) and a cryogenic mill with a self-contained liquid nitrogen bath (MA 775 model, Marconi, Brazil) were used for preparation of tuna fish candidate reference material.

2.2 Reagents and materials

All solutions were prepared using high-purity deionized water obtained from a Milli-Q water purification system (Millipore, Bedford, MA, USA). Analytical reference solutions of As were prepared by successive dilutions of a stock solution containing 1000 mg L⁻¹ As(III) and As(V) (Sigma–Aldrich, Germany) and analytical reference solutions of AsB were prepared from stock solutions containing 200 mg L⁻¹ AsB (Sigma Aldrich, Brazil).

Solutions of 10 g L⁻¹ Pd(NO₃)₂ (Suprapur, Merck) and 10 g L⁻¹ Mg(NO₃)₂ (Suprapur, Merck) were used to prepare the chemical modifier solutions. Triton X-100 (Merck) was added to the chemical modifier solution (0.1% w/v).

Calibration analytical curves for total As determination were obtained by using reference solutions with concentrations between 5.0 and

100.0 µg L⁻¹ of As(III) in TMAH 0.2% (v/v) or HNO₃ 0.1% (v/v). Calibration analytical curves for AsB determination were obtained using analytical solutions with concentrations between 12 and 240 µg L⁻¹ AsB in 0.1% v/v HNO₃.

2.3 Samples

Tuna fish candidate RM and robalo liver were collected at a fish market in São Paulo (Brazil) and prepared according to the procedure described by Carioni *et al.*²⁶ and Naozuka and Nomura²⁷. Briefly, the tissue was separated, cleaned with deionized water, cut into 2 cm³ pieces, frozen and freeze-dried for 48 h. The milling of the dried samples was performed using a cutting mill for 3 min at 5,000 rpm, followed by cryogenic milling (5 min of freezing followed by 3 cycles of 2 min of grinding, with 1 min of freezing between each cycle). The resulting final product was radiation-sterilized, bottled, and stored.

Tuna fish certified reference material (CRM BCR 627) from the Institute for Reference Materials and Measurements (IRMM, Belgium) was used to check the accuracy of the methods developed for measurement of As species and total As mass fraction.

2.4 Procedures

2.4.1 Evaluation of pyrolysis temperature

Pyrolysis temperature curves were evaluated in the absence and presence of two different chemical modifiers: 5 μg Pd + 3 μg Mg + 0.1% w/v Triton X-100 and 25 μg Pd + 15 μg Mg + 0.1% w/v Triton X-100. The temperature was evaluated in a range of 180-1600 $^{\circ}\text{C}$ using increments of 20 $^{\circ}\text{C}$. Slurries were prepared for this purpose using the procedure described by López-García, Briceño and Hernández-Córdoba²⁵ with modifications in the mass of tuna fish and TMAH concentration. Briefly, the slurries were prepared using 100 mg of tuna fish candidate reference material in 5.0 mL of TMAH 0.2% (v/v)²⁵.

2.4.2 Sample preparation for total As and species determination

Slurries were prepared using 100 mg of sample, 5.0 ml of H₂O and agitation in Vortex (Quimis, Q220, Diadema, São Paulo) at 25 $^{\circ}\text{C}$. Before each measurement, the sample slurry was homogenized using a pipette and then aliquots of 20 μL were injected into the atomizer together with 10 μl of different chemical modifiers: 5 μg Pd + 3 μg Mg + 0.1% w/v Triton X-100, 25 μg Pd + 15 μg Mg + 0.1% w/v Triton X-100 or 100 μg Pd + 0.1% w/v Triton X-100. The heating program optimized for the analysis is presented in Table 1. Analytical calibration curves were obtained using solutions containing different As(III) concentrations (5.0 and 100.0 $\mu\text{g L}^{-1}$) prepared in 0.1% v/v HNO₃.

3. Results and discussion

3.1 Heating program optimization

The pyrolysis temperature was evaluated in order to find the best conditions for measurement of total As and AsB species by SLS-GF AAS. Triton X-100 was used in combination with Pd + Mg to improve the interaction between the solid sample and the chemical modifier solution²⁸.

Figure 1 shows the pyrolysis temperature curves obtained for tuna fish slurry in TMAH media. The atomization, drying, and cleaning temperatures were used according to Carioni *et al.*²⁶.

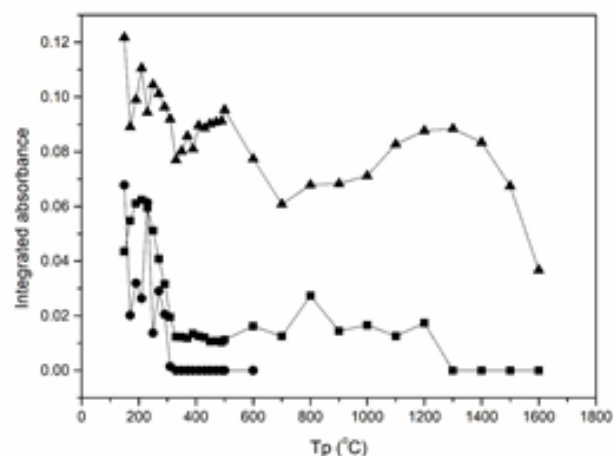


Figure 1. Pyrolysis temperature curves for slurry tuna fish candidate reference material in TMAH (●) in the absence of chemical modifiers, (■) in the presence of 5 μg Pd + 3 μg Mg + 0.1% w/v Triton X-100, (▲) in the presence of 25 μg Pd + 15 μg Mg + 0.1% w/v Triton X-100.

In the absence of chemical modifiers As was lost by volatilization at temperatures higher than 300 $^{\circ}\text{C}$. However, in the presence of chemical modifiers, higher masses of Pd and Mg resulted in higher sensitivity, and the best pyrolysis temperature was 1200 $^{\circ}\text{C}$ for both modifier solutions. We observed that different pyrolysis curve profiles were obtained when 5 μg Pd + 3 μg Mg + 0.1% w/v Triton X-100 was used in comparison with 25 μg Pd + 15 μg Mg + 0.1% w/v Triton X-100. In this case, the mass of chemical modifiers may have an impact on the atomization mechanism of some As species present in the candidate RM used for this study. This hypothesis was further investigated in this work.

Using 25 μg Pd + 15 μg Mg + 0.1% w/v Triton X-100 as chemical modifiers at the pyrolysis temperature of 1200 $^{\circ}\text{C}$, analytical calibration curves prepared in the presence of 0.2% of TMAH (v/v) were compared to those prepared in the presence of 0.1% of HNO₃ (v/v) to determine the chemical interference promoted by these reagents. Thus, the slopes and correlation coefficients of those calibration curves were respectively 0.0023 and 0.9998 for the curve prepared in the presence of 0.1% of HNO₃ and 0.0022 and 0.9993 for the curve prepared in the presence of 0.2% of TMAH. The slope ratio between both calibration curves was 1.05, showing no significant effect of TMAH on As measurement enabling the use of 0.1% HNO₃ media for further analytical calibration curves preparation.

The integrated absorbance signals of As at the optimized heating program were also compared in samples slurries prepared in 0.2% TMAH with those prepared using only H₂O. No significant difference (Student's *t*-test 95% level) was found between those solutions, suggesting the use of TMAH is not imperative. For this reason, slurries prepared in H₂O were used for further analysis.

3.2 Total As determination and direct chemical speciation

Thermal behavior of total As and As species in tuna fish tissue and robalo liver in the absence and in the presence of chemical modifiers were investigated. Significant difference was observed

in the results for As concentration when 5 µg Pd + 3 µg Mg + 0.1% w/v Triton X-100 was compared with 25 µg Pd + 15 µg Mg + 0.1% w/v Triton X-100. When masses of Pd and Mg were increased by a factor of 5, the results were 1.3 - 1.2 times higher. In addition, the values obtained for a fish tissue CRM after using the 5 µg Pd + 3 µg Mg + 0.1% w/v Triton X-100 and 25 µg Pd + 15 µg Mg + 0.1% w/v Triton X-100 as chemical modifiers corresponded to the certified values for AsB and total As, respectively (Table 2). Results for total As tuna fish candidate reference material were also in agreement (Student's *t*-test, *p* > 0.05) with previous results obtained by our group using SS-GFAAS ($4.8 \pm 0.2 \text{ mg kg}^{-1}$)²⁶ and INAA ($5.1 \pm 0.1 \text{ mg kg}^{-1}$)¹⁴.

Table 2. Results of As mass fractions obtained for Tuna Fish certified reference materials (BCR 627) and Tuna fish candidate reference material for Arsenobetaine (AsB)^a and Total Arsenic (AsT)^b by SLS-GF AAS, *n* = 3.

| Concentration/mg kg ⁻¹ ± standard uncertainty and coefficient of variation (CV, %) | Certified value (BCR 627) | Measured value (BCR 627) | CV (%) | Tuna fish (RM) | CV (%) |
|---|---------------------------|--------------------------|--------|----------------|--------|
| 5 µg Pd + 3 µg Mg + Triton* | 3.9 ± 0.2^a | 3.5 ± 0.2 | 5.4 | 3.6 ± 0.4 | 11.9 |
| 25 µg Pd + 15 µg Mg + Triton* | 4.8 ± 0.3^b | 4.5 ± 0.3 | 5.8 | 4.4 ± 0.3 | 5.9 |

*0.1% w/v Triton X-100

Results obtained for As content in tuna fish candidate reference material (Table 2) using the 5 µg Pd + 3 µg Mg + 0.1% w/v Triton X-100 chemical modifier corresponded to the certified value of AsB (Student's *t*-test, *p* > 0.05). The results for AsB in tuna fish candidate reference material (Table 2) are also in agreement with a previous work ($3.99 \pm 0.08 \text{ mg kg}^{-1}$), when the same sample was analyzed by HPLC-ICP-MS¹⁴. In this study, we observed that differences in the behavior of As species, when atomized in the presence of different chemical modifiers, allowed the direct speciation of AsB by SLS-GF AAS. The dependence of As atomization on the chemical modifier have already been reported in previous works^{25,29}. Differences in the behavior of organic and inorganic arsenic were observed when solutions containing different composition and/or masses of chemical modifiers were used^{25,29}.

Although the proposed procedure did not allow the discrimination of other As species in fish, AsB could be separated from the toxic As species DMA and other unknown As species. DMA is also a constituent of tuna fish tissue and its presence was reported in the tuna fish SRM 627³⁰.

The same procedure used for determination of total As in tuna fish was applied to robalo liver. The obtained result ($6.9 \pm 0.8 \text{ mg kg}^{-1}$) was not in agreement with a previous work in which total As in the same sample was determined by INAA ($11.0 \pm 0.2 \text{ mg kg}^{-1}$)¹⁴. This problem can be the result of different As species in robalo liver, which may result in a different mechanisms of atomization. The As species in robalo liver are still unknown, although some evidences have shown that part of As is likely present in the form of arsenolipids¹⁴. The difference in the behavior of As species was discussed in a recent work by Pereira and co-workers²⁹. Their work has identified differences in pyrolysis curves from As(III) aqueous solutions and As in fish oil when Pd + Ru were used as chemical modifiers, which may be related to the presence of other As species besides of As(III), such as arsenolipids.

When 100 µg Pd + 0.1% w/v Triton X-100 was used as a chemical modifier, better recovery was obtained. In this condition, the value obtained for total As ($10.3 \pm 0.6 \text{ mg kg}^{-1}$) is in agreement with the literature¹⁴. This indicates that the composition of the chemical modifier should be adjusted for each sample, since the atomization mechanism for

total As determination was clearly altered by matrix constituents. In addition, the use of a sufficient mass of the chemical modifiers allowed the measurement of total As content in the slurries, irrespective of the chemical species in which it is present^{25,26}.

The detection and quantification limits and characteristic masses are shown in Table 3, using the three different chemical modifiers. These detection limits are appropriate for the determination of these species, avoiding the need of extraction processes and/or chromatographic separations²⁵.

Table 3. Analytical parameters of SLS-GF AAS for total and direct chemical speciation of arsenic.

| | 5 µg Pd + 3 µg Mg + Triton* | 25 µg Pd + 15 µg Mg + Triton | 100 µg Pd + Triton |
|----------------------------|-----------------------------|------------------------------|--------------------|
| LOD (µg kg ⁻¹) | 34.6 | 19.9 | 18.5 |
| LOQ (µg kg ⁻¹) | 103.9 | 59.9 | 55.5 |
| m_o^a (pg) | 35 | 33 | 34 |

LOD = $(3 \times SD_{bco} / \text{slope})$, LOQ = $(3 \times \text{LOD})$, m_o = characteristic mass (1% absorbance or 0.0044 absorbance signal), SD_{bco} = standard deviation of blank (n = 10).

*0.1% w/v Triton X-100.

When 5 µg Pd + 3 µg Mg + 0.1% w/v Triton X-100 was used for As determination in robalo liver, 5.1 ± 0.2 mg kg⁻¹ of As was measured. The identification of As species, however, remains to be elucidated. Previous analyses have demonstrated poor results for As speciation in this samples when extractions were performed using methanol/H₂O and acetone/methanol/H₂O (44 and 49% of total As, respectively). The high amount of lipids in this kind of sample may prevent the extraction of part of the As to the aqueous phase, preventing the identification of As species¹⁴. In view of these analytical difficulties, more investigations on the quantification and identification of the different arsenic species are still required for robalo liver.

In summary, the direct total As and As speciation methods for tuna fish were performed by a simple slurry preparation in water, using aqueous calibration. In the case of total As, there was no need of digestion and dilution steps when the chemical modifiers were used for tuna fish and robalo liver analysis. In the case of determination of AsB, the use of 5 µg Pd + 3 µg Mg + 0.1% w/v Triton X-100 as a chemical modifier allowed the direct measurement of this As compound in tuna fish without prior separation of species. It implies that all laborious steps of extraction, centrifugation and separation were not necessary. Considering that tuna fish is extensively consumed by many populations in the world, the present study represents a valuable tool for the assessment of non-toxic As species, which brings the possibility

to assure the safety of tuna consumers using two simple complementary methods to distinguish AsB from other As compounds in tuna fish.

4. Conclusions

This work described the use of different chemical modifier compositions for the development of a direct speciation method for AsB measurement in tuna fish tissue by SLS-GF AAS. Methods for total As measurements in tuna fish and robalo liver were also evaluated.

The direct determination of AsB was achieved when a solution containing 5 µg Pd + 3 µg Mg + 0.1% w/v Triton X-100 was used as chemical modifier in tuna fish tissue. The use of 25 µg Pd + 15 µg Mg + 0.1% w/v Triton X-100 and 100 µg Pd + 0.1% w/v Triton X-100 allowed the total As measurement in tuna fish tissue and robalo liver, respectively. This work demonstrated that the behavior of arsenic in SLS-GF AAS may depend on the species of the element and composition or concentration of chemical modifiers. In addition, the simplicity of the proposed method enables its use for routine analyses as a valuable tool for quality control of tuna in the fishing industry.

5. Acknowledgments

The authors acknowledge the support of the Fundação de Amparo à Pesquisa do Estado de São Paulo for financial support (FAPESP no. 2007/56504-6, 2012/11998-0, 2017/10346-2) and

Conselho Nacional de Desenvolvimento Científico e Tecnológico (CNPq) for financial support and fellowships.

6. References

- [1] Leermakers, M., Baeyens, W., De Gieter M., Smedts, B., Meert, C., De Bisschop, H. C., Morabito, R., Quevauviller, P., Toxic arsenic compounds in environmental samples: Speciation and validation, *Trends Anal. Chem.* 25 (1) (2006) 1-10. <https://doi.org/10.1016/j.trac.2005.06.004>.
- [2] Shakoor, M. B., Nawaz, R., Hussain, F., Raza, M., Ali, S., Rizwan, M., Oh, S., Ahmad, Human health implications, risk assessment and remediation of As-contaminated water: A critical review, *Sci. Total Environ.* 601-602 (2017) 756-769. <https://doi.org/10.1016/j.scitotenv.2017.05.223>.
- [3] Yunus, F. M., Khan, S., Chowdhury, P., Milton, A. H., Hussain, S., Rahman, M., A review of groundwater arsenic contamination in Bangladesh: the millennium development goal era and beyond, *Int. J. Environ. Res. Public Health.* 13 (215) (2016) 1-18. <https://doi.org/10.3390/ijerph13020215>.
- [4] McSheehy, S., Szpunar, J., Morabito, R., Quevauviller, P., The speciation of arsenic in biological tissues and the certification of reference material for quality control, *Trends Anal. Chem.* 22 (4) (2003) 191-209. [https://doi.org/10.1016/S0165-9936\(03\)00404-7](https://doi.org/10.1016/S0165-9936(03)00404-7).
- [5] Ysart, G., Miller, P., Croasdale, M., Crews, H., Robb, P., Baxter, M., L'Argy, C., Harrison, N., 1997 UK total diet study: aluminium, arsenic, cadmium, chromium, copper, lead, mercury, nickel, selenium, tin and zinc, *Food Addit. Contam.* 17 (9) (2000) 775-786. <https://doi.org/10.1080/026520300415327>.
- [6] Cfia - Canadian Food Inspection Agency, Certification Requirements: China, 2017. <http://www.inspection.gc.ca/food/fish-and-seafood/exports/by-jurisdiction/china/eng/1373555071317/1373555185449>.
- [7] Comlaw, Australia New Zealand Food Standards Code: Standard 1.4.1: Contaminants and Natural Toxicants. <http://www.comlaw.gov.au/details/f2011c00121>.
- [8] Pétursdóttir, Á. H., Gunnlaugsdóttir, H., Jörundsdóttir, H., Raab, A., Krupp, E. M., Feldmann, J., Determination of inorganic arsenic in seafood: Emphasizing the need for certified reference materials, *Pure Appl. Chem.* 84 (2) (2012) 191-202. <https://doi.org/10.1351/PAC-CON-11-10-03>.
- [9] The Commission of the European Communities, Commission directive 2009/141/EC of 23 November 2009 - amending Annex I to Directive 2002/32/EC of the European Parliament and of the Council as regards maximum levels for arsenic, theobromine, *Datura sp.*, *Ricinus communis L.*, *Croton tiglium L.* and *Abrus precatorius L.* <http://eur-lex.europa.eu/legal-content/EN/ALL/?uri=CELEX%3A32009L0141>.
- [10] ABNT, Associação Brasileira de Normas Técnicas, "Termos e definições relacionados com materiais de referência", 1 ed. Rio de Janeiro, 2000a (ABNT ISO Guia 30).
- [11] Zschunke, A., The role of reference materials in analytical chemistry, *Accred. Qual. Assur.* 8 (2003) 247-251.
- [12] Comar - International database for certified reference materials. <http://www.comar.bam.de/en/>. Accessed July 20, 2018.
- [13] Chelegão, R., Carioni, V.M.O., Naozuka, J., Nomura, C. S., Feasibility of using AAS for the characterization of a tuna fish candidate reference material for total Hg and methyl-Hg measurement, *J. Braz. Chem. Soc.* 27 (4) (2016) 712-718. <https://doi.org/10.5935/0103-5053.20150320>.
- [14] Carioni, V. M. O., Nomura, C. S., Yu, L. L., Zeisler, R., Use of neutron activation analysis and LC-ICP-MS in the development of candidate reference materials for As species determination, *J. Radioanal. Nucl. Chem.* 299 (2014) 241-248. <https://doi.org/10.1007/s10967-013-2790-6>.
- [15] Fang, Y., Pan, Y., Li, P., Xue, M., Pei, F., Yang, W., Maa, N., Hua, Q., Simultaneous determination of arsenic and mercury species in rice by ion-pairing reversed phase chromatography with inductively coupled plasma mass spectrometry, *Food Chem.* 213 (2016) 609-615. <https://doi.org/10.1016/j.foodchem.2016.07.003>.
- [16] Jia, X., Gong, D., Wang, J., Huang, F., Duan, T., Zhang, X., Arsenic speciation in environmental waters by a new specific phosphine modified polymer microsphere preconcentration and HPLC-ICP-MS determination, *Talanta.* 160 (2016) 437-443. <https://doi.org/10.1016/j.talanta.2016.07.050>.
- [17] Kalantzi, I., Mylona, K., Sofoulaki, K., Tsapakis, M., Pergantis, S.A., Arsenic speciation in fish from Greek coastal areas, *J. Environ. Sci.* (2017). <https://doi.org/10.1016/j.jes.2017.03.033>.

- [18] Cornelis, R., Crews, H., Caruso, J., Heumann, K.G., Handbook of Elemental Speciation II: Species in the Environment, Food, Medicine & Occupational Health, John Wiley & Sons, 2005, p. 488.
- [19] Nomura, C. S., Silva, C. S., Nogueira, A. R. A., Oliveira P. V., Bovine liver sample preparation and micro-homogeneity study for Cu and Zn determination by solid electrothermal atomic absorption spectrometry, *Spectrochim. Acta Part B*. 60 (5) (2005) 673-680. <https://doi.org/10.1016/j.sab.2005.02.021>.
- [20] Anawar, H. M., Arsenic speciation in environmental samples by hydride generation and electrothermal atomic absorption spectrometry, *Talanta* 88 (2012) 30-42. <https://doi.org/10.1016/j.talanta.2011.11.068>.
- [21] Serafimovski, I., Karadjova, I. B., Stafilov, T., Tsalev, D. L., Determination of total arsenic and toxicologically relevant arsenic species in fish by using electrothermal and hydride generation atomic absorption spectrometry, *Microchem. J.* 83 (2006) 55-60. <https://doi.org/10.1016/j.microc.2006.01.021>.
- [22] Shah, A. Q., Kazi, T. G., Baig, J. A., Arain, M. B., Afridi, H. I., Kandhro, G. A., Wadhwa, S. K., Kolachi, N. F., Determination of inorganic arsenic species (As^{3+} and As^{5+}) in muscle tissues of fish species by electrothermal atomic absorption spectrometry (ETAAS), *Food Chem.* 119 (2010) 840-844. <https://doi.org/10.1016/j.foodchem.2009.08.041>.
- [23] Zmozinski, A. V., Llorente-Mirandes, T., Damin, I. C. F., López-Sánchez, J. F., Vale M. G. R., Welz, B., Silva, M. M., Direct solid sample analysis with graphite furnace atomic absorption spectrometry-A fast and reliable screening procedure for the determination of inorganic arsenic in fish and seafood, *Talanta*. 134 (2015) 224-231. <https://doi.org/10.1016/j.talanta.2014.11.009>.
- [24] Mihucz, V. G., Bencs, L., Koncz, K., Tatár, E., Weiszbürg, T., Zárny, G., Fast arsenic speciation in water by onsite solid phase extraction and high-resolution continuum source graphite furnace atomic absorption spectrometry, *Spectrochimica Acta Part B: Atomic Spectroscopy*. (2017). <https://doi.org/10.1016/j.sab.2016.12.010>.
- [25] López-García, I., Briceño, M., Hernández-Córdoba, M., Non-chromatographic screening procedure for arsenic speciation analysis in fish-based baby foods by using electrothermal atomic absorption spectrometry, *Anal. Chim. Acta*, 699 (2011) 11-17. <https://doi.org/10.1016/j.aca.2011.05.005>.
- [26] Carioni, V. M. O., Chelegão, R., Naozuka, J., Nomura, C. S., Feasibility study for the preparation of a tuna fish candidate reference material for total As determination, *Accred. Qual. Assur.* 16 (2011) 453-458. <https://doi.org/10.1007/s00769-011-0796-8>.
- [27] Naozuka, J., Nomura, C. S., Total determination and direct chemical speciation of Hg in fish by solid sampling GF AAS, *J. Anal. At. Spectrom.* 26 (2011) 2257-2262. <https://doi.org/10.1039/C1JA10188A>.
- [28] Naozuka, J., Oliveira, P. V., Minimization of Sample Pretreatment for Al, Cu and Fe Determination in Coconut Water by Electrothermal Atomic Absorption Spectrometry, *J. Braz. Chem. Soc.* 17 (2006) 521-526. <https://doi.org/10.1590/S0103-50532006000300014>.
- [29] Pereira, E. R., Almeida, T. S., Borges, D. L. G., Carasek, E., Welz, B., Feldmann, J., Menoyo, J. C., Investigation of chemical modifiers for the direct determination of arsenic in fish oil using high-resolution continuum source graphite furnace atomic absorption spectrometry, *Talanta* 150 (2016) 142-147. <https://doi.org/10.1016/j.talanta.2015.12.036>.
- [30] Maier, E. A., Demesmay, C., Olle, M., Lamotte, A., Lagarde, F., Heimburger, R., Leroy, M. J. F., Asfari, Z., Muntau, H., The certification of the contents (mass fractions) of arsenobetaine in solution (CRM 626) and of total arsenic, arsenobetaine, dimethylarsinic acid in tuna fish tissue (CRM 627), Luxembourg: Office for Official Publications of the European Communities, 1997.

Effects of garnet particles and chill casting conditions on properties of aluminum matrix hybrid composites

Haider Tawfiq Naeem¹  Firas Fouad Abdullah¹

¹ Al-Muthanna University, 72001 Samawah, Al-Muthanna, Iraq

+Corresponding author: Haider Tawfiq Naeem, email addresses: haidertn@mu.edu.iq, dr.haider.naeem@gmail.com

ARTICLE INFO

Article history:

Received: December 11, 2018

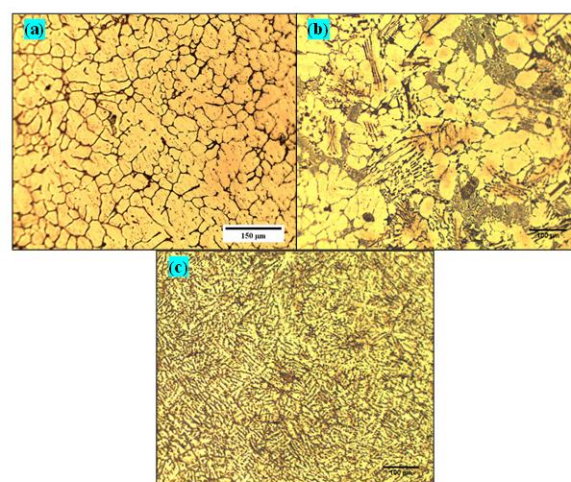
Accepted: Maarch 31, 2019

Published: April 25, 2019

Keywords:

1. copper chill casting
2. aluminum hybrid
3. hard ceramic particles

ABSTRACT: In recent years, the demand of high-performance and light-weight materials was increasing for industrial applications. The present research aims to study microstructural and mechanical properties of aluminum matrix hybrid reinforced 6-12 wt.% of garnet under the effects of materials chill casting during the manufacturing aluminum matrix composite. In this research work, metallic mold and no chills were used. In order to evaluate the quality of the chill end casting microstructure, hardness, and tensile tests were conducted on the prepared composite specimens. Aluminum matrix composites underwent the chill casting process have been examined using the optical microscope, scanning electron microscopy and X-ray diffraction. Microstructure outcomes of the casted Al-composites alloy indicated that having precipitations (Al₂Si, AlCuMg₂Si) and Garnet particulates hard within the Al-matrix. The results showed that the copper chill casting is the better one in terms of improving the mechanical properties because of its high volumetric heat capacity. Aluminum composite with addition of 9% Garnet composite produced via copper chill casting exhibits better mechanical properties.



The optical micrograph of the Al-samples

1. Introduction

Aluminum matrix hybrid composites with dispersion of two or more ceramic reinforcements have been widely used in various applications of automotive and aerospace sectors¹. Aluminum matrix composite have light specific-weight, good resistance of corrosion with excellent thermal properties. These composites are becoming wide using as the high performance materials. Ceramic materials are generally used to reinforce aluminum-alloys with silicon carbide (SiC), titanium carbide (TiC), alumina (Al₂O₃), silicon oxide, TiB₂, ZrB₂, AlN, Si₃N₄ and SiO₂^{2,3}. These ceramic materials have high strength and high hardness. However, it displays brittle behavior and

has low resistance to fracture which can be improved by modifying the reinforcement grain size, shape and by incorporating additional phases⁴. It has been widely reported that aluminum alloys can be readily developed with two or more reinforcement and recently there has been a growing interest in the use of hybrid composites. Particulate reinforced hybrid composites exhibit excellent isotropic properties⁵. Ghoncheh *et al.*⁶ found that experiments carried out on a mold having high cooling rates have the solidification parameters such as nucleation temperature, recalescence undercooling temperature, and range of solidification temperature influenced by variation of cooling rates. Generally, the improvement in the overall properties of

composites is made using the hybrid composites through adding insoluble reinforcements to the base matrix⁷. Many of studies focused on the utilization of various forms of artificial reinforcements in aluminum matrix alloys such as TiC, WC, SiC, SiO₂, Al₂O₃ etc. for getting the desired properties^{8,9}. The composite hardness is improved using hard ceramic reinforcements. Saravanakumar, Sasikumar and Sivasankaran¹⁰ started their investigation on hybrid composites by fabricating of Al-6063/Al₂O₃/Gr using liquid metallurgy technique, and then they have studied wear property using conventional tribometer apparatus for different parameters like sliding speed, applied loads as well the reinforcements effect addition of Gr (Garnet) is particularly useful and led to the improvement of the mechanical properties. Anju¹¹ has studied effect of particle size of Al-garnet composites on wear behavior showed enhancement for the wear property with Gr particles.

Kumar, Sait and Subramanian¹² studied aluminum alloy boron carbide and garnet composites were fabricated by the stir casting process. They discovered that by increasing the amount of garnet in the aluminum alloy mixture, the tensile strength and hardness were increased. Also, the wear test analysis proved that the addition of reinforcements improve the wear property of composite.

Uthayakumar, Aravindanb and Rajkumar¹³ discovered that the addition of Graphite particles led to decrease the microhardness values but significantly improved the wear resistance of the aluminum composite specimens.

In recent years many researchers have worked on the combination of graphite with SiC and Al₂O₃ and it was found similar results. The study of Suresh and Hemanth¹⁴ focused on the effect of chills on mechanical characteristics and wear properties of the composite. Whereas, Sharifi and Karimzadeh¹⁵ investigated wear behavior of aluminum matrix hybrid nanocomposites by

reinforcing of 1 wt.% Gr and 10 wt.% SiC with A356 using powder metallurgy technique to investigate the tribological properties.

Directional and fast solidification is one of a broadly reasonable method to refine the grain sizes and hence improves the mechanical properties of aluminum composite, which can be achieved by the application of chills.

In this research paper, the garnet was used as reinforcement with a matrix of Al-6000 alloys to produce new material alloys with optimum properties. Another goal of the research is to investigate the effect of the best chill castings. The application of chills will be used to improve the directional solidification and hence to achieve finer microstructure with improved mechanical properties.

2. Materials and methods

2.1 Materials

In the present study, commercially available Al-alloy (ASTM LM 13 as given in [Table 1](#)) piston alloy was used, which is a multicomponent Al-Si-Ni-Cu-Mg alloy with lower concentrations of Fe and Mn. In the present investigation low cost and naturally available hard ceramic Garnet (chemical formula of Gr is Fe₃Al₂Si₃O₁₂) are used to reinforcements Al-alloy. Garnet was added in the proportion of 6 wt.% to 12 wt.% in steps of 3 wt.% [Table 2](#) shows the nominal of Al-composites samples.

Metallic chills of dimension 25 mm x 35 mm x 170 mm were used to investigate the influence of the directional solidification on characteristics of the composite. The effect is compared with composites developed without using chills. The used material provides superior casting characteristics thermo-physical properties. So, it is suitable for some of the industries such as the automotive industry.

Table 1. Chemical composition of Al-alloys (LM13) during this study.

| Element | Weigh Percentages (%) |
|---------|-----------------------|
| Al | 83.4 |
| Si | 10.89 |
| Fe | 0.53 |
| Cu | 1.3 |
| Mg | 2.32 |
| Ni | 0.51 |

Table 2. Nominal of aluminium composites alloys in this study

| Elements | Gr | Mg | Si | Cu | Fe | Ni | Al |
|----------|---------------|------|-------|-----|------|------|------|
| | Weight (wt.%) | | | | | | |
| Al-C0 | 0 | 2.32 | 10.89 | 1.3 | 0.53 | 0.51 | 83.4 |
| Al-C1 | 6 | 2.32 | 10.89 | 1.3 | 0.53 | 0.51 | 83.4 |
| Al-C2 | 9 | 2.32 | 10.89 | 1.3 | 0.53 | 0.51 | 83.4 |
| Al-C3 | 12 | 2.32 | 10.89 | 1.3 | 0.53 | 0.51 | 83.4 |

2.2 Experimental Procedure

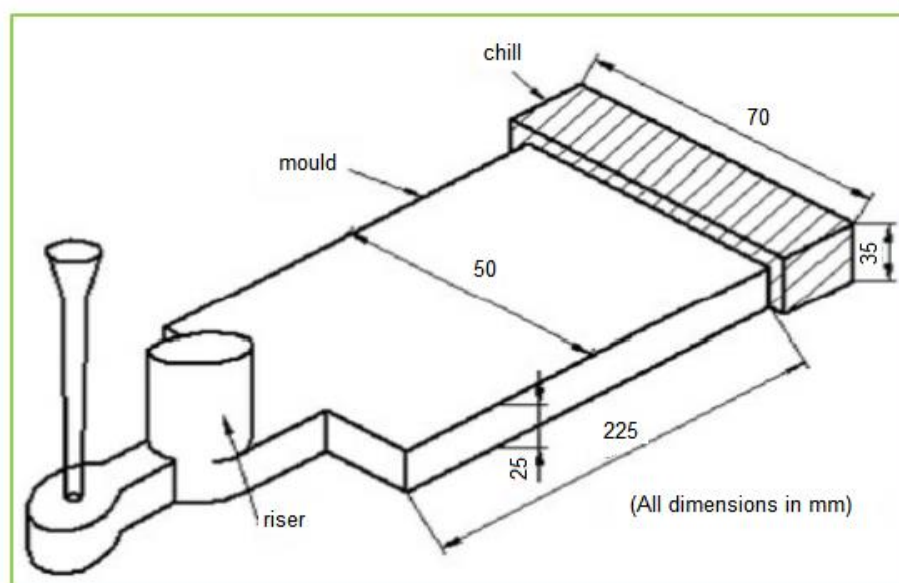
2.2.1 Fabrication of the Composite:

Cost reduction is the key factor for wider application of aluminum hybrid metal matrix composites-(Al-HMMCs) in modern industry which can be achieved by cheaper reinforcements, simpler fabrication methods, and higher production volume. Thus, the fabrication process via a stir casting technique was used to develop the composites with greater bonding of reinforcement particles with the metal matrix. Stir casting method

is well known for uniform distribution of the reinforcements because of stirring action and flexible for materials with different low melting temperature.

In the present study, a resistance furnace was used for melting the Al-alloy at about 850 °C.

Garnet (Gr) particles were preheated then added into the molten Al-alloy matrix, thereby the mixed Al-mixture poured into the different molds with and without chill. First mold which made of sand and also poured into different chills such as steel and copper is shown in [Figure 1](#).

**Figure 1.** Scheme of sand mold.

2.2.2 Mechanical Properties

Hardness tests were performed on the composites using Vickers hardness tester with a square-base diamond pyramid as the indenter. Ultimate tensile strength of the samples was tested using an electronic tensile testing machine based on ASTM standard. For a particular cast Al-HMMC, three specimens were tested and the mean value along with standard deviation of the mechanical properties reported. The micrographs of specimens were examined in the optical microscope and the scanning electron microscope. Chill end materials were machined on lathe to get the required dimensions.

3. Results and discussion

3.1 Microstructure and mechanical behavior

Figure 2 shows the optical micrograph and Figure 3 shows scanning electron microscope of microstructures of the different three aluminium samples. It shows the uniform distribution of the reinforcements and good bonding between reinforcement and matrix. Although the stir casting process is known for better bonding between Al-matrix and reinforces particles, it is not developed for mass production. The stir casting method is simple and convenient successful fabrication of the composite.

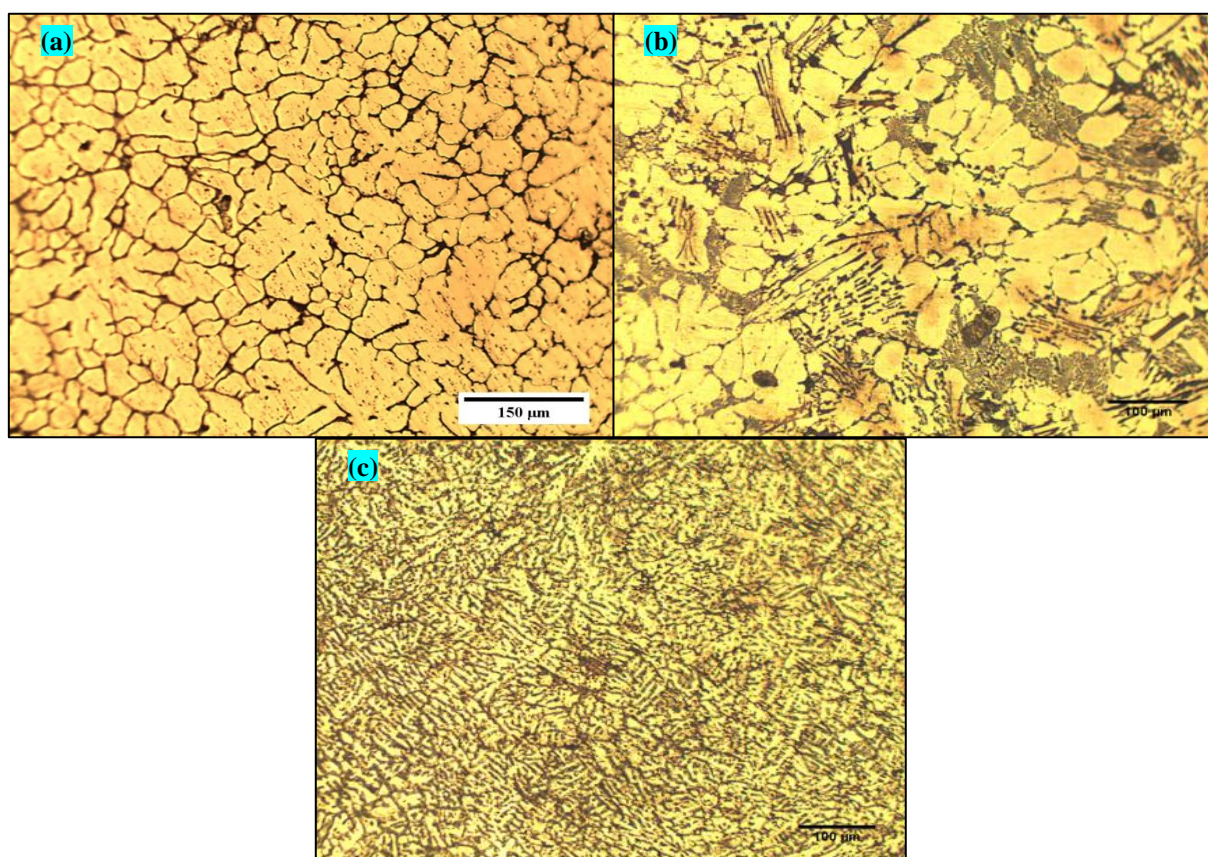


Figure 2. The optical micrograph of the Al-samples (a) Al-HMMC with 6% Garnet without chill, (b) Al-HMMC with 9% Garnet under mold of steel and (c) Al-HMMC with 9% Garnet under copper mold chill.

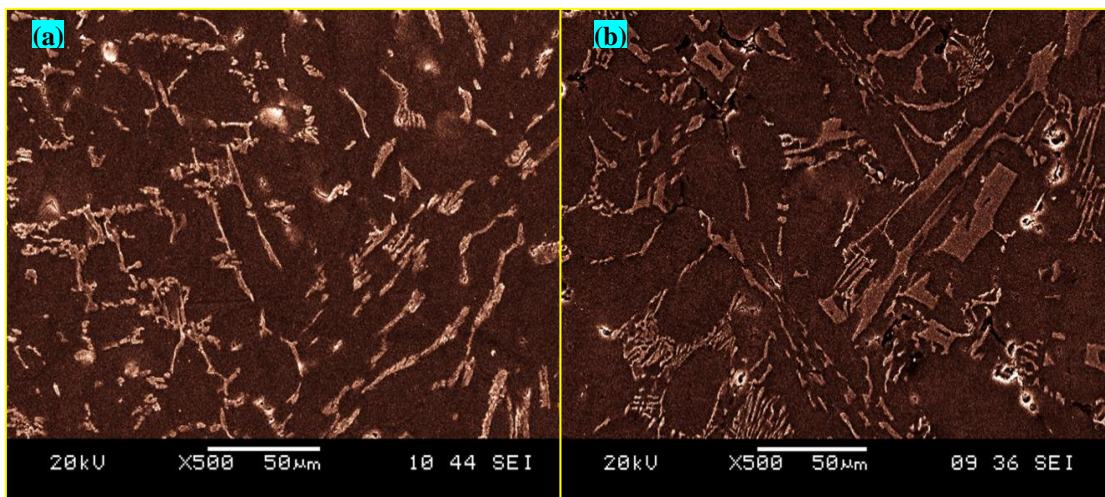


Figure 3. SEM images of microstructure of the Al-samples (a) Al-C2 under mold of steel chilling and (b) Al-C3 under mold of steel chilling.

The X-ray diffraction analytic as given in Figure 4 manifests the XRD peaks of Al-Mg-Si-Cu-Ni matrix alloy with and without adding Garnet particles after applying the casting treatment processing. The XRD results for the stir casted Al-Mg-Cu-Si-Ni-9%Gr composite (Al-C2 sample), as presented in Figure 4a, exhibited many peaks which were alpha-Al, Al₂Si, AlCuMg₂Si as well the peak of garnet particles. The XRD peaks of the stir casted Al-Mg-Si-Cu-Ni matrix alloy (Al-C0) sample is presented in Figure 4b. The peaks of Al-

C0 sample consisted of the alpha-Al and the high peak of Al₂Si. The peak Al₂Si was created due to the high dissolution percent of silicon within the Al matrix during the high temperature as results casting processing. Generally, it was observed that the cause of the presence of the Al₂Si, AlCuMg₂Si compounds implicit alloying elements (Mg, Si, Cu and others) dissolution within the aluminum matrix, due to high temperature during the heat process.

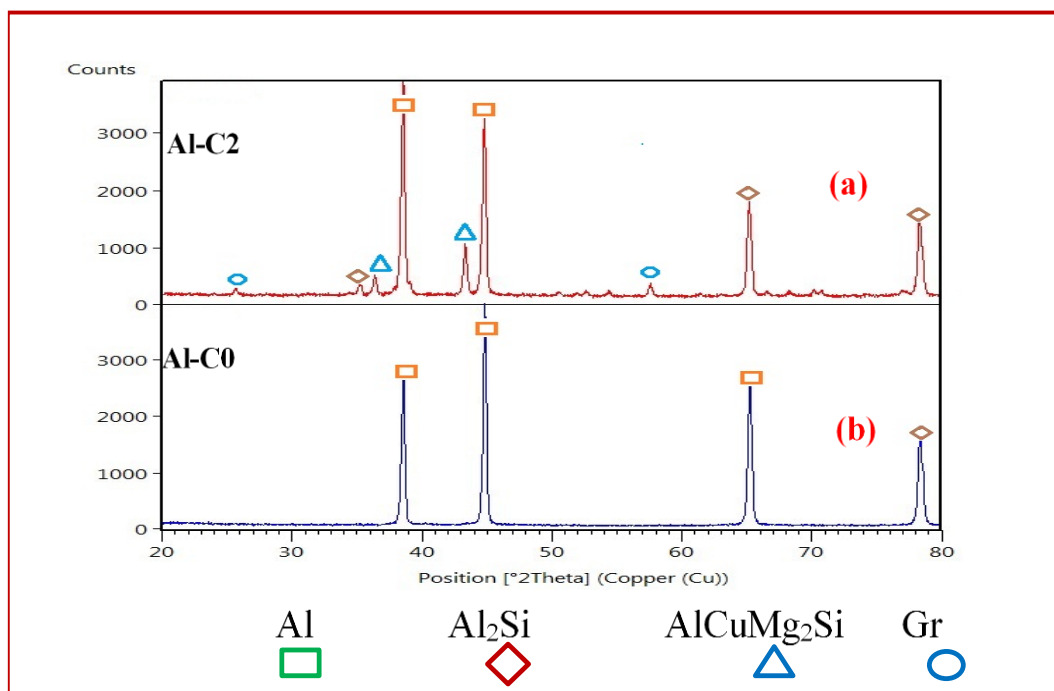


Figure 4. X-ray diffraction patterns of aluminium matrix composites (a) Al-C2 (after adding 9% garnet) under mold of copper chilling and (b) Al-C0 (without garnet particles).

Vickers hardness values of the Al-Mg-Si matrix under the different chill casting conditions (in Figure 5). It was observed that Al-composite samples which have the highest Vickers hardness values were underwent the copper chill casting compared to mold steel chill and mold without chill. The recently studies¹⁶⁻¹⁸ proved that the use copper chill end (in the casting process) was not only favors in the directional solidification but also enhances solidification. The rapid cooling rate was helping to get finer structures and improved mechanical properties as investigated in this study. It is seen that the casted Al-HMMC samples under copper chill has a significant increase of Vickers hardness value. The major reason for increasing of Vickers hardness due to the actions of mold copper chill end and also to the presence of garnet particles (Gr) were coherent grains and their uniform distribution within Al-matrix alloy composite samples.

The ultimate tensile strength of Al-matrix composite samples under the different of mold-chills casting process shown in Figure 6. It was obvious that Al-composite with 9 wt.% garnet (using copper chill casting) has the high tensile strength. This high of tensile is due to increasing the weight percent of Gr. It was observed that tensile strength of Al-matrix composites reinforced with garnet is higher than the Al-matrix alloy without addition Gr particles. Recently studies by Nityanand and Prasad¹⁹ and Bandekar and Prasad²⁰ referred to the advantages of the copper chill casting coupled with the reinforcement of Gr particles within Al-matrix alloy. However, the current study proved that copper chill casting condition with using Gr particles as reinforcement led to the very fine, uniform and coherent grains of microstructural (as aforementioned in Figure 2c) in addition to the obtaining improvements of mechanical properties of Al-matrix composites samples.

It has observed that the values of hardness and tensile were significant decreasing for Al-HMMC composite sample after added 12 wt.% Gr particles. This the decrease is due to that aluminum matrix become a semi-brittle matrix and, then, has a less ductility property thus losing strength.

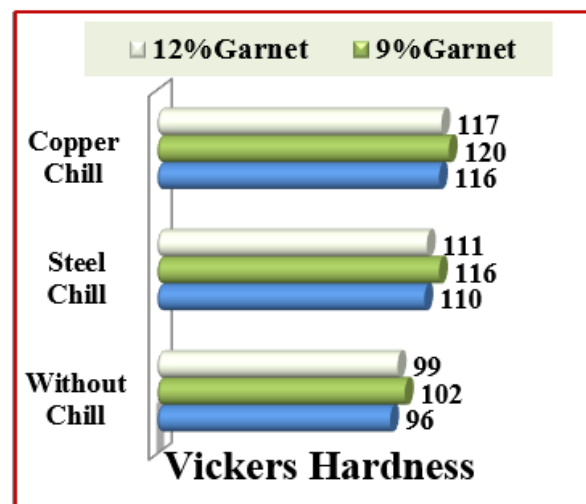


Figure 5. Vickers Hardness of the chill cast composites at various of Garnet.

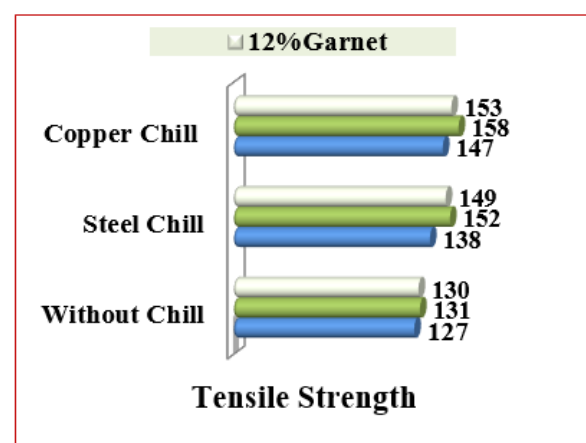


Figure 6. Ultimate tensile strength of the composite samples with respective to various of Garnet for different chill materials.

4. Conclusions

Al-Si-Ni-Cu-Mg alloy composites were successfully synthesized with garnet ceramic particles using the stir casting method under different chilling casting. Microstructural analyses showed that grains were uniform distributed, and they have a good bonding with the Al-matrix.

The results presented that the casted Al-matrix composite fabricated via copper chill block has significant high Vickers hardness and tensile strength values. The outcomes showed that the adding of Garnet particles and using copper chill casting have strongly effects on properties of aluminum metal matrix composites samples.

5. Acknowledgments

This study was conducted in workshops of College of Engineering-Al Muthanna University-Al Muthanna Governorate-Iraq. The authors appreciatively acknowledge the work provision provided by the technicians of the workshop in college of engineering.

6. References

- [1] Sharma, P., A study on microstructure of aluminium matrix composites, *Integr. Med. Res.* 3 (3) (2015) 240-244. <https://doi.org/10.1016/j.jascer.2015.04.001>.
- [2] Lakshmipathy, J., Kulendran, B., Reciprocating wear behavior of 7075Al/SiC in comparison with 6061Al/Al₂O₃ composites, *International Journal of Refractory Metals and Hard Materials* 46 (2014) 137-144. <https://doi.org/10.1016/j.ijrmhm.2014.06.007>.
- [3] Sarada, B. N., Srinivasa, P. L. M., Ugrasen, G., Hardness and wear characteristics of hybrid aluminium metal matrix composites produced by stir casting technique, *Mater. Today Proc.* 2 (4-5) (2015) 2878-2885. <https://doi.org/10.1016/j.matpr.2015.07.305>.
- [4] Aruria, D., Adepua, K., Adepub, K., Bazavada, K., Wear and mechanical properties of 6061-T6 aluminum alloy surface hybrid composites [(SiC-Gr) and (SiC-Al₂O₃)], *Journal of Materials Research and Technology* 2 (4) (2013) 362-369. <https://doi.org/10.1016/j.jmrt.2013.10.004>.
- [5] Sharifi, E. M., Karimzadeh, F., Wear behavior of aluminum matrix hybrid nanocomposites fabricated by powder metallurgy, *Wear* 271 (7-8) (2011) 1072-1079. <https://doi.org/10.1016/j.wear.2011.05.015>.
- [6] Ghoncheh, M. H., Shabestari, S. G., Abbasi, M. H., Effect of cooling rate on the microstructure and solidification characteristics of Al2024 alloy using computer-aided thermal analysis technique, *J. Therm. Anal. Calorim.* 117 (2014) 1253-1261. <https://doi.org/10.1007/s10973-014-38673>.
- [7] Radhika, N., Subramanian, R., Effect of reinforcement on wear behaviour of aluminium hybrid composites, *Tribology-M. S. I.* 7 (1) (2013) 36-41. <https://doi.org/10.1179/1751584X13Y.0000000025>.
- [8] Sharma, S. C., The sliding wear behavior of Al6061–garnet particulate composites, *Wear* 249 (12) (2001): 1036-1045. [https://doi.org/10.1016/S0043-1648\(01\)00810-9](https://doi.org/10.1016/S0043-1648(01)00810-9).
- [9] Mishra, S., Patnaik, A., Kumar, S. R., Comparative analysis of wear behavior of garnet and fly ash reinforced Al7075 hybrid composite, *Wiley Online Library* 50 (1) (2019) 86-96. <https://doi.org/10.1002/mawe.201800121>.
- [10] Saravanakumar, A., Sasikumar, P., Sivasankaran, S., Synthesis and Mechanical Behavior of AA 6063-x Al₂O₃ wt.%-1% Gr (x = 3, 6, 9 and 12 wt.%) Hybrid Composites, *Procedia Engineering* 97 (2014) 951-960. <https://doi.org/10.1016/j.proeng.2014.12.371>.
- [11] Sharma, A., Kumar, S., Singh, G., Pandey, O. P., Effect of particle size on wear behavior of Al–garnet composites, *Particulate Science and Technology* 33, (3) (2015) 234-239. <https://doi.org/10.1080/02726351.2014.954686>.
- [12] Kumar, R. A., Sait, A. N., Subramanian, K., Mechanical properties and microstructure of stir casted Al/B₄C/garnet composites, *Materials Testing* 59 (4) (2017) 338-343. <https://doi.org/10.3139/120.111007>.
- [13] Uthayakumar, M., Aravindanb, S., Rajkumarb, K., Wear performance of Al–SiC–B₄C hybrid composites under dry sliding conditions, *Materials and Design* 47 (2013) 456-464. <https://doi.org/10.1016/j.matdes.2012.11.059>.
- [14] Suresh, R., Hemanth, J., Assessment of dispersoid content and chill effect for improved mechanical properties of chilled aluminium alloy quartz particulate composite, *ASME International Mechanical Engineering Congress and Exposition* 12 (2008) 631-634 <https://doi.org/10.1115/IMECE2008-67433>.
- [15] Sharifi, E. M., Karimzadeh, F., Wear behavior of aluminum matrix hybrid nanocomposites fabricated by powder metallurgy, *Wear* 271 (7-8) (2011) 1072-1079. <https://doi.org/10.1016/j.wear.2011.05.015>.
- [16] Seah, K. H. W., Hemanth, J., Sharma, S. C., Mechanical properties of aluminum/quartz particulate composites cast using metallic and non-metallic chills, *Materials & Design* 24 (2) (2003) 87-93. [https://doi.org/10.1016/S0261-3069\(02\)00144-9](https://doi.org/10.1016/S0261-3069(02)00144-9).
- [17] Spinelli, E. J., Cheung, N., Goulart, P. R., Quaresma, J. M. V., Garcia, A., Design of mechanical properties of Al-alloys chill castings based on the metal/mold interfacial heat transfer coefficient, *International Journal of Thermal Sciences* 51 (2012) 145-154. <https://doi.org/10.1016/j.ijthermalsci.2011.08.014>.
- [18] Wankhede, D. M., NarkhedeS, B. E., Mahajan, K., Choudhari, C. M., Influence of Copper Chills and Pouring Temperature on Mechanical Properties of LM6

Castings, *Advances in Materials and Metallurgy In: Conference paper* 2019 207-216.
https://doi.org/10.1007/978-981-13-1780-4_21.

[19] Nityanand, B., Prasad, M. G. A., Fractographic and three body abrasion behaviour of Al-Garnet-C hybrid chill cast composites, *IOP Conference Series: Materials Science and Engineering* 225 (1) (2017)
<https://doi.org/10.1088/1757-899X/225/1/012290>.

[20] Bandekar, N., Prasad, M. G. A., Study of Dispersoid Content and Chill Effect for Improved Mechanical Properties of Aluminum-Garnet-Carbon Hybrid Metal Matrix Composites, *International Journal of Engineering Technology, Management and Applied Sciences* 3 (2015) 616-623.
<http://www.ijetmas.com/admin/resources/project/paper/f201503111426091722.pdf>.

Cobalt(II) chloride complexes with some phosphine oxides: compatibility between structural data for the solid complexes and their stability constants in acetone medium

Antonio Carlos Massabni^{1,2} , Cristo Bladimiro Melios¹

¹ São Paulo State University (Unesp), Institute of Chemistry, 55 Prof. Francisco Degni St, Araraquara, São Paulo, Brazil

² Araraquara University (Uniará), 1217 Carlos Gomes St, Araraquara, São Paulo, Brazil

+Corresponding author: Antonio Carlos Massabni, email address: amassabni@uol.com.br

ARTICLE INFO

Article history:

Received: December 22, 2018

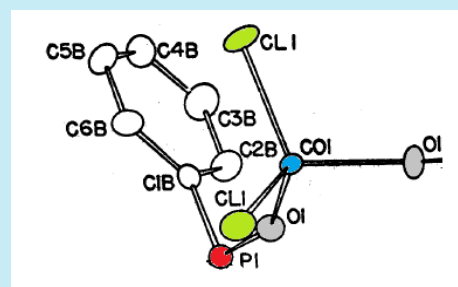
Accepted: March 30, 2019

Published: April 25, 2019

Keywords:

1. cobalt(II) chloride
2. phosphine oxides
3. structural data
4. stability constants

ABSTRACT: Binary complexes of general formula CoCl_2L_2 , where L = triphenylphosphine oxide (TPPO), benzyldiphenylphosphine oxide (BDPPO), dibenzylphenylphosphine oxide (DBPPO) and tribenzylphosphine oxide (TBPO) were considered concerning X-ray structural data for the complexes in the solid state and their stability constants in acetone solution. Compatibility between structural data and stability constants are pointed out. Previous investigations showed that in acetone medium, with CoCl_2 as reference acceptor, the following basicity order is obeyed: $\text{TBPO} > \text{DBPPO} > \text{BDPPO} > \text{TPPO}$. This sequence is supported by X-ray diffraction data of the solid complexes and by electrolytic conductance values for these complexes both in acetone and in nitromethane media.



1. Introduction

First attempts made to correlate variations in bands assigned as carbonyl stretching frequencies in the infrared region for solid metal ion complexes with the stability constants of these same complexes in solution date back to early 1950s.

In some cases, very good correlations were found¹; on the other hand, complexes comprising the same oxygen donors showed no correlation at all¹.

So far as we know, correlations between X-ray structural data for the solid complexes and their stability constants in solution have not been reported. Very recently, an attempt to correlate bond lengths (in solids) and stability constants (in solution) involving organometallic complexes has been published². However, the work is quite restricted (explicitly, only two solid complexes – and these are not directly comparable – are

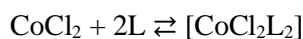
considered). Furthermore, the goal stated by the authors² namely, to establish correlations between solid structures and their corresponding thermodynamic data in solution was certainly not achieved.

The present article deals with X-ray data for the solid complexes of general formula CoCl_2L_2 , where L = triphenylphosphine oxide (TPPO), benzyldiphenylphosphine oxide (BDPPO), dibenzylphenylphosphine oxide (DBPPO) or tribenzylphosphine oxide (TBPO) as well as with formation constants of these complexes in acetone medium, at 25 °C.

2. Materials and methods

Solid complexes, appropriate for X-ray examination were prepared as previously described³. Equipment used for collection of X-ray diffraction data, measurements of diffraction

intensities, solution and refinement of the diffraction data were already described^{4,5}. Spectra in the visible region and absorbances at fixed wavelengths have been gathered as described elsewhere⁶. Stability constants for the equilibria:



$$\text{and hence: } \beta_2 = \frac{[\text{CoCl}_2\text{L}_2]}{[\text{CoCl}_2][\text{L}]^2}$$

were determined at 25 °C in acetone medium by combining the spectrophotometric method of the corresponding solutions with the Fronaeus' computation technique⁶.

3. Results and discussion

Relevant results from both X-ray examination and stability constants given in Table 1 indicate that in acetone medium, and with CoCl₂ as a reference acceptor the following basicity order holds^{7,8}: TBPO > DBPPO > BDPPO > TPPO.

Table 1: Main bond (Å) and angles (°) for the coordination sphere of the complexes and their stability constants in acetone medium.

| Ligand | Co-O ₁ | Co-O ₂ | P-O ₁ | P-O ₂ | O-Co-O | Ref. | logβ ₂ | Ref. |
|--------|-------------------|-------------------|------------------|------------------|--------|------|-------------------|------|
| TPPO | 1.997 | 2.001 | 1.500 | 1.498 | 100.04 | 9 | 6.82 | 6 |
| BDPPO | 1.977 | 1.977 | 1.513 | 1.513 | 100.25 | 5 | 7.31 | 7, 8 |
| DBPPO | 1.974 | 1.974 | 1.529 | 1.529 | 103.07 | 5 | 8.06 | 7 |
| TBPO | 1.937 | 1.920 | 1.505 | 1.547 | 104.98 | 4 | 8.10 | 7 |

These results are in line with the X-ray data for the solid complexes, i.e., the stronger the donor, the shorter the Co-O distances (stronger coordination) and the greater the P-O lengths. The sole exception is one of the P-O distances concerning the TBPO complex. The reason for this is unknown. The above basicity sequence has been further confirmed by conductivity data of the complexes both in acetone¹⁰ and in nitromethane³ (in this last solvent, only data for the BDPPO, DBPPO and TBPO complexes are available).

In a previous investigation⁸, no simple correlation was found between the Co-O stretching frequencies (infrared) of the solid complexes and their stability constants in acetone solution.

4. Conclusions

The basicity sequence for the phosphine oxides considered herein has been substantiated both by X-ray diffraction data of the corresponding cobalt(II) solid complexes and by their stability constants in acetone medium. The aim of this article is also to foster other people in searching possible connections between the structure of solid complexes (even in solution, through X-ray scattering and diffraction data; see *e. g.* ref. 11) and their stability constants in liquid media.

6. References

- [1] Cotton, F. A., The infrared spectra of transitional metal complexes, Modern Coordination Chemistry (Lewis, J. and Wilkins, RG., ed.), Interscience, New York, 1960. p. 386.
- [2] Mészáros, J. P., Dömötör, O., Hackl, C. M., Roller, A., Keppler, B. K., Kandioller, W., Enyedy, É. A., Structural and solution equilibrium studies on half-sandwich organorhodium complexes of (N,N) donor bidentate ligands, New J. Chem. 42 (2018) 11174-11184. <https://doi.org/10.1039/c8nj01681j>.
- [3] Massabni, A. C., Serra, O. A., Cobalt(II) complexes with phosphine oxides, J. Coord. Chem., 7 (1977) 67-73.
- [4] Santos, R. H. A., Mascarenhas, Y., The crystal and molecular structure of bis(tribenzylphosphine oxide)dichloro cobalt(II), J. Coord. Chem., 9 (1979) 59-64. <https://doi.org/10.1080/00958977908073102>.
- [5] Santos, R. H. A., Contribuição ao estudo da estrutura de complexos de fosfinóxidos com cobalto(II). PhD Dissertation, Instituto de Física e Química de São Carlos, USP. São Carlos (SP), Brazil, 1979.
- [6] Molina, M., Melios, C. B., Massabni, A. C., Takaki, T., Equilibria involving cobalt(II) halides and phosphine oxides I. A spectrophotometric study of the cobalt(II) chloride – triphenylphosphine oxide system in acetone

medium, *J. Coord. Chem.* 7 (1978) 133-140.
<https://doi.org/10.1080/00958977808073052>.

[7] Molina, M., Melios, C. B., Massabni, A. C., Yamanaka, H., Equilibria in acetone medium: binary systems involving cobalt(II) chloride and phosphine oxides, Proc. 4th. Internat. Symp. on Solute-Solute-Solvent Interactions, Vienna (Gutmann, V. and Schuster, P. eds.) Pergamon Press, Oxford, UK, 1978, 211-213.

[8] Molina, M., Melios, C. B., Massabni, A. C., Yamanaka, H., Equilíbrios em meio acetônico. Sistema cloreto de cobalto(II) – benzildifenilfosfinóxido, *Eclét. Quím.*, 3 (1978) 17-25. <https://doi.org/10.26850/1678-4618eqj.v3.1.1978.p17-25>.

[9] Mangion, M. M., Smith, R., Shore, S. G., X-ray structural data for the CoCl_2 -triphenylphosphine oxide complex, *Cryst. Struct. Comm.*, 5 (1976) 493-496.

Mangion, M. M., Smith, R., Shore, S. G., Dichlorobis(triphenylphosphine oxide)cobalt(II), $\text{C}_{36}\text{H}_{30}\text{Cl}_2\text{CoO}_2\text{P}_2$, *Crystal Structure Communications* 5(3) (1976), 493-500.

[10] Melios, C. B., Molina, M., Tognolli, J. O., Espeleta, A. C. F., Equilibria in acetone médium. VI. The cobalt(II) chloride-tri-n-octylphosphine oxide system, *Eclética Química*, 4 (1979) 39-46. <https://doi.org/10.26850/1678-4618eqj.v4.1.1979.p47-53>.

[11] Wertz, D. L., Kruh, R. F., Solute-solvent interactions in some concentrated cobalt(II) bromide solutions, *Inorg. Chem.*, 9 (1970) 595-598.